Copyright Warning & Restrictions

The copyright law of the United States (Title 17, United States Code) governs the making of photocopies or other reproductions of copyrighted material.

Under certain conditions specified in the law, libraries and archives are authorized to furnish a photocopy or other reproduction. One of these specified conditions is that the photocopy or reproduction is not to be "used for any purpose other than private study, scholarship, or research." If a, user makes a request for, or later uses, a photocopy or reproduction for purposes in excess of "fair use" that user may be liable for copyright infringement,

This institution reserves the right to refuse to accept a copying order if, in its judgment, fulfillment of the order would involve violation of copyright law.

Please Note: The author retains the copyright while the New Jersey Institute of Technology reserves the right to distribute this thesis or dissertation

Printing note: If you do not wish to print this page, then select "Pages from: first page # to: last page #" on the print dialog screen

ABSTRACT

DEVELOPING AN INSULIN PRODUCING TISSUE USING MOUSE EMBRYONIC STEM CELLS

by
Neha Mahendrakumar Jain

This thesis describes derivation of pancreatic insulin producing cells (IPCs) from mouse embryonic stem cells and development of three-dimensional (3D) engineered tissue system to provide physiologic culture conditions for IPCs. Upon using a previously established protocol, IPCs have been successfully derived from mouse embryonic stem cells and characterized *in vitro*. IPCs not only express classical markers of pancreatic beta cells but also exhibit glucose responsive behavior. Interestingly while deriving IPCs from mouse embryonic stem cells, islet endothelial cells have also been identified and successfully isolated from the culture. Derivation of a pure population of endothelial cells expressing specific markers of islet microvasculature, differentiated from mouse embryonic stem (mES) cells is entirely novel and is demonstrated for the first time in this study. To better mimic the native environment, a 3D engineered tissue system has been created using stem cell-derived IPCs. IPC survival, glucose responsiveness and gene expressions under both static and flow culture conditions were examined. Furthermore, the effects of endothelial cells on IPC function was examined using a 3D co-culture system of IPCs and islet endothelial cells under both static and flow culture conditions.

While no significant improvements are seen in the glucose responsiveness and gene expression analysis of the IPC clusters in 3D culture conditions in static or flow culture conditions, this study describes includes preliminary design considerations that

can be further extended in developing functional 3D insulin-producing tissues, and ultimately establishing a long-term clinically relevant strategy.

DEVELOPING AN INSULIN PRODUCING TISSUE USING MOUSE EMBRYONIC STEM CELLS

by
Neha Mahendrakumar Jain

A Dissertation
Submitted to the Faculty of
New Jersey Institute of Technology
and Rutgers, The State University of New Jersey - Newark
in Partial Fulfillment of the Requirements for the Degree of
Doctor of Philosophy in Biomedical Engineering

Department of Biomedical Engineering

January 2015

APPROVAL PAGE

DEVELOPING AN INSULIN PRODUCING TISSUE USING MOUSE EMBRYONIC STEM CELLS

Neha Mahendrakumar Jain

Dr. EunJung Lee, Dissertation Advisor — Date
Assistant Professor of Biomedical Engineering, NJIT

Dr. Treena Arinzeh, Committee Member — Date
Professor of Biomedical Engineering, NJIT

Dr. Pranela Rameshwar, Committee Member — Date
Professor of Department of Medicine, Rutgers New Jersey Medical School

---

Dr. Samuel Leibovich, Committee Member — Date
Professor of Department of Cell Biology and Molecular Medicine, Rutgers New Jersey Medical School

---

Dr. Cheul Cho, Committee Member — Date
Assistant Professor of Biomedical Engineering, NJIT

BIOGRAPHICAL SKETCH

Author: Neha Mahendrakumar Jain

Degree: Doctor of Philosophy

Date: January 2015

Undergraduate and Graduate Education:

- Doctor of Philosophy in Biomedical Engineering,
  New Jersey Institute of Technology, Newark, NJ, 2015

- Master of Science in Biomedical Engineering,
  New Jersey Institute of Technology, Newark, NJ, 2010

- Bachelor of Science in Chemical Engineering,
  L.D. College of Engineering, Ahmedabad, India, 2006

Major: Biomedical Engineering

Presentations and Publications:

Peer-Reviewed Articles

Jain NM, Lee EJ. (2014) Islet endothelial cell-derived from mouse embryonic stem cells – Accepted to Cell Transplantation.

Posters

Jain NM, Lee EJ. Islet endothelial cell-derived from mouse embryonic stem cells. Presented at: New York Stem Cell Conference; 2013 Oct 16-17; New York City, New York

Jain NM, Haq-Siddiqi N, Lee EJ. A 3D microfluidic gel system for stem cell derived endothelial cells. Presented at: Bio Medical Engineering Society Annual Meeting; 2013 Sep 25-28; Seattle, Washington

Jain NM, Lee EunJung. Endothelial cells as a side product from mouse embryonic stem cell differentiation into pancreatic islet cells. Presented at: Cellular and Molecular Bioengineering Conference; 2013 Jan 1-5, Waimea, Hawaii

Jain NM, Pfister BJ, Perez-Castillejos R. Microfluidic devices to study the interaction between endothelial cells and neurons. Paper presented at: Faraday Discussion 146- Graduate Research Seminar; 2010 April 9-14; Richmond, Virginia

Jain NM, Pfister BJ, Perez-Castillejos R. Microfluidic devices to study the interaction between endothelial cells and neurons. Presented at: 2010 Metro Area Micro Electro Mechanical Systems/Nano Electro Mechanical Systems Workshop; 2010, July 26; Hoboken, New Jersey

Jain NM, Pfister BJ, Perez-Castillejos R. PDMS devices for studying Dorsal Root ganglia (DRG). Presented at: 2010 Bio Medical Engineering Society Annual Meeting; 2010, October 6-10; Austin, Texas

I dedicate this dissertation
To Gurudev
For guiding me through my life and
For inspiring me to be more than I ever thought myself capable of…

&

To
Ankur
In you have found a friend, a lover, a child and a parent
May we abound in love and laughter!

ACKNOWLEDGMENT

I would like to thank Dr. Eun Jung Lee for being my advisor and teaching me the value of patience, persistence and perfection. I would also like to thank Dr. Pranela Rameshwar, Dr. Treena Arinzeh, Dr. Samuel Leibovich and Dr. Cheul Cho for being part of my PhD dissertation committee. I would like to specially thank Dr. Pranela Rameshwar for her kindness, friendliness and helping me get past the obstacles I faced in research. I would like to thank Dr. Steve Grecco for his invaluable support, friendliness and kindness. The space here is not enough to capture my gratitude for you!

I would like to thank Dr. Dino Magou for teaching me cell culture and for being my first friend and mentor in NJIT. I would like to thank Dr. Willis Hammond for encouraging me and setting me on the path to do research and for being a kind friend. I would like to thank Dr. George Collins for being a friend, mentor and for comforting me in tough times. My immense gratitude to Dr. Raquel Perez-Castillejos for giving me an opportunity to start a PhD in her laboratory and to Dr. Treena Arinzeh for bearing with me when I would go to her office with all my PhD issues. A thank you goes out to Dr. Bharat Biswal for being a pillar of support, a friend and an amazing mentor. A big thanks to Dr. Bruno Mantilla, for teaching me the value of excellence and for being a dear friend. I will miss you a lot and the class!!

I will like to thank Rosa Tolentino, Dr. Mevan Siriwardane, Dr.Anil Srirao, Eric Wong, Veton Vejseli, Smruti Ragunath, Nada Haq, Lakshit Tripathi, Matthew Marsh, Pamela Hitscherich, Jessica Ma, Khaditou Guiro, Roseline Menezes, Garima Sinha and Niki for their love, support and friendliness. Without you all, this journey wouldn't have been so enjoyable! Finally, I would like to thank my parents who have always loved and

believed in me unconditionally. I am truly the luckiest person to have you Mummy & Pappa. I would like to thank my brother Niku for being the strength, support and my best buddy since I was born! Believe it or not, I have learned so much from you. I love you a lot Sardar! Finally, I would also like to thank my dearest friend and husband Ankur, who did not let me quit when it seemed almost impossible for me to take a step further. You have been instrumental in making me realize my strengths. Thanks for always being there, I love you!

A big shout out to all the Art of Living fellas from Jersey City gang for being a family away from family. Thank you Amit, Shubhra, Anish, Pooja, Vidya, Kushal, Archie, Deepu, Uday, Alak, Suchi, Harish, Sweta and Bashu! You guys are the best!

TABLE OF CONTENTS

TABLE OF CONTENTS
(Continued)

Chapter **Page**

TABLE OF CONTENTS
(Continued)

Chapter **Page**

TABLE OF CONTENTS
(Continued)

TABLE OF CONTENTS
(Continued)

Chapter **Page**

LIST OF TABLES

LIST OF FIGURES

LIST OF FIGURES
(Continued)

Figure **Page**

LIST OF FIGURES
(Continued)

Figure **Page**

LIST OF FIGURES
(Continued)

Figure **Page**

LIST OF FIGURES
(Continued)

Figure **Page**

LIST OF FIGURES
(Continued)

Figure **Page**

LIST OF FIGURES
(Continued)

Figure **Page**

LIST OF FIGURES
(Continued)

Figure **Page**

LIST OF ABBREVIATIONS

2D	Two Dimension
3D	Three Dimension
AAT	Alpha Anti-Trypsin
ANOVA	Analysis of Variance
ANG-1	Angiopoetin-1
BSA	Bovine Serum Albumin
CTGF	Connective Tissue Growth Factor
DAPI	4',6-diamidino-2-phenylindole
DE	Definitive Endoderm
DMSO	Dimethyl Sulfoxide
DTZ	Dithizone
EB	Embryoid Body
EC	Endothelial Cell
ECM	Extracellular Matrix
eNOS	Endothelial Nitric Oxide Synthase
ELISA	Enzyme Linked Immuno Assay
FACS	Fluorescence Activated Cell Sorting
FBS	Fetal Bovine Serum
FGF	Fibroblast Growth Factor
FLK1	Fetal Liver Kinase 1
GAPDH	Glyceraldehyde-3-Phosphate Dehydrogenase

GC	Guanine Cytosine
GLUT2	Glucose Transporter Type 2
HBSS	Hanks Buffer Salt Solution
H&E	Hematoxylin and Eosin
HGF	Hepatocyte Growth Factor
ICAM	Intercellular Adhesion Molecule 1
IEC	Islet Endothelial Cell
IPC	Insulin Producing Cell
ITSFn	Insulin Transferrin Selenium and Fibronectin
LDL	Low Density Lipoprotein
LIF	Leukemia Inhibitory Factor
KRBH	Krebs Ringer Bicarbonate Hepes Buffer
MEF	Mouse Embryonic Fibroblast
MESC	Mouse Embryonic Stem Cell
MESC-EC	Mouse Embryonic Stem Cell derived Endothelial Cell
NO	Nitric Oxide
NOS	Nitric Oxide Synthase
PAX4	Paired Box Gene 4
PBS	Phosphate Buffered Saline
PCR	Polymerase Chain Reaction
PDMS	Polydimethylsiloxane
PDX1	Pancreatic and Duodenal Homeobox 1
PECAM1	Platelet Endothelial Cell Adhesion Molecule 1

PET	Poly Ethylene Terephthalate
PFA	Para Formaldehyde
PTFE	Poly Tetra Fluoro Ethylene
RAEC	Rat Aortic Endothelial Cell
RTPCR	Reverse Transcription Polymerase Chain Reaction
S1P	Sphingosine 1 Phosphate
SDS	Sodium Dodecyl Sulfate
TGF-β	Transforming Growth Factor Beta
VEGF	Vascular Endothelial Growth Factor

CHAPTER 1

INTRODUCTION

1.1 Background

Diabetes is an epidemic disease that affects about 371 million people worldwide [3]. In the United States alone, diabetes has been reported as the 7th leading cause of death, with the total economical cost of $245 billion in 2012 [7]. Diabetes is also a major cause of various other diseases including heart disease, kidney failure, non-traumatic lower limb amputations, blindness, dental disease and complications during pregnancy among adults [10].

Pancreas transplantation has been considered the gold standard for treatment of diabetes type I. But, due to shortage of healthy donor tissue available, transplantation of pancreas or islets is extremely limited. Even if the transplantation is performed, immune rejection poses a serious problem to the health of the patient. Most patients need to be on life long immune suppression drugs, which compromise their health and wellbeing. Xenografts i.e., animal derived tissue are comparatively readily available for transplantation, but pose a serious risk of unknown disease transmission if used for transplantation. Alternatively, insulin injections are used by a majority of the patients suffering from diabetes Type I & II, but these can lead to hypoglycemia or hyperglycemia which themselves can cause major health issues, including death [11]. Further, insulin injections provide temporary relief of symptoms while not addressing the underlying cause.

Recently, islet transplantation has emerged as one of the promising treatment options. Isolated islets are encapsulated inside semipermeable membranes and then transplanted or simply delivered inside the body through a catheter [12]. This is a simpler procedure compared to the pancreas transplantation as the volume of islets is much less than the pancreas [13]. In addition, the encapsulation prevents the islets from being destroyed by the body's immune system [13, 14]. Recently, the Edmonton protocol for islet transplantation has been described [15]. The Edmonton protocol involves isolating islets from a cadaveric donor pancreas using a mixture of liberases. Each recipient receives islets from one to as many as three donors. The islets are infused into the patient's portal vein, and are then kept from being destroyed by the recipient's immune system through the use of two immunosuppressants, sirolimus and tacrolimus as well as a monoclonal antibody drug used in transplant patients called daclizumab [15]. But, the islet transplantation by Edmonton protocol has shown that the islets suffer from low retention and viability after transplantation [15]. As multiple donors are needed for providing islets for one patient, this further limits the procedure. There are other obstacles to successful microencapsulated islet transplantation such as deficient nutrient diffusion, local fibrosis and issues with biocompatibility [16, 17]. All these factors indicate the need for achieving a large pool of functional beta cells and providing a physiological environment for these cells *in vitro*, which can be used for therapeutic intervention for patients with diabetes.

To better understand the pathophysiology of diabetes, Type 1 and 2 diabetes are reviewed in Section 1.1.1. The physiology of pancreatic islet cells is summarized in Section 1.1.2. Recent efforts in deriving stem cell-derived pancreatic islet cells are

described in Section 1.1.3. Furthermore, section 1.1.4 describes the past and current efforts in the field of pancreatic tissue engineering. The several interactions that occur between the beta cells and endothelial cells during development have been described in Section 1.1.5.

1.1.1 Diabetes

The term diabetes mellitus describes a metabolic disorder characterized by chronic hyperglycemia with disturbances of carbohydrate, fat and protein metabolism resulting from defects in insulin secretion, insulin action, or both. The effects include long term damage, dysfunction and failure of various organs [18]. There are several different types of diabetes, among which diabetes Type 1 and Type 2 are the most common.

Type 1 diabetes is classified as Type 1A and Type 1B. Type 1A diabetes is caused by autoimmune destruction of the beta cells of the pancreas [19]. The slowly progressive form of diabetes type 1A generally occurs in adults and is sometimes referred to as latent autoimmune diabetes in adults (LADA). Islet cell autoantibodies, and autoantibodies to insulin, and glutamic acid decarboxylase (GAD65) are present in almost 85–90% of patients with Type 1 diabetes mellitus [20]. It has been shown that genetic background, ethnicity and environmental factors play a role in the disease occurrence [21]. Type 1B, also known as the Idiopathic Type 1 diabetes is characterized by the absence of an autoimmune disorder and diabetes related antibodies [22, 23]. It is known to have a severe and sudden onset and is characterized by high serum pancreatic enzyme concentrations [23]. It has been found that individuals of African and Asian origin are more prone to getting affected by this disease [24].

The current treatment options for patients with Type 1 diabetes include pancreas transplantation and islet transplantation. Current limitation with the transplantation option is the shortage of healthy donor organ/tissue. Typically more than one donor organ in needed for each patient. This significantly increases the need for healthy donor tissue for such islet transplant options. Moreover, these patients require continuous immunosuppression. The immunosuppression is not only needed for preventing graft rejection, but also to prevent the recurring autoimmune attack on the islets.

Another limitation is the low survival of transplanted islets. While Edmonton protocol showed unprecedented success as 17 consecutive patients became insulin independent after the treatment [15], only 10% of them maintained the insulin dependence after 5 years [25]. Moreover, it has been reported that approximately 60% of pancreatic islets are destroyed due to instant blood-mediated inflammatory reaction after intraportal transplantation through a catheter [17]. This reaction leads to the disruption of islets due to the activation of complement and coagulation systems [26, 27]. Further, the devascularization caused during the isolation, as well as the implantation of the islets into low oxygen tension within the liver, directly damages the islet cells [16]. The activation of innate immune system by the hypoxia environment and the release of inflammatory cytokines, such as tumor necrosis factor-α (TNF-α), interferon-γ (IFN-γ), and interleukin-1 (IL-1) also leads to damage to the islet graft [28].

Type 2 diabetes, also known as non-insulin-dependent diabetes, or adult-onset diabetes is a term used for individuals who have relative, rather than absolute, insulin deficiency. Insulin resistance is often observed in patients with diabetes Type 2 [29, 30]. As the hyperglycemia is not severe enough to induce symptoms, diabetes Type 2 can go

unnoticed for a long time [31, 32]. Nevertheless, this increases the risk for developing macrovascular and microvascular complications [31, 32]. With the advent of science and identification of specific pathogenetic processes and genetic defects that cause diabetes, it is likely that the number of people in this category will decrease in the future [18].

Weight reduction, increased physical activity, and pharmacological treatment of hyperglycemia have been shown to improve insulin resistance [33, 34]. The risk of developing Type 2 diabetes increases with age, obesity, and lack of physical activity [35, 36]. It has been shown that women who suffered from gestational diabetes are more likely to develop diabetes Type 2. Individuals suffering with hypertension and dyslipidemia are also at increased risk for developing diabetes type 2 [35-38]. Familial and genetic disposition play an important role [37-39]. However, the genetics of this form of diabetes are complex and not clearly defined.

Most patients with diabetes type 2 are dependent on insulin injections to maintain a normal blood glucose level. Although availability of insulin improves the symptoms of the patient, administration of insulin is not a treatment for diabetes. Lifestyle change, healthy eating habits, exercise, weight loss and medications such as Metformin are the recommended treatment options [40]. Recently, increasing evidence has demonstrated that islet and cell transplantation, which has only been applied to patients with Type I diabetes, is also effective in patients with Type 2 diabetes [41].

1.1.2 Pancreas and Pancreatic Cells

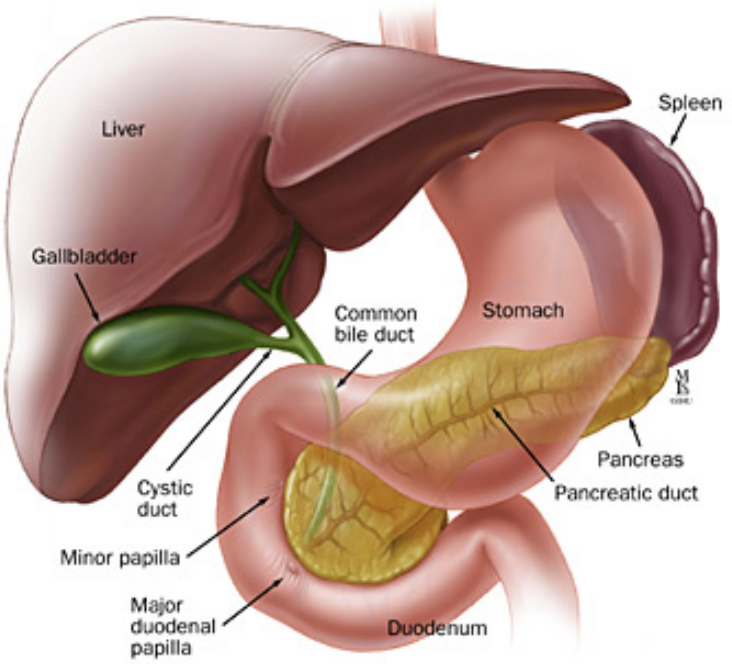

Figure 1.1 Anatomical Position of the Pancreas. The pancreas is shown in relation to the liver, stomach, spleen and the duodenum. Adapted from Moses *et al.*
Source: [42].

The pancreas is a narrow, 6-inch long gland that lies posterior and inferior to the stomach on the left side of the abdominal cavity [43]. Figure 1.1 shows the anatomical position of the pancreas in relation to the surrounding organs such as stomach, liver and the spleen. For descriptive purposes, it is divided into a head, neck, body and tail [6]. The pancreas is a highly vascularized organ. There are numerous arteries that supply the pancreas with freshly oxygenated blood as illustrated in Figure 1.2. The pancreas is vascularized by the superior and inferior pancreatico-duodenal arteries, which form an anastomosis between the coeliac and superior mesenteric arteries, and by numerous short branches from the splenic artery.

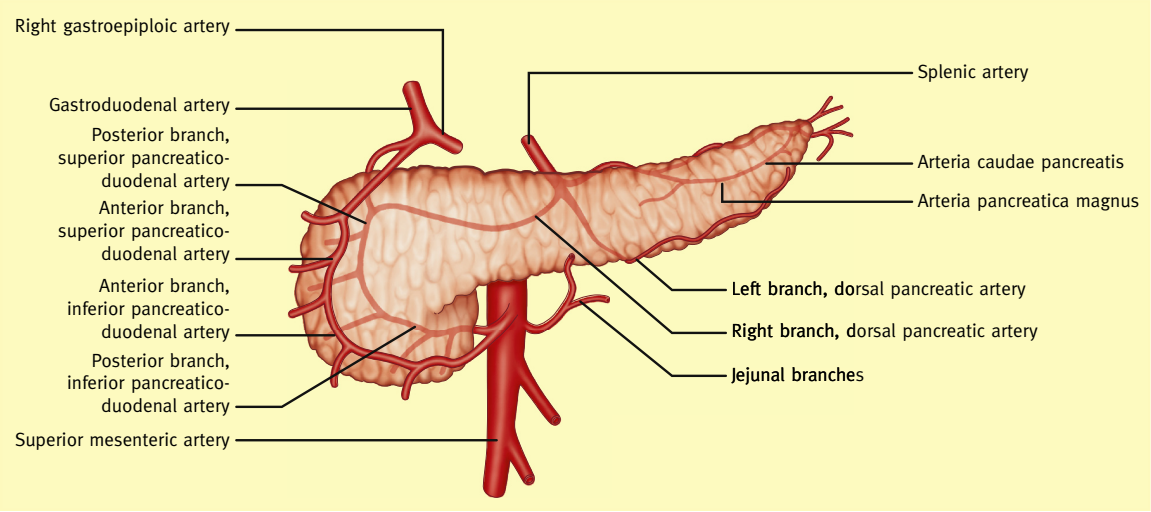

Figure 1.2 Arterial Supply to the Pancreas. Adapted from Moses *et al.*
Source: [6].

The pancreas is the largest of the digestive glands and performs a range of vital exocrine and endocrine functions. The pancreas macroscopically is finely lobulated and is contained within a delicate fibrous capsule. These lobules are made up of alveoli of serous secretory cells, which drain via their ductules into the principal ducts. The islets of Langerhans are located between the alveoli and most of them are located in the pancreatic tail. The islets of Langerhans taken together form ~1% of the pancreas [44] and studies using microspheres have shown that they receive 10% of the total pancreatic blood flow [45]. In most rodents, β cells compose the core of the islets and the non beta cells, including α, δ and pancreatic polypeptide (PP) cells, form the mantle region [46-50]. However, in the human islets not only are the β cells lower in number compared to rodents [51-53], they are dispersed throughout the islets [51, 54].

Pancreatic beta cells play an important role in the maintenance of glucose homeostasis in the body. This begins with the entry of glucose in the beta cells via the GLUT2 receptor [55]. Glucose is then phosphorylated to glucose-6-phosphate by glucokinase, which is also the main glucose sensor in the beta cell [56, 57]. Elevation in the ATP/ADP ratio induces closure of ATP-sensitive potassium channels on the cell surface leading to cell membrane depolarization [58]. This causes the voltage gated Ca2+ channels to open and facilitates the influx of Ca2+ inside the beta cell. A rise in free Ca2+ levels in the cytoplasm trigger the exocytosis of insulin [59]. The primary action of insulin, which is secreted by the beta cells, is to facilitate glucose uptake. This is done primarily in three different ways. Initially, insulin signals the cells of insulin-sensitive peripheral tissues, primarily skeletal muscle, to increase their uptake of glucose [60]. Secondly, insulin acts on the liver to promote glycogenesis. Finally, insulin simultaneously inhibits glucagon secretion from pancreatic α-cells, thus signaling the liver to stop producing glucose via glycogenolysis and gluconeogenesis [61]. Other actions of insulin include the stimulation of fat synthesis, promotion of triglyceride storage in fat cells, promotion of protein synthesis in the liver and muscle, and proliferation of cell growth [62].

Amylin is a neuroendocrine hormone also secreted by beta cells in response to nutrient stimuli [63-65]. Amylin complements the effects of insulin on circulating glucose concentrations via two main mechanisms. Amylin suppresses glucagon secretion after a meal [66], thereby decreasing glucagon-stimulated hepatic glucose output following nutrient ingestion. This suppression of glucagon secretion is mediated via efferent vagal signals. Importantly, amylin does not suppress glucagon secretion during

insulin-induced hypoglycemia [67, 68]. Amylin also slows the rate of gastric emptying and thus, the rate at which nutrients are delivered from the stomach to the small intestine for absorption [69].

Glucagon is a key catabolic hormone secreted from the alpha cells in the islets. Some studies have described diabetes as a bihormonal disease resulting from inadequate insulin as well as excessive glucagon [70]. Glucagon regulates hepatic glucose production and maintains basal blood glucose concentrations within a normal range during the fasting state. When the level of glucose in plasma falls below the normal range, glucagon secretion increases, resulting in hepatic glucose production and return of plasma glucose to the normal range [71, 72]. This endogenous source of glucose is not needed during and immediately following a meal, and glucagon secretion is suppressed.

1.1.3 Stem Cell Derived Pancreatic Cells

It has been shown that embryonic stem cells from both mouse [73-75] and human [73, 76-82] can be differentiated into pancreatic islet cells. Soria *et al.* first described the derivation of insulin producing cells from mouse embryonic (mES) cells [83], while Assady *et al.* demonstrated human embryonic stem (hES) cell derived insulin producing cells for the first time [76]. Other studies have reported the effects of chemical factors affecting the efficiency of differentiation. Some of these protocols used a serum free ITSFn (Insulin, Transferrin, Selenium and Fibronectin) medium and basic fibroblast growth factor (bFGF) treatments [84], while others involved treatment with PI3 kinase inhibitors [85]. However, it was later shown that this protocol might trigger apoptotic pathways of the cells and promote neuronal differentiation [77, 86]. Cells derived from these protocols did not show a controlled insulin release or insulin positive secretory

granules [77, 86, 87], indicating that they are immature and not fully functional under *in vitro* culture conditions [5]. The cells produce insulin but are not able to upregulate their insulin response when exposed to high glucose conditions. Upon transplantation of stem cell derived IPCs to mice, they were able to transiently correct the glucose levels but the effect faded in time [84, 85, 88]. This may be a result of cell death or de-differentiation following transplantation. To increase the yield of endodermal cells, selection of nestin positive cells has been used for both mES cells [79, 84-87, 89-92] and hES cells [87, 91, 93]. Teratoma formation is another drawback of this strategy, which makes it impractical to be used as a clinical therapy [74, 85, 88].

Another approach is to use the knowledge derived from pancreatic development to develop strategies for ESC differentiation into insulin producing cells. A five-stage protocol that mimics pancreatic organogenesis and comprises the sequential phases of inducing a definitive endoderm, primitive gut tube, posterior foregut, pancreatic endoderm and cells that express endocrine hormones, was successfully used to differentiate hES cells to IPCs [94]. After two weeks of differentiation, endocrine hormone expression was noticed. The drawback to this approach was that most of the cells co-expressed more than one hormone indicating that the cells produced were not fully mature. Further, the yield of insulin producing cells was limited to ~7% and the C-peptide release in response to a glucose challenge was marginal [94]. A similar multi stage protocol was also developed using mES cells [84]. Two signaling pathways, the Wnt and transforming growth factor TGF-β are crucial to induce formation of the definitive endoderm. Previous studies have shown that differentiation of human ESCs into definitive endoderm can be achieved via treatment with activin-A and Wnt3a and

can be confirmed by expression of endodermal markers such as Sox17, FoxA2, Gata4, Cxcr4, and Cerberus [94, 95]. Nodal, CHIR99021, IDE1 and IDE2 are molecules that have been shown to induce development of the definitive endoderm in mouse [96, 97] and human cells (19). Also, retinoic acid (RA) is a strong teratogen and can induce ES cells into different cell types including neuronal [98], cardiac [99] and smooth muscle cell [100] based on time and concentration of exposure.

Yet another protocol with four stages of differentiation and a timeline of 12 days was developed that helped generation of glucose responsive insulin producing cells [95]. In brief, during the first stage, human ESCs were treated with activin-A and Wnt3a, followed by activin-A treatment. In the second stage, cyclopamine treatment was eliminated and keratinocyte growth factor was substituted for FGF10. In the next stage, differentiating cells are treated with B27 (a proprietary serum free supplement by Life Technologies), KAAD-cyclopamine, all-trans retinoic acid and Noggin instead of Fibroblast growth factor (FGF). In the fourth stage (pancreatic endoderm formation), cells were cultured in the absence of all factors except B27. Finally, the pancreatic endoderm was transplanted into immunodeficient mice for an *in vivo* maturation step.

Although previous studies have focused on inducing the expression of PDX1, which is a pancreatic progenitor marker by RA, the generation of insulin producing cells was not increased [10] using this approach in mES cells. Some studies have also used a combination of RA with activin A for mES cells, which has also been shown to lead to both pancreatic and neuronal population [101]. Another strategy was to use conditioned medium from embryonic pancreatic buds [102], but the variable composition of secreted growth factors can have an impact on the differentiation process from mES cells. These

challenges suggest that deriving a high yield of functional insulin producing cells from mouse embryonic stem cells is a challenging process and requires a robust approach. Low cell yield, low insulin secretion and lack of glucose responsiveness are the major challenges that need to be overcome. Recently, in a breakthrough study Pagliuca *et al*., demonstrated the derivation of a large amount of functional human pancreatic beta cells using ESCs [103]. This protocol is scalable and can be used for large-scale production of glucose responsive insulin producing cells. Transplantation of these cells into diabetic mice led to ameliorated hyperglycemia. However, more studies will need to replicate the results before they can be used as a therapy.

Mesenchymal stem cells (MSCs) derived from human bone marrow have also been shown to differentiate into insulin producing cells (IPCs) by induced expression of PDX1 [104]. These cells were glucose responsive and were able to reduce hyperglycemia upon transplantation, but only half of the differentiated cells expressed insulin, while glucagon, somatostatin and ghrelin was expressed by all the differentiated cells [104]. Another study used adipose tissue derived MSCs to produce IPCs [105]. Upon induction into a pancreatic endocrine phenotype, the cells expressed transcription factors important for pancreatic development such as Isl-1, Ipf-1, and Ngn3.

1.1.4 Pancreatic Tissue Engineering

In the past, perifusion setups have been used for *in vitro* culture of islets prior to transplantation. The term ‘perifusion’ is used to distinguish the design that involves the flow of culture medium around the islets in a continuous-flow chamber, from the term ‘perfusion’ which involves flow of medium through an intact tissue [106]. In perifusion studies, freshly isolated islets are freely suspended in a column. This column is typically

under 95 % O_2 and 5% CO_2 exposure at 37 °C. Krebs ringer bicarbonate buffer with different glucose concentrations is applied to stimulate insulin release from the islets. The outflow of the column is collected and used for assays or saved for future use. Such assays are typically done over short time intervals ranging from a few minutes to a few hours.

Long term culture of islets in 2D condition have shown that endocrine cells transdifferentiate into exocrine cells and undifferentiated cells [107]. Also, 2D tissue culture surfaces do not provide the cell-matrix interactions that are present *in vivo.* Perifusion methods were developed to improve survivability and function of islets after isolation [108]. In perifusion studies, freshly isolated islets are freely suspended in a column that is typically under 95 % O_2 and 5% CO_2 exposure at 37 °C. These systems allow for rapid testing of the glucose sensitivity of the islets prior to transplantation.

Past studies have shown that islets or individual beta cells have improved survival and function when cultured on ECM-derived substrates, both cell-secreted matrices [109-115], and individual purified ECM proteins [113, 116-119]. Various ECM components have been tested to improve the islet survival and function in *in vitro* culture. It has been shown that matrix secreted by bovine corneal endothelial cells improved islet survival [120], insulin secretion [121] and induced adult β-cell proliferation [109]. Studies of rat β-cells cultured on matrix produced using a rat bladder carcinoma line (804G) revealed that the integrin α6β1 interacted with laminin in the 804G-secreted matrix and influenced β-cell function and insulin secretion [122, 123]. Similar to studies with cell-derived matrices, culture experiments with purified individual ECM proteins resulted in better islet survival and function. Collagen type IV [118] and laminin [113],

both components of the basement membrane, contributed to greater insulin release. Islets cultured on collagen type I–coated surfaces and those treated with soluble fibronectin exhibited less apoptosis and greater insulin secretion [119]. Vitronectin influenced β-cell adhesion and migration via αv integrin interactions [117]. In most of these studies islet–matrix interactions have been studied with insulin-producing cells cultured on 2D ECM-coated tissue culture surfaces. However, there is a growing interest in using ECM components, such as collagens and Matrigel for forming three-dimensional (3D) gels, allowing for the entrapment of islets or individual β-cells and the study of cell–matrix interactions in 3D culture conditions.

Previous studies have demonstrated the encapsulation of xenobiotic islets in semipermeable membranes prior to transplantation prevents the immune rejection by the host animal while allowing insulin secretion out of the membrane and maintenance of normal blood glucose levels [124-128]. The major obstacles to successful microencapsulated islet transplantation are deficient nutrient diffusion, local fibrosis, and the use of inadequate materials for capsules, thus compromising biocompatibility. Further, islets to be implanted should be homogenously dispersed inside the capsules to facilitate maximum oxygen and nutrient diffusion. It is important that the membrane is permeable to insulin and low molecular weight components such as oxygen, glucose, electrolytes and other nutrients and impermeable to cellular components of the immune system.

Recently, three-dimensional islet culture experiments have been demonstrated by a number of groups. Brendel *et al.*, showed that human islets embedded in agarose gel compared with islets in suspension culture were able to consistently induce

normoglycemia in nude mice even after 14 days in *in vitro* culture [129]. Daoud *et al.,* investigated the effects of human islet culture within various three-dimensional environments including collagen I gel and collagen I gel supplemented with ECM components fibronectin and collagen IV and found that the incorporation of ECM components within the three-dimensional support significantly improved insulin release profile and gene expression when compared to suspension culture [130].

Moreover, it was also shown that the entrapment of freshly harvested islets in a 3D collagen matrix helped maintain the islet integrity in culture as the contraction of collagen fibrils counteracted the dispersion of islets [131]. It was observed that the entrapped islets maintained satisfactory morphology, viability, and capability of glucose-dependent insulin secretion for over two weeks [131]. A study by Wang *et al*., reported the development of a 3D ESC pancreatic differentiation system to derive insulin producing glucose sensitive cells. The study showed that about 50-60% of the differentiated cells produce insulin. However, teratoma formation upon transplantation was not studied.

Various microfluidic systems were explored in efforts to improve the survival of islets in *in vitro* culture by perfusing islets and doing rapid quality assessment following donor isolation [132]. Culturing mouse islets in a microfluidic device resulted in twice the endothelial cell density inside the islets and connected length of capillaries compared to classically cultured islets [133]. Microfluidic devices have also been used to perfuse islets and doing rapid quality assessment following donor isolation [132]. Microfluidic devices can serve as unique platforms to optimize islet culture by introducing intercellular flow to overcome the restricted diffusion of media components. Microfluidic

devices offer ease of operation, high customization abilities and the capability to do single islet analysis [134-136]. At the same time, they also suffer from limitations such as islet damage due to potential shear and mechanical stresses [134-136], complexity of microfluidic devices [134-138], low throughput [137-140] and the difficulty of monitoring/imaging the islets real time [132, 137, 138, 141].

1.1.5 Interaction of Pancreatic Cells and Vascular Cells

Islets are highly vascularized structures [142]. Although, islets form only 1-2% of the pancreatic mass, they receive approximately 10% of the blood supply [143]. The blood perfusion is meticulously regulated, predominantly [144] by a complex interplay of locally produced factors, gastrointestinal hormones and the nervous system, to meet the needs for hormone secretion imposed on the pancreatic tissue [143]. This not only allows for adequate nutrient supply and glucose sensing, but also facilitates adequate and rapid dispersal of islet hormones secreted to the blood stream.

It has been shown that various vascular mediated signals are important during pancreatic development. In vitro tissue interaction studies have shown that the dorsal aorta, which is near the dorsal pancreatic endoderm, induces the budding of the dorsal pancreas and expression of pancreatic transcription factors such as the pancreatic and duodenal homeobox 1 (Pdx1) transcription factor and pancreas transcription factor 1a (PTF1a), as well as insulin and glucagon [145, 146], as shown in Figure 1.3. The aorta also induces the dorsal pancreatic mesenchyme, which signals towards the dorsal pancreatic bud via fibroblast growth factor 10 (FGF10) [147]. An important blood-derived factor is sphingosine-1- phosphate (S1P), which binds to G-protein-coupled S1P receptors on mesenchymal cells and induces their proliferation. In turn, these

mesenchymal cells stimulate growth and budding of the dorsal pancreatic endoderm [148]. In summary, there is convincing evidence of the inductive potential of vascular tissue during pancreatic development in mice that might also apply to human pancreatic development [1].

Differentiating endocrine cells start to secrete vascular endothelial growth factor-A (VEGF-A) to attract endothelial cells and induce them to form an islet vascular bed [149].

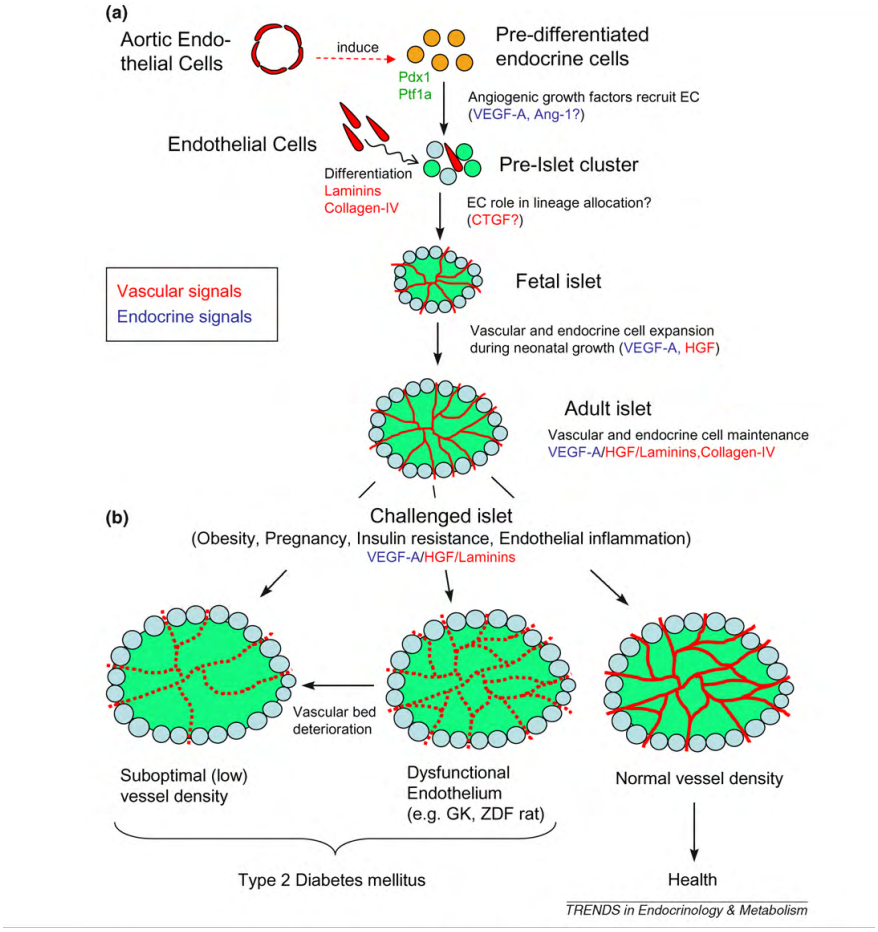

Figure 1.3 Interactions Between Endothelial Cells and Endocrine Cells Throughout Life. Adopted from Eberhard *et al.*
Source: [1].

It has been shown that VEGF-A is essential not only for development of the islet microvasculature, but also for the formation of endothelial fenestration, which might facilitate effective glucose sensing and interstitial flow in the adult islet [149-152]. However, VEGF-A deficient mouse islets do not completely lack blood vessels, so other factors might also contribute, to some extent, to endothelial cell attraction and vessel

formation [150]. Angiopoietin-1 (Ang-1), another angiogenic growth factor expressed in beta cells [149], promotes the survival and integrity of blood vessels [153].

Apart from enabling blood flow in islets, endothelial cells are the source of many extracellular matrix (ECM) proteins that support beta cell differentiation and proliferation [154, 155]. It has also been shown that a novel EC-derived factor, connective tissue growth factor (CTGF), is involved in endocrine cell lineage allocation and beta cell proliferation [156]. CTGF is highly expressed in the islet vasculature, albeit at lower levels in future β cells in the embryonic pancreas. More α cells were found in islets of CTGF-deficient mice, so CTGF might be required for directing endocrine precursor cells towards the beta cell lineage. CTGF also interacts with several growth factor signaling pathways, such as the TGF beta (Transforming growth factor beta) and Wnt pathways, but its specific receptor in the pancreas has not been identified yet [156]. The various molecular interactions between the endothelial cells and beta cells are tabulated in Table 1.1.

The beta cell and endothelial cell interaction continues even in adulthood. In the healthy individual, the beta cell adapts to higher insulin demands, such as during postnatal development, increased body weight (in extreme to obesity) or pregnancy, by upregulation of insulin production and growth [157]. The growing islet requires oxygen and nutrients, as well as paracrine signals from the blood vessels, so expansion of the microvasculature is needed. This expanding microvasculature results from mutual signals between blood vessels and beta cells. VEGF-A signaling is also essential for maintaining the vascular bed in adult islets, because systemic administration of VEGF receptor antagonists quickly and significantly reduced the islet vascular density [158].

Apart from its role during embryonic pancreas development, VEGF-A also seems to play a role in islets after birth. More specifically, VEGF-A has been suggested to stimulate endothelial cell growth in the neonatal pancreas [159], because low perinatal levels of VEGF-A were associated with reduced vascular density, early insulin secretory defects and a decrease in beta cell mass in intrauterine growth restricted rats [160]. In addition, increased levels of VEGF-A were observed during islet growth in pregnant rats and it was shown that EC proliferation precedes beta cell division [159]. Thus, islet cell mass expansion either during body growth from a neonate to an adult or during pregnancy are accompanied by increased VEGF-A expression to ensure a sufficient density of capillaries within islets.

Table 1.1 Molecular Interactions Between Endothelial Cells and Beta Cells

Secreted molecule	Function	Receptor or target
β-Cells		
VEGF-A	VEGF-A_{165} dimer secretion by β-cells in embryo and adult and EC attraction and maintenance	VEGFR2 on endothelial cells
Ang-1	Angiogenic factor	Tie-2
Tsp-1	Angiostatic factor; induction of apoptosis in EC and regulation of blood vessel density	CD36
Vasculature		
Collagen IV	Potentiation of insulin secretion	Integrins
Laminins	Induction of β-cell differentiation and normal insulin production, secretion and β-cell proliferation	Integrins, Lutheran
CTGF	Potential role in endocrine lineage specification; expression to a lesser extent in β-cells	Interaction with integrins
HGF	Support of β-cell proliferation in embryonic and postnatal pancreas	c-Met

Source: [1]

Furthermore, studies have shown evidence that isolated islets in co-culture with endothelial cells have shown better survival, integration and functionality [159, 161-164]. Although the participation of ECs in β-cell differentiation and function has been well studied *in vivo* [1, 145, 154, 165, 166], the influence of these cells in the specific differentiation of ESCs into insulin-producing β cells as well as the factors involved have not been fully explored *in vitro*. A recent paper by Adame *et al.*, showed that co-culturing endothelial cells with differentiating embryoid bodies resulted in an increase in the expression of the pancreatic markers PDX-1, Ngn3, Nkx6.1, Pro-insulin, GLUT-2 and Ptf1a [167]. These studies suggest that endothelial cell mediated factors might play a very critical role in the differentiation of stem cells into functional beta cells.

1.2 Significance

This thesis dissertation describes research in the field of pancreatic tissue engineering with the goal of making fundamental advances in the development of functional pancreatic tissues for basic research as well as for long-term clinical application to treat patients with diabetes.

One of the main challenges in pancreatic tissue engineering is obtaining a large number of functional insulin producing cells. Past studies have used various stem cell sources and protocols to derive insulin-producing cells using pluoripotent stem cells. Despite the considerable progress in the field of stem cells, the yield of insulin producing cells using stem cells remains low at about 0.8-7.3% [94, 168]. Furthermore, cells are still immature as they co-express more than one endocrine hormones and are not fully responsive to glucose.

Therefore, the overall objective of this dissertation was to establish a three-dimensional (3D) engineered tissue system to provide a proper culture condition for stem cell-derived beta cells to become fully functional *in vitro*. The effects of physical cues including application of flow to 3D tissues were examined. In addition, the effects of cellular factors on stem cell-derived islet cell function were examined by co-culturing with endothelial cells. The overall objective was achieved by the following specific aims:

Specific Aim 1) To improve the survival and functionality of mES derived insulin producing cells (IPCs).

Working Hypothesis: Encapsulation of IPCs in a 3D ECM environment will improve their survival and glucose responsiveness.

a) *Characterization of mES cell derived IPCs in a 2D system.* IPCs will be derived from mES cells and their phenotype and function will be examined using techniques such as RT-PCR, immunohistochemistry, western blotting, and insulin ELISA. Specifically, the expression of genes such as PDX1, Insulin, Pax4, Nkx6.1, GLUT-2, EphrinA5 and GAPDH will be examined.

b) *Characterization of mES cell derived IPCs in 3D system.* The optimal density of IPCs to be encapsulated in an ECM based gel will be determined based on previous studies by other groups using islet cells. IPCs will be encapsulated in a collagen hydrogel matrix. The IPC performance in the 3D systems will be measured and compared to that of the 2D system based on cell survival and glucose stimulated insulin release measured by insulin ELISA. The expression of genes such as PDX1, Proinsulin, Pax4, Nkx6.1, EphrinA5, GLUT-2 and GAPDH will be examined by using RT-PCR.

c) *Effects of flow on IPC function and survival in a 3D gel system.* The 3D gel system will be subjected to perfusion flow using an existing flow bioreactor system. The function of IPC in the 3D system will be assessed and compared in static vs. flow conditions through protein and gene analysis.

Specific Aim 2) To characterize the endothelial cell population derived from mES cell differentiation into IPCs

Working Hypothesis: mESC-ECs derived from IPC differentiation protocol express islet endothelial cell specific markers.

a) *Characterization of mES -EC phenotype and function in a 2D culture.* ECs will be characterized in detail for expression of classic EC markers such as PECAM-1, Thrombomodulin, ICAM-1, EphB2 and eNOS as well as islet endothelial cell specific markers such as Nephrin and Anti alpha trypsin-1 (AAT).

b) *Characterization of mESC-EC phenotype and function in a 3D engineered tissue.* 3D hydrogel tissues will be formed using mESC-ECs and collagen type I (derived from rat tail). They will be analyzed for formation of tubular networks, lumens and deposition of ECM proteins such as laminin, collagen type IV and fibronectin.

c) *Effects of flow on 3D vascularized tissues.* mESC-EC hydrogels will be subjected to flow using an existing perfusion bioreactor system. A flow rate of 0.5 ml /min which corresponds to a shear stress of approximately 0.71 dynes/cm^2 will be used. This value falls in the shear stress range that is estimated to be present in the circulation [169]. These tissues will be analyzed for formation of tubular networks and lumens.

Specific Aim 3) To develop a 3D vascularized insulin producing tissue.

Working Hypothesis: IPCs co-cultured with ECs will maintain higher viability, glucose responsiveness and will have a higher expression of islet specific markers compared to that of IPCs mono-cultured in collagen.

a) *To develop a co-cultured 3D tissue with mES cell-derived insulin producing cells and mESC-ECs.* The cell and matrix densities will be optimized based on the literature and experimental trials.

b) *To characterize the effects of flow on a co-cultured 3D tissue on mES cell-derived insulin-producing cell maturation and function.* An existing perfusion bioreactor system will be used for the application of flow to the 3D co-culture

tissue construct. Flow parameters will be optimized based on the literature and experimental trials. A static co-culture will be used as a control.

c) *To study the expression profile of EphrinA5 in mES derived insulin producing cells*. The expression profile of EphrinA5 will be studied and compared under flow and static co-culture condition and its co-relation to insulin secretion and glucose responsiveness will be studied.

Derivation and characterization of IPCS from mES cells are described in Chapter 2. Extended from the studies in chapter 2, the techniques were devised to embed the IPCs in collagen hydrogels. Characterization of the survivability and functionality of the IPCs in 3D collagen tissue under static and flow culture condition is described in Chapter 3. The co-culture of mESC-IPCs and mESC-ECs is also described in Chapter 3. The derivation, isolation and characterization of islet specific endothelial cells from mES cells in 2D and 3D conditions are described in Chapter 4. A summary of the entire work and future directions are discussed in Chapter 5. This is the first demonstration of islet specific endothelial cells derived from mouse embryonic stem cell, which is *in press* for Cell Transplantation Journal. An appendix section includes details of all the protocols, medium recipes and methods used.

CHAPTER 2

DIFFERENTIATION OF MOUSE EMBRYONIC STEM CELLS INTO PANCREATIC BETA CELLS

2.1 Introduction

Diabetes Mellitus is a chronic progressive metabolic disorder. Currently, pancreas or islet transplantation is considered the best therapeutic option for Type I diabetes patients, while most Type 2 diabetes patients depend on life long medication for maintaining glucose homeostasis. However, several limitations to these treatments include side effects of immune suppression drugs used during transplantation, immune rejection and the dependency on medication. Further, there is a shortage of healthy donor organs, which led scientists to investigate alternative methods to obtain suitable cell source for transplantation. Recently, a number of studies have shown the possibility of deriving insulin-producing cells using embryonic and adult stem cell populations as summarized in Table 2.1 [75-77, 81, 170-172].

Soria *et al.*, demonstrated the first derivation of insulin producing cells from mouse embryonic stem (mES) cells [83]. This study used a cell trapping system and genetic approaches to create an insulin secreting cell clone. Although the cells were able to reverse hyperglycemia upon implantation in mice, the hyperglycemia was reversed in 12 weeks suggesting that the cells either stopped making insulin or dedifferentiated. A study by Hori *et al.* showed that the use of growth inhibitors such as LY294002 and Wortmannin promoted differentiation of mES cells into IPCs [85]. They used a simple protocol in contrast to the complex genetic approaches employed previously, and the cells maintained their insulin producing

status after engraftment in mice. However, widespread teratoma formation was observed in the treated mice within three weeks of implantation.

Lumelsky *et al.* demonstrated derivation of insulin producing cells (IPCs) from a highly enriched nestin positive cell population [84]. It has been shown that nestin positive cells give rise to both neuronal cells [173] and beta cells [174]. This method used a serum free medium with insulin, transferrin, selenium and fibronectin (ITSFn), which promotes cell death of most types of cells excluding the nestin positive cells, thus enriching their population [175]. The study resulted in IPCs that were glucose responsive and provided the first evidence of the IPCs self-assembling into islet like structures *in vivo*. But the IPCs transplanted subcutaneously in the shoulder of diabetic mice were not able to correct hyperglycemia consistently, as the insulin produced by these cells was about 50 times lower per cell compared to a native islet cell [84]. Recent evidence suggested that these IPCs may not have produced insulin endogenously but had absorbed insulin from the culture medium [77, 87].

In contrast to a study by Lumeskly *et al*., Blyszczuk *et al.* showed that nestin selection was not necessary to produce IPCs from mES cells. However, their differentiated IPCs showed a partial CK19 expression which is highly expressed in pancreatic ductal cells [176, 177] but not in functional islets [178]. The IPCs also exhibited relatively low levels of insulin, suggesting that they were immature [172]. In addition, upon transplantation of the graft in mice, there was a delay of two weeks before the hyperglycemia was reversed; suggesting that further *in vivo* maturation step was necessary for mES derived IPCs [172].

Assady *et al.*, demonstrated derivation of IPCs from human embryonic stem (hES) cells [76]. The differentiated cells expressed beta cell markers such as glut-1, glut-2, insulin and glucokinase, but the glucose responsiveness of the cells was not tested. D'Amour *et al.* used a five step protocol that mimicked the *in vivo* pancreatic organogenesis by directing hES cells into sequential developmental stages. These stages led the cells to progress from definitive endoderm stage into mature insulin producing cells [94]. However, this protocol resulted in cells that co-expressed more than one hormone including glucagon, somatostatin and PP. In addition, these cells failed to respond to glucose stimulation. To improve the maturation of these cells, Kroon *et al.,* transplanted endocrine precursor cells derived from hES cells into mice for further *in vivo* maturation [95]. The mice were able to maintain normal glucose levels after >100 days of transplantation. Upon graft extraction, it was found that the hES derived IPCs had insulin secretory properties similar to that of engrafted adult human islets [95].

Despite all the recent advancements, low differentiation efficiency still remains a challenge. The current yield of IPC differentiated from hES cells is 0.8-7.3% [94, 168]. To improve the differentiation efficiency, studies have explored the effects of growth factors such as retinoic acid (RA) and activins. RA is a strong teratogen and shown to induce ES cells into different cell types including neuronal [98], cardiac [99] and smooth muscle cell [100] depending on the time and concentration of exposure. A previous study reported that the addition of RA did not affect the differentiation efficiency [10]. However, when RA was used in combination with activin A, increase in both pancreatic and neuronal population from mES cells was observed [73]. Moreover, the use of conditioned medium from embryonic pancreatic buds [179], resulted in significant

upregulation of certain genes involved in beta cell development. A summary of various factors used in IPC differentiation is presented in Table 2.2.

Table 2.1 Differentiation Factors and Cell Type

Cell type	Differentiation factors	References
Embryonic stem cells	B27, nicotinamide, insulin, transferin, selenium, FN, exendin-4, LY294002, activin-A, LAM, RA, GLP-1, Nodal, IDE1, IDE2, FGF-10, cyclopamine, extendin-4, DAPT	Bai et al. (2005); Boyd et al. (2008); Cho et al. (2008); D'Amour et al. (2006); Hori et al. (2002); Kroon et al. (2008); Shi et al. (2005)
BM-MSCs	Activin-A, conophyline, BTC-δ4, BTC, nicotinamide, L-glutamine, FN, LAM, HGF, extendin-4	Hisanaga et al. (2008); Lin et al. (2010); Sun et al. (2007)
Umbilical cord blood derived MSCs	Glucose, RA, nicotinamide, epidermal growth factor, exendin-4, B27	Chao et al. (2008); Gao et al. (2008)
Adipose tissue-derived MSCs	Glucose, nicotinamide, activin-A, exendin-4, HGF, pentagastrin, BTC	Timper et al. (2006)
Progenitor cells	Glucose, poly-L-ornithine, FN, apo-transferin, L-glutamine, RA, nicotinamide, insulin-like growth factor, matrigel, FGFR2IIIb, HGF, EGF	Elghazi et al. (2002); Feng et al. (2005); Gao et al. (2003); Hori et al. (2005); Suzuki et al. (2002)

DAPT N-[N-(3,5-difluorophenacetyl)-L-alanyl]-S-phenylglycine t-butyl ester, *RA* retinoic acid, *BTC-δ4* betacellulin-delta4, *FN* fibronectin, *LAM* laminin, *HGF* hepatocyte growth factor, *EGF* epidermal growth factor

Source: [5]

Table 2.2 Extrinsic Factors Promoting Beta Cell Differentiation and Proliferation

Extrinsic factors	Abbreviation	Function	References
Glucagon like peptide	GLP-1	The most potent stimulator of oral glucose-induced insulin secretion, GLP-1 is released in response to meal intake and is rapidly metabolized and inactivated by dipeptidyl-peptidase-4	Bai et al. (2005); Hardikar et al. (2002)
Betacellulin	BTC	Plays an important role in regulating growth and differentiation of pancreatic β cells	Cho et al. (2008); Li et al. (2004); Oh et al. (2011); Shi et al. (2005); Sun et al. (2007)
Activin-A		Regulates neogenesis of β cells in vivo	Li et al. (2004); Shi et al. (2005); Sun et al. (2007)
Hepatocyte growth factor	HGF	Promotes β-cell proliferation and regeneration, regulates the pancreatic islet differentiation	Wang et al. (2004)
Endothelial growth factor	EGF	Promotes the proliferation of nestin-positive cells	Kelly et al. (2005); Schwindt et al. (2009); Tureyen et al. (2005)
Basic fibroblast growth factor	bFGF	Promotes the proliferation of nestin-positive cells	Kelly et al. (2005); Schwindt et al. (2009); Tureyen et al. (2005)
Nicotinamide		Promotes formation of fetal porcine islet-like cell clusters and increases the rates of proinsulin biosynthesis in these clusters	Cho et al. (2008); Tang et al. (2004)
β-mercaptoethanol		Increases the potency of nicotinamide	Chen et al. (2004)
Laminin	LAM	Affects β cells differentiation, proliferation, and insulin secretion	Lin et al. (2010)
Fibronectin	FN	Affects β cells differentiation, proliferation, and insulin secretion	Lin et al. (2010)
Extendin 4		Promotes growth and maturation of β cells	Degn et al. (2004)

Source: [5]

Another challenge is to obtain fully functional insulin producing cells. Most studies using pluripotent stem cells have reported that the differentiated cells were either not glucose responsive [76, 84, 94] or required additional *in vivo* maturation steps [95, 180]. Immature cells also typically co-express multiple hormones and are not glucose sensitive [94]. On the other hand, mature beta cells are defined by a switch from $MafB^{+}$ $MafA^{-}$ to $MafB^{-}$ $MafA^{+}$ status in their gene expression [181]. This switch occurs in cells that already express Nkx6.1 and is preceded by an increase in Pdx1 expression [94]. It is of paramount importance to produce a glucose sensitive IPC in *in vitro* conditions so that the insulin secretion kinetics of these cells can be studied in detail before they are utilized for therapeutic transplantation.

In this study, a previously published protocol [73] was used to derive insulin-producing cells from mouse embryonic stem cells. This protocol involves formation of embryoid bodies (EBs), spontaneous differentiation of EBs into ectodermal, mesodermal and endodermal lineages and differentiation into C-peptide and insulin producing cells. The differentiation into multilineage progenitors, including endoderm progenitor cells, is supported by a basic culture medium, followed by differentiation induction into the pancreatic lineage by insulin, nicotinamide and laminin supplemented medium.

2.2 Materials and Methods

2.2.1 Mouse Embryonic Stem (mES) Cell Culture

MES cells (a generous gift from Dr. Qyang) were cultured on a layer of mouse embryonic fibroblasts (MEF) in high glucose DMEM supplemented with 15% knockout serum, 1% L-Glutamine, 1% sodium pyruvate, 1% non essential amino acids and 1%

penicillin-streptomycin, β- mercaptoethanol and Leukemia inhibitory factor (LIF). Colonies were passaged every 2-3 days onto freshly plated MEF cell layers. Medium was exchanged everyday.

2.2.2. Derivation of Insulin Producing Cells (IPCs) from mES Cells

MES cells were used to derive IPCs using a previously established protocol [73]. To induce differentiation into pancreatic beta cells, mES cells were differentiated by formation of embryoid bodies (EB). A cell suspension made with a total of 0.3 million cells in 10 ml of differentiation medium #1 (IMDM medium supplemented with 20% FBS, 1% L-Glutamine, 1% pencillin-streptomycin and 1-thioglycerol. Refer to Appendix A for details) was use for making hanging drops in P100 petri dishes (USA Scientific). A total of 8 rows of hanging drops were added in each dish to give 64 EBs/plate. After two days of hanging drop culture, the EBs from each dish were collected in a P60 Petri dish using differentiation medium #1 and cultured in suspension culture conditions for two days. The EBs were then transferred into a 0.1% gelatin coated P60 tissue culture treated dish. 4 mls of medium was added and the dishes were moved in the "8" pattern seven times for even distribution of EBs in the dish. The dishes were incubated and were not disturbed for at least 36 hours to facilitate proper attachment of the EBs to the surface of the dish. Medium was exchanged every 2-3 days.

After 9 days of culture, the cells on the dishes were digested and replated. To digest the cells, the medium was first aspirated, and the spread out cells were washed 2X with PBS. Then 0.5% trypsin and 0.25% trypsin were added in 1:3 ratio to the cells and incubated for 3 min at 37 °C. Trypsin was gently removed and the cells were detached using a cell scraper (USA Scientific). 4 mls of differentiation medium #2 (Refer to

Appendix A for details) supplemented with 10% FBS was added to each dish containing trypsinized cells. The cells were mixed well by pipetting and the resulting cell suspension contained single cells and cell aggregates. 428 µl of cell suspension was added to each well of a 6 well plate previously coated with 0.01% poly-ornithine & 1 µg/ml laminin. Additional 2 ml of medium was added and the plates were incubated for 18 days. The dishes were moved vertically and horizontally seven times to distribute the cells evenly throughout the wells. The medium was switched to serum free conditions the day after digestion. Medium was exchanged every 2-3 days. A schematic of the protocol is shown in Fig. 2.1.

2.2.3 Dithizone Staining

Dithizone (DTZ) is a zinc chelating agent and has been shown to selectively stain the insulin producing cells crimson [182]. DTZ stock solution was prepared by dissolving 50 mg of dithizone (Sigma) powder in 5mls of DMSO (Sigma). After vortexing, the mixture was aliquoted in 200 µl tubes and stored at -20 °C for long term use. For staining the cells, 10 µl of DMSO stock solution/ml of medium was used. The solution was filtered using a 0.2 µm syringe filter (Nalgene) and placed briefly at -20 °C for 30 seconds.

The cells were washed with Hanks balanced salt solution (HBSS) 2X prior to the addition of DTZ staining solution. Cells were then incubated with DTZ staining solution for 15 minutes at 37 °C. To image the cells, they were washed 3X with HBSS. The DTZ positive cell clusters that were stained with crimson color were detected and marked at the bottom of the plate.

2.2.4 Immunofluorescence Studies

Cells at Day 33 of differentiation were fixed with 4% p-formaldehyde (PFA) for 2 hours at room temperature, washed 3X with PBS and then were either stored at 4 °C till they were ready to be used for immunofluorescence or were used directly. Fixed cells were first blocked for 1 hour with 10% goat serum (Sigma) in PBS at room temperature. Then the primary antibodies were added and incubated overnight at 4 °C. Primary antibodies used were polyclonal rabbit anti FoxA2 (Abcam, 1:1000), polyclonal rabbit anti PDX1 (Abcam, 1:2000), polyclonal mouse anti insulin/Proinsulin (Abcam, 1:1000), polyclonal rabbit anti C-peptide (Abcam, 1:1000). After multiple washes with PBS, cells were incubated with secondary goat anti-rabbit IgG FITC (Abcam, 1:2000) or secondary goat anti-mouse IgG Texas Red (Santa Cruz, 1:200) for 1 hour at room temperature. Cells were mounted on a glass slide using a mounting medium with DAPI (Vectastain Lab) for imaging.

2.2.5 Immunohistochemistry Studies

Cells were fixed with 4% PFA for 2 hours at room temperature, washed 3X with PBS and then were either stored at 4 °C till they were ready to be used or were used directly. Samples were first boiled for 25 min in antigen retrieval buffer (0.01M citric acid, pH=4.4) at 95-100 °C loosely covered in foil. After allowing to cool at 20 min at room temperature, cells were blocked for 1 hour with 10% goat serum (Sigma) in PBS at room temperature. Polyclonal mouse anti insulin/Proinsulin (Abcam, 1:1000) was added and incubated overnight at 4 °C on a rocker. After multiple washes with PBS, cells were incubated with secondary goat anti-mouse IgG HRP (Santa Cruz, 1:200) for 30 min at room temperature. Cells were then treated with the Vectastain Elite ABC reagent kit

(Vector Labs) and Vector NovaRed substrate solution (Vector Labs) following the manufacturers instructions. Cells were washed with DI water for 5 minutes and then counterstained with Hematoxylin (Vector labs). The samples were allowed to dry overnight and then mounted using a Permount mounting medium (Fisher). Images were captured using a color camera mounted on an inverted microscope (Nikon C1Si).

2.2.6 Glucose Challenge Test

To perform a glucose challenge test, cells at the end of differentiation i.e., Day 33 were treated separately. Cells were washed 2X with sterile warm PBS and were switched to insulin free medium so that the insulin uptook from the medium does not contribute to the detected insulin levels when performing an ELISA. After 24 hours the medium was removed and the cells were washed 2X with warm PBS, and then incubated with Krebs Ringer Bicarbonate Hepes buffer (KRBH, See Appendix for details) supplemented with 2.5mM glucose for 90 minutes. The supernatant was collected and aliquoted in 200 µl tubes and stored at -20 °C. The cells were then incubated with KRBH buffer supplemented with 27.7 mM glucose for another 2 hours. The supernatant was again collected, aliquoted in 200 µl tubes and stored at -20 °C until ready to be analyzed.

2.2.7 Insulin ELISA

An ELISA was performed on the samples using the Mouse Insulin ELISA kit (Mercodia) as per the manufacturers instructions. The plate was read using an Emax plate reader (Molecular devices) at 450 nm. A standard curve was drawn using the absorbance values of the calibrators with known insulin concentration and an equation was derived, which was used to calculate the concentration of insulin in the samples. A high positive control

(Mercodia) was used to verify experimental values. All samples were prepared in duplicates.

2.2.8 IPC Yield Calculation

In order to calculate the yield of IPC clusters, DTZ staining was performed as described in Section 2.3. Once DTZ+ clusters were identified, they were manually isolated using a sterile fine bent tip forceps. Isolated IPC clusters were collected in a 1.5 ml micro centrifuge tube filled with FBS. Most IPC clusters were found to be closely associated with cell sheets, and these were carefully teased apart using another pair of fine tip forceps or scissors. After all the IPCs were collected, FBS was removed and the IPCs were washed with PBS 3X to remove traces of serum. IPC clusters were then incubated with 0.25% trypsin for 3 min and pipetted multiple times to facilitate the dissociation of the clusters into single cells. Cells were suspended in trypan blue solution and the cell counting was performed using a hemacytometer. The yield of IPC was calculated as the DTZ+ cells/total number of cells.

2.2.9 RNA Isolation

Frozen IPC cluster pellet were used for RNA isolation using the RNeasy mini kit (Qiagen). Once the pellets were thawed out, RLT buffer supplemented with 10% of 2-beta mercaptoethanol was added directly to the cell pellet and vortexed to mix well. The lysate was passed 8-10 times through a 20 G needle attached to RNase free syringe (Fisher) to homogenize the samples. The samples were centrifuged at 14,000 rpm for 3 min in a microcentrifuge (Eppendorf) and the supernatant was transferred to a new RNase free tube. One volume of 70% ethanol was added to the lysate and mixed well by pipetting. Up to 700 µl of the sample was added to the spin column placed in a 2 ml

collection tube and centrifuged at 10,000 rpm for 30 sec. The flow-through was discarded and 700 µl of RW1 buffer was added to the spin column and centrifuged at 10,000 rpm for 30 sec. The flow through was discarded once again and 500 µl of RPE buffer was added to the spin column and centrifuged at 10,000 rpm for 30 sec. The flow-through was discarded at the end and the procedure was repeated with centrifugation at 10,000 rpm for 2 min. The flow through and the collection tube were both discarded and the spin column was placed in a fresh collection tube. The empty spin column was centrifuged at 14,000 rpm for 1min to remove the final traces of impurities. The collection tube was discarded after this step and the spin column was placed in an RNase free 1.5 ml collection tube. 35 µl of RNase free water was added directly at the center of the spin column in one swift stroke. The membrane appeared to become completely wet by this addition of water. The cap of the tube was cut off and the spin column was centrifuged at 10,000 rpm for 1 min to elute the RNA. The isolated RNA was stored on ice for use within 2 hours or kept at -80 °C for long term storage.

2.2.10 RNA Quantification

RNA quantification was performed using a Nanodrop spectrophotometer (Nanodrop). First the instrument was blanked using RNase free water. 1 µl of the RNA sample was then placed on the measurement area and the $A_{260/280}$ ratio was recorded along with the concentration in ng/µl. $A_{260/280}$ is the ratio of absorbance of the RNA sample at 260 nm to 280 nm. $A_{260/280}$ value of 1.8-2 is acceptable quality of RNA. $A_{260/280}$ value of 2 is characteristic of pure RNA.

2.2.11 Primer Design

Primers were designed using the Oligoperfect^{TM} designer by Life technologies. The reference sequence of the species and gene of interest were obtained from RefSeq (NCBI reference sequence). All the primers were designed for detection only. The primers with Guanine – Cytosine (GC) content of approximately 50% and Tm close to 55 °C were selected. Once the primers were selected, the 5' sequence of the forward and reverse primer were added in the Oligoanalyzer software 3.1 (Intergrated DNA technologies). Self dimerization and hairpin formation were assessed at the temperature range of interest i.e., 50 °C- 60 °C. The primer sequences were then tested using the Primer blast software (NCBI) to check homology with other genes/species. Primers were purchased from Sigma Aldrich and were diluted to 20 μM concentration using RNase free water and stored at -80 °C before use.

2.2.12 RT PCR Studies

cDNA synthesis was done using a high capacity cDNA reverse transcription kit (Life Technologies). All the kit components were thawed over ice and the cDNA synthesis was done as per the manufacturers instructions. The reaction mixture contained purified RNA, 10X reverse transcription buffer, 25X 100 mM dNTP mix, 10X Reverse transcription random primers, multiscribe reverse transcriptase and nuclease free water. The reaction conditions were 25 °C for 10 min, 37 °C for 120 min, 85 °C for 5 min and a final hold at 4 °C. 400 ng of RNA was used per reaction and the cDNA synthesis was performed in a T100 thermal cycler (Biorad). The cDNA produced was either stored at 4 °C for short-term storage or at -20 °C for long-term storage. PCR was performed using iTaq DNA polymerase kit (BioRad). All the kit components were thawed over ice. The reaction

mixture included 10X iTaq buffer, 50mM $MgCl_2$, 10mM dNTP mix, iTaq DNA polymerase, forward and reverse primers, RNase free water and cDNA. About 10 ng cDNA was used per reaction. All samples were run in triplicates and included a no template control. The reaction was run in a T100 thermal cycler (Biorad) with the following conditions: (i) 95 °C for 3 min (ii) 40 repeats of 95 °C for 30 sec, 55 °C for 30 sec and 72 °C for 30 sec (iii) 72 °C for 10 min and (iv) 4 °C hold. All reagents were purchased from BioRad unless otherwise stated.

For RT-PCR, 10 ng of cDNA was added per well of a clear 96-well PCR plate (Life Technologies). A mastermix containing Sso Advanced SybrGreen supermix (BioRad), 20 μM forward primer, 20 μM reverse primer and RNase free water was added to each well. All samples were run in duplicates. Once all the reagents were added, the plate was covered with a clear adhesive film. The plate frame was tapped gently to mix the contents and then placed inside a plate spinner to remove the bubbles. The reaction was run in an Applied biosystems 7300 (Life technologies) with the following conditions: (i) 30 sec at 95 °C (ii) 40 repeats of 95 °C for 30 sec and 60 °C for 30 sec.

2.2.13 DNA Gel Electrophoresis

One percent agarose solution was made using PCR grade agarose dissolved in Tris acetate EDTA (TAE) buffer. The solution was heated in a microwave for 3 min to ensure that the agarose was completely dissolved. 10 μl of Ethidium bromide was added per 100 mls of the 1% agarose solution. At this point, the solution turned from clear white to clear pink. The solution was poured into a casting tray covering about 75% of the comb teeth height and then placed in the fridge for 10 min. Once the gel appeared firm to touch by hand, the casting tray was lifted and connected on to the electrophoresis setup. TAE

buffer was added to fill the gel run chamber and the combs were carefully removed. 8 µl of 1kB+ DNA ladder (Life Technologies) was added to the first lane of the gel. 2 µl of nucleic acid sample loading buffer (5X, BioRad) was added to 10 µl of PCR sample and loaded onto the wells. The electrophoresis was performed at 100 V till all the bands separated. When the lower dye front was about half way down, the run was paused and the gel was lifted manually, placed inside the UV tray of the Chemi doc XRS (BioRad) and imaged using the UV transiluminator. Image Lab software (BioRad) was used to capture and process the image. All reagents were purchased from BioRad unless otherwise stated.

2.2.14 Statistical Analysis

Results are presented as mean± standard deviation to account for sample size. A one-way paired student T-test was used for comparing statistical significance between two data sets and a one-way ANOVA test was used when more than two data sets were involved. Statistical significance was accepted for $p<0.05$.

2.3 Results

2.3.1 Differentiation of Insulin Producing Cells (IPCs) from mES Cells

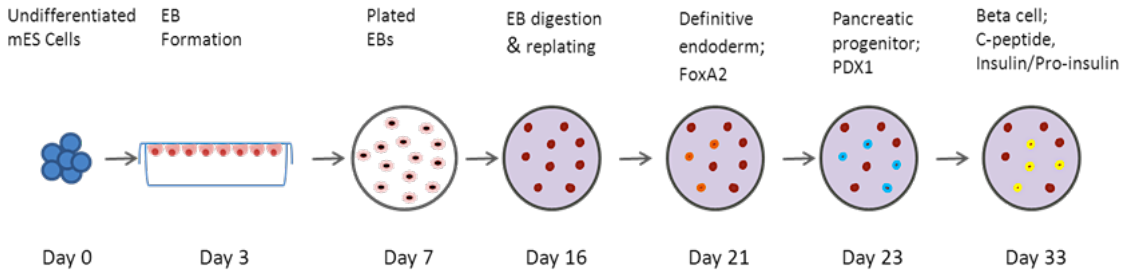

Figure 2.1 Schematic of the IPC Differentiation Protocol. Undifferentiated mES cells were formed into EBs using a hanging drop method. The resulting EBs were collected and plated on a gelatin coated dish on day 7. The spread out cells were digested and were re-plated on a poly-ornithine and laminin coated dish on day 16. The definitive endoderm marker, FoxA2 was detected on Day 21, while C-peptide and Insulin, pancreatic progenitor marker PDX1 and beta cell marker, respectively, were detected on Day 23 and 33 of differentiation.

MES cells were used to derive insulin producing cells by following a previously established protocol [73]. Figure 2.1 shows a schematic of the differentiation protocol used in this study. This differentiation protocol yielded IPC (insulin producing cells) clusters that have size range of 300-400 μm in diameter. The size of these clusters was much larger compared to native mouse islets which are 50-200 μm in size [2]. Other cell types including endothelial cells often accompanied the clusters.

During the entire differentiation period, cells were examined at various stages to check for specific markers. Figure 2.2 shows a western blot analysis confirming the expression of definitive endoderm (DE) markers such as FoxA2 and Sox17 as early as

Day 6, which corresponds to when the EBs were in suspension culture conditions. The expression of these markers continued till the end of differentiation i.e., Day 33. This is in agreement with previous studies that have shown that FoxA2 expression is found in developing pancreas and continues in adulthood, mainly in islets of Langerhans, ductal cells and acinar cells [183].

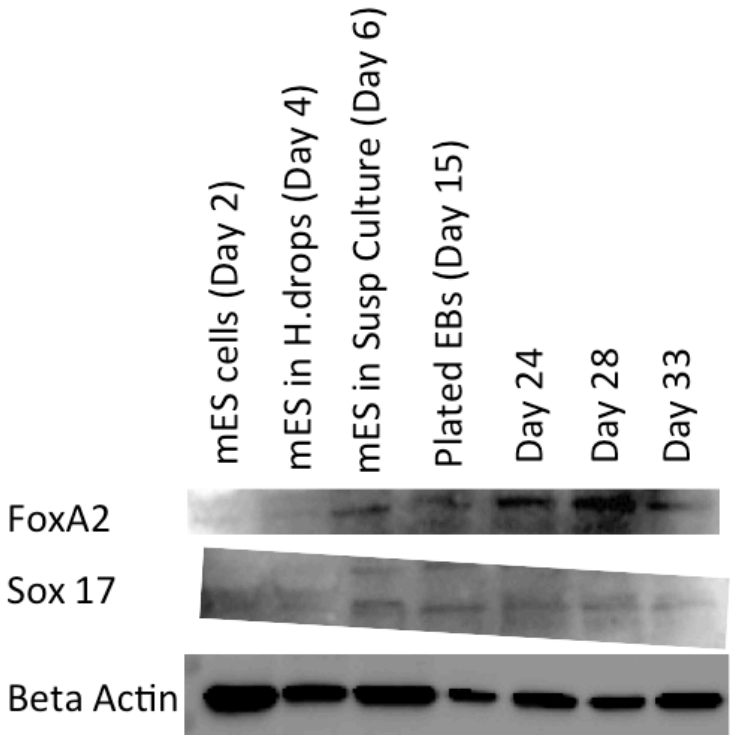

Figure 2.2 Expression of Definitive Endoderm by Differentiating MES Cells. EBs formed by a hanging drop method and subsequent the suspension culture showed expression of definitive endoderm markers such as FoxA2 and Sox17 as early as Day 6 of culture and continued expression till Day 33.

Immunofluorescence studies were performed to detect important markers along the beta cell development pathway. Figure. 2.3A shows the expression of FoxA2, which started as early as Day 6. The pancreatic progenitor marker, PDX1, was detected on Day 23 of differentiation as shown in Figure. 2.3B. At the end of the differentiation protocol i.e., Day 33, the presence of C-peptide was detected, as demonstrated in Figure. 2.3C. An immunohistological analysis showed that the cells were also positive for Insulin/Proinsulin expression at Day 33 as shown in Figure. 2.3D.

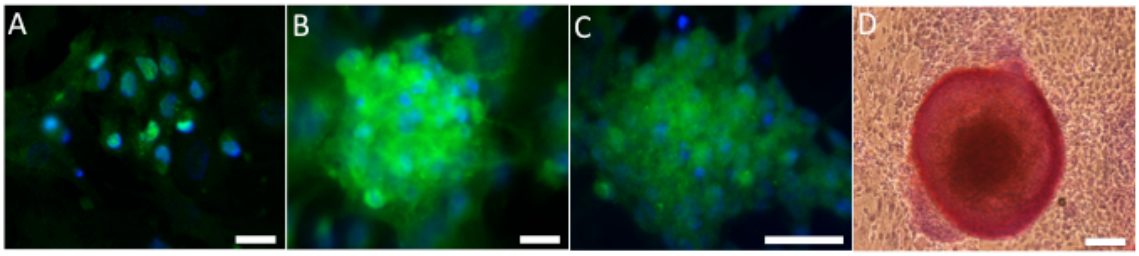

Figure 2.3 Expression of Pancreatic Specific Markers by IPC Clusters. Immunofluorescence images showing cells positive for (A) FoxA2 confirming endodermal lineage at D21, (B) Pdx1 confirming pancreatic progenitor cells at D23, and (C) C-peptide at D33 of differentiation. (D) A representative immunohistochemistry image at Day 33 shows the presence of insulin/pro-insulin. Scale bar: 100 μm.

2.3.2 Yield of IPC from mES Cell Differentiation

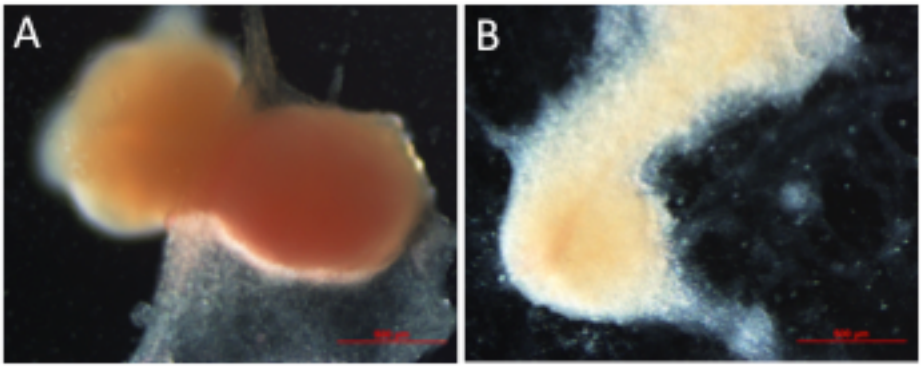

Figure 2.4 Dithizone (DTZ) Staining. A DTZ positive cluster at D33 of differentiation is shown on the left with crimson color cluster whereas an unstained negative cluster is shown on the right for comparison. Scale bar: 500 μm.

To determine the differentiation yield, differentiated cells were stained using a Dithizone (DTZ) staining method at Day 33 of differentiation [182]. Figure. 2.4(A) shows a DTZ+ IPC cluster stained crimson and an unstained cluster for comparison (Figure. 2.4B). Figure. 2.5 shows the yield of DTZ+ IPC clusters from individual batches. On average, six DTZ positive cell clusters were found in a 9.5 cm^2 surface area (area corresponding to one well of a 6-well plate) as shown in Figure. 2.6A. This corresponds to approximately 5.76% of the total number of cells present in the same size dishes (Figure. 2.6B).

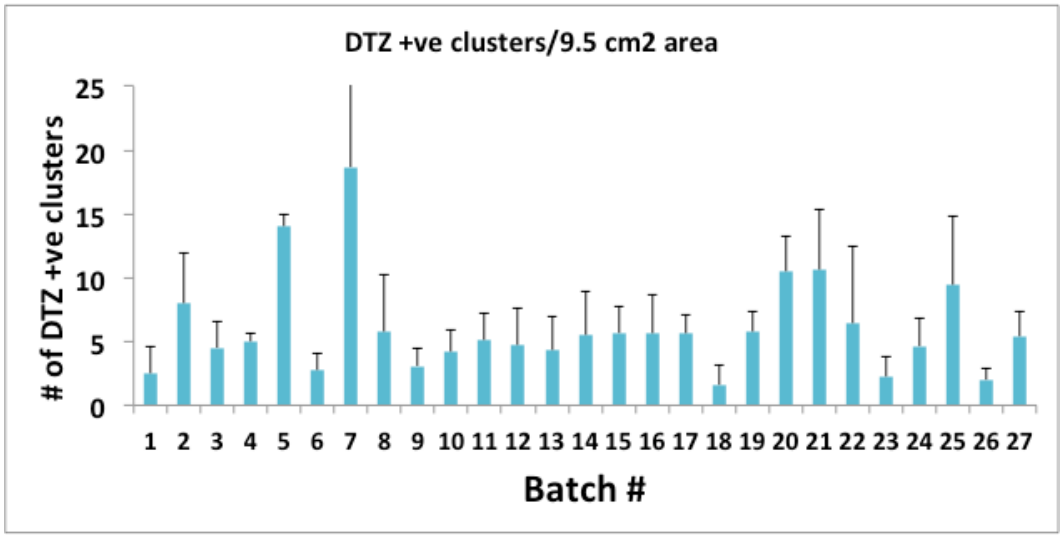

Figure 2.5 Yield of DTZ+ Cell Clusters. A graphical representation of the yield of individual batches is shown (n=27, Mean±SD).

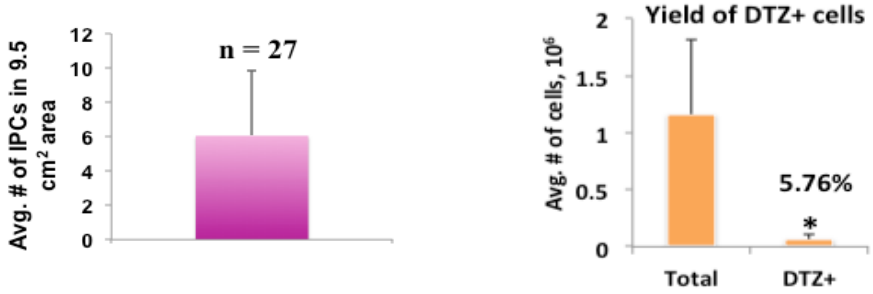

Figure 2.6 Differentiation Efficiency of IPC Clusters from mESCs. (A) The graph shows the average number of IPC clusters obtained from 9.5 cm^2 area, which corresponds to either a P35 dish or a well of a 6 well plate (n=27). (B) The graph compares the average number of IPCs obtained/9.5 cm^2 to the total number of cells present in the same size dishes (n=27, $p<0.05$).

2.3.3 Factors Effecting Differentiation Yield

During differentiation process, digestion of EBs yielded a mix of single cells and cell aggregates. The differentiation process requires these single cells and cell aggregates to be plated for additional 18 days until the completion of differentiation. To determine whether the presence of cell aggregates in the culture affects the overall differentiation efficiency, three different conditions were prepared. Differentiation cultures were prepared either with no aggregates, with no aggregates but with additional cells to maintain similar cell density or aggregates and single cells mix. Culture with a mix of single cells and cell aggregates was used as a control. Our results show that the yields were lower in the test samples and no significant differences were observed when compared to control samples as shown in Figure 2.7.

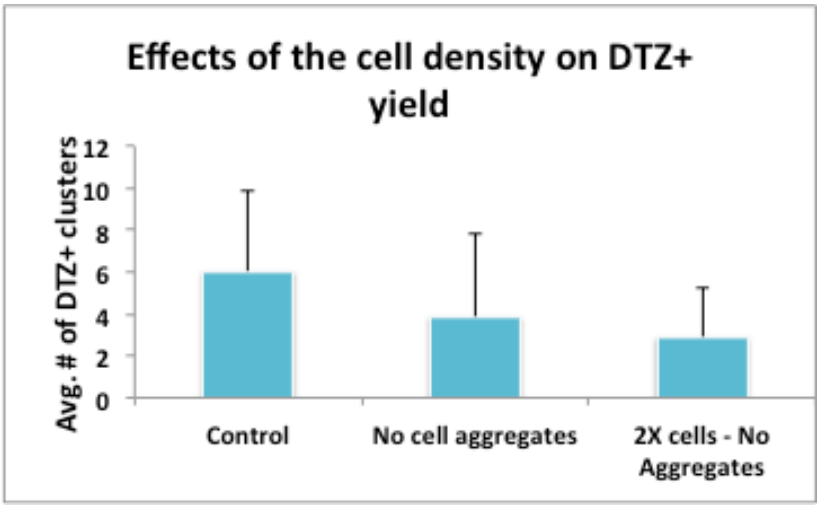

Figure 2.7 Factors Affecting Differentiation Efficiency – Presence of Cell Aggregates (n=10).

In addition, when the differentiation culture was extended for an additional 7 days beyond 33 days of culture, a significant increase in the number of DTZ+ cell clusters was observed indicating that the culture duration was a critical factor in determining IPC cluster yield (Fig. 2.8)

Figure 2.8 Factors Affecting Differentiation Efficiency – Culture Duration. A significant increase in the average number of IPC clusters was observed in longer culture (Mean ± SD, $p < 0.05$).

2.3.4 Glucose Responsiveness of Differentiated IPCs

An insulin ELISA was performed to quantify the amount of insulin produced by differentiated IPCs as well as to determine whether the IPCs were glucose responsive. Our ELISA results demonstrated that the IPC secrete significantly higher insulin when exposed to higher glucose concentrations, indicting that they are glucose responsive as shown in Fig. 2.9.

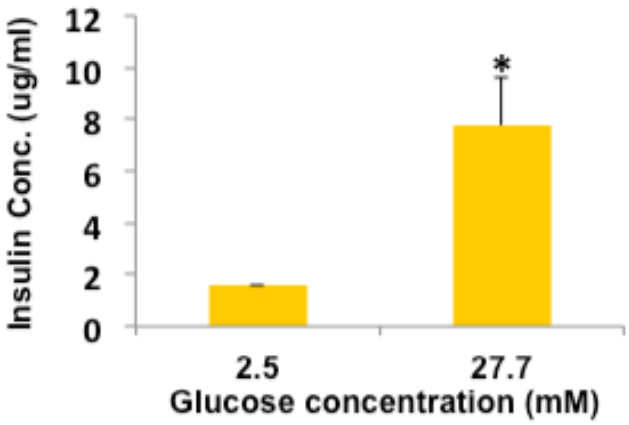

Figure 2.9 Insulin ELISA Assay. An insulin ELISA followed by a glucose challenge test demonstrated that mES derived IPCs are glucose responsive (n=6, $p<0.005$).

2.3.5 Pancreatic Gene Expression by Differentiated IPCs

Freshly isolated DTZ+ IPC clusters were used for RNA extraction and subsequent gene expression analysis. PCR revealed that the insulin-positive cell clusters express beta cell specific genetic markers such as Ins2, PDX1, Nkx6.1, Pax4, Glut2 and EphrinA5 as shown in Figure. 2.10. GAPDH was used as a housekeeping control. Beta cell specific markers are important genetic markers that are expressed by a mature beta cell.

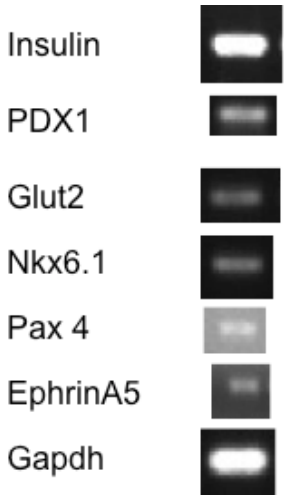

Figure 2.10 Gene Expression Analysis of IPC Clusters. IPCs expressed beta cell specific markers such as Insulin, PDX1, Glut2, Nkx6.1, Pax4 and EphrinA5. GAPDH was used as a housekeeping control.

2.4 Discussion

In this study, a previously established protocol was used to derive IPCs from mES cells [73]. At the end of a 33 days long protocol, IPC clusters, identified by DTZ staining, were successfully obtained. DTZ is known to form a chelate complex with the zinc ions stored inside the beta cells. DTA staining is widely used for detecting endogeneous insulin secretion by beta cells as the beta cells secrete zinc along with insulin [184, 185], The differentiated cells express both FoxA2 and Sox17 throughout the differentiation timeline. FoxA2 and Sox17 genes are widely known as definitive endoderm (DE) markers [186-190]. The pancreas develops from the DE, and so the expression of these markers suggests that the cells differentiate towards DE lineage, which is the first step in progressing them towards a beta cell fate. Previous studies have shown that FoxA2

expression is found in the developing pancreas and continues in adulthood, mainly in islets of Langerhans, ductal cells and acinar cells [183]. This is consistent with our study where the expression of FoxA2 at Day 33 of culture is detected by western analysis.

To further characterize the identity of IPCs derived from mES cells, gene expression analysis was performed. Our mES-derived IPCs expressed beta cell specific markers such as insulin and C-peptide demonstrating insulin production by these cells. Both of these genes have been shown to play an important role in the beta cell development. As beta cells are known to secrete insulin in response to a glucose stimulus, secretion of insulin is one of the key characteristics of beta cells. However, previous reports have shown that in *in vitro* cultures, dead cells can take up insulin from the medium and thus account for a false positive [77, 87]. C-peptide, which is formed when a proinsulin molecule cleaves to form an insulin molecule, has thus been used as a more reliable marker for insulin producing cells. C-peptide is not present in the medium and thus detection of C-peptide indicates endogenous insulin production by cells. Ins 2 or Pro-insulin is the uncleaved version of Insulin. The expression of Ins 2 and C-peptide confirms the endogenous production of insulin by mES-derived IPCs demonstrating that these cells were functional in terms of insulin production.

Moreover, differentiated cells express PDX1 and Nkx6.1, which are important for pancreatic development and beta cell function. PDX1 has been shown to serve as a master regulator of β cell fate by simultaneously activating genes essential for β cell identity and repressing those associated with α cell identity [191]. Low levels of PDX1 have been associated with beta cell death during onset of diabetes [192, 193]. Nkx6.1 gene is necessary and sufficient for expression of beta cell specific markers in

differentiating endocrine precursors in the embryo [194]. *In vitro* studies using beta cell lines and isolated islets have also suggested that Nkx6.1 may play a role in the regulation of glucose-stimulated insulin secretion as well as beta cell proliferation [195, 196]. Deletion of Nkx6.1 causes rapid-onset diabetes due to defects in insulin biosynthesis and secretion followed by ectopic activation of delta cell genes in beta cells [197]. Nkx6.1 gene is therefore important in maintaining the phenotype and genotype of beta cells.

Pax4 is known to be a key regulator of beta cell mass [198]. Inactivation of Pax4 results in the absence of mature β and δ cells in the pancreas but increases the number of alpha cells, suggesting that the early expression of Pax4 is essential for the differentiation of the β and δ cell lineages [199]. The expression of Pax4 by the culture indicates the development of endocrine progenitor cells in the differentiation culture. It also suggests the possibility of the presence of δ cells in the cell culture.

Moreover, it was demonstrated that our IPCs also express GLUT2 and EphrinA5. Glucose transporter 2 (GLUT2) also known as solute carrier family 2 (facilitated glucose transporter), member 2 (SLC2A2) is a transmembrane carrier protein, that enables glucose movement across cell membranes unclear [200]. GLUT2 is known to be the principal glucose transporter in beta cells in rodent islets, but is not the principal glucose transporter in human islets [201]. GLUT2 mediates the bidirectional transport of glucose in beta cells and forms part of the glucose sensing mechanism of the beta cell [200] and thus plays an important role in making beta cells glucose responsive. The differentiating cells also expressed GLUT2. EphrinA5 is a ligand for Eph receptor proteins and is localized on the plasma membrane and thus needs direct cell-to-cell contact for activation [202-204]. It is important in beta cell-to-cell communication and also in glucose

stimulated insulin secretion [205]. The expression of these genes indicates that the differentiated IPCs exhibit beta cell specific markers.

As one of the important characteristics of pancreatic beta cells is their ability to regulate insulin secretion depending on the level of glucose they are exposed to, functional characterization of differentiated IPCs was performed. Our differentiated IPCs secrete insulin and upregulated their insulin secretion in response to higher glucose conditions. The insulin secretion from 10 islets at 2 mM and 20 mM has been reported to be 1 ng/ml/hr and 2 ng/ml/hr, respectively [206]. This number can vary depending upon the age and sex of the animal and also the methods used for isolating the islets and duration of islet culture after isolation before the glucose challenge was performed. As the differentiating IPCs were significantly bigger in size than the islets, it is difficult to compare the results.

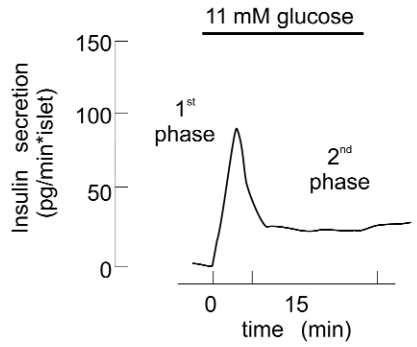

Fig. 2.11 Biphasic Insulin Secretion Response to Glucose Stimuli. Adopted from Rorsman *et al.*
Source: [4]

A normal mouse has an average blood glucose of around 80 mg/dl [207], which is similar to humans. When this level increases for example, due to diet intake, insulin is secreted. Glucose stimulated insulin secretion in mice and rat islets is biphasic in nature and consists of a transient first phase followed by a sustained second phase [208-211] as shown in Figure. 2.11. However, in *in vitro* conditions only the first phase of the response is seen [4].

While IPCs were obtained in this study, the differentiation efficiency however, was rather low, yielding approximately 5.76% of insulin-producing cells from the entire cell population. As differentiation of beta cells is a complex process, multiple factors can affect the efficiency. Our results from examining several factors affecting the yield of differentiation suggest that presence or absence of cell aggregates after digestion was not a critical factor in determining the differentiation yield. However, the cell density for re-plating was found to be a critical determinant for the IPC yield. Further studies will be needed to confirm whether a lower cell density can result in higher differentiation yield and vice versa. In addition, the effects of Exendin-4, a potent agonist of GLP-1 [212] and activin A can be explored as they are shown to promote islet differentiation, maturation and increased insulin content in various cell lines [213, 214].

It was observed that an increase in duration of culture period resulted in a significant increase in the differentiation yield. This suggests that the cells continue to differentiate beyond Day 33, which is the end point of current protocol used. Further studies are needed to determine whether a further increase of the culture duration will result in an even higher yield of IPCs and whether the glucose responsiveness of the IPCs is also affected.

The presented study followed a previously described protocol [73] with just one minor change. The suspension culture was done for two days instead of three days. It was noticed that at the end of three days, the EBs did not stay in suspension. Instead they attached to the petri dish and started spreading out. In order to transfer them to the gelatin coated dish they had to be lightly scraped off the surface of the Petri dish. As this might cause mechanical damage to the cells, the suspension culture was terminated after two days when the EBs were still in suspension. The exact effect of this change on the final outcome is yet unclear.

In conclusion, this study presents the differentiation and characterization of IPCs obtained from mES cells. Although the protocol has been previously reported [73], the study presents approaches to improve the yield of IPC clusters. It was found that an increase in culture duration for up to seven days resulted in a higher yield of IPCs, while excluding the cell aggregates and doubling the cell density after re-plating resulted in a decrease of yield. Further experiments are required to study the specific effects of cell density on the IPC differentiation yield.

CHAPTER 3

DEVELOPMENT OF IPC CLUSTER EMBEDDED 3D TISSUES

3.1 Introduction

Islets of Langerhans are micro-organs located in the pancreas and composed of at least four types of endocrine cells. The α and βcells are the most abundant and also the most important ones as they secrete the hormones glucagon and insulin, which are crucial for maintaining glucose homeostasis. It is generally accepted that endocrine cells in rodents are not randomly distributed into islets, but are arranged in specific patterns. β cells compose the core of the islets and the non-β cells, including α, δ and pancreatic polypeptide (PP) cells, form the mantle region [46-50]. This unique architecture appears to have important functional implications [46]. In several murine models in which insulin secretion is decreased, normal organization of islet cells was found to be perturbed [215] and β cells were found intermingled with non β cells.

In addition, *in vitro* experiments showed that homologous contacts between rat β cells improved their function, as compared to heterologous contacts between β and non β cells that had no effect [216]. This observation suggests that a core-mantle segregation of islet cells is useful in favoring homologous contacts between β cells, which in turn improves insulin secretion. The characteristic islet architecture may also serve to facilitate interactions among the different islet hormones via interstitial or vascular routes [47, 217]. It has also been shown that the proportion of islet β cells is lower in humans compared with rodents [51-53] and that the various endocrine cell types are dispersed

throughout the human islets [51, 54]. Figure 3.1 shows a schematic representation of rat and human islets.

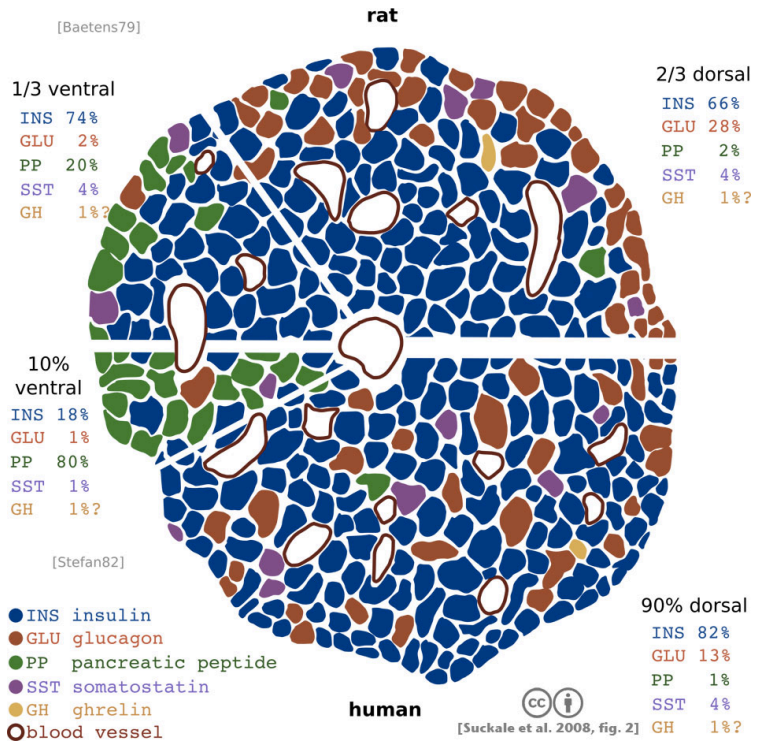

Figure 3.1 Islet Architecture in Rodents and Humans. The above schematic shows the distribution of various cell types in rodents and human islets.
Source: [8].

Currently, 2D cultures are the most common method of culturing islets *in vitro*. However, 2D culture systems do not provide the much needed ECM support that is available to islets *in vivo* which is important in mediating cell adhesion, providing structural support and activating intracellular chemical signaling pathways [118, 218-220]. It has been shown that culturing islets as monolayers in a 2D culture system

disrupts their characteristic arrangement and hence negatively impacts function and survival of the cells [221]. In the absence of this crucial microenvironment, cells either do not mimic their physiological phenotype or many times differentiated cells fail to maintain their functions over longer periods of time. A study by London *et al.* showed that only ~56% of the islets survive after a 48 hour culture period in 2D conditions [222]. These studies suggest that 3D culture models that closely mimic physiological environment may be necessary to promote optimum survival and function of the islets in *in vitro* culture conditions.

In fact, previous studies have demonstrated that the use of biomaterials may enhance islet function by providing a three-dimensional cellular support and delivering proteins, growth factors, and immunosuppressive agents [223, 224]. A study by Montesano *et al.* showed that when dissociated islets were embedded inside 3D collagen gels, not only did the collagen environment provide the necessary permissive environment for the heterozygous cells to reform the islet like spherical morphology, but also the different cells re-assembled mimicking their topographical location [225, 226]. Another study by Zhang *et al.,* demonstrated that culturing human islets in 3D scaffolds reduced the formation of the toxic islet amyloid, which is known to be a pathological characteristics of diabetes type II [227].

Moreover, a previous study showed improvement in viability and insulin secretion profile of human islets cultured in 3D agarose gels compared to that of islets cultured in 2D condition [129]. Various other studies using collagen and other ECM materials to encapsulate islet cells have shown improved functionality, insulin secretion, and higher expression of pancreatic specific genes of beta cells [130, 221, 228]. Nagata *et*

al. cultured islets in a hydrogel of collagen type I mixed with collagen type III, type IV and laminin. They found that all the mixtures suppressed cell death effectively [116]. These studies suggest that a 3D system comprised of ECM proteins may be beneficial in improving the maturation and function of insulin producing cells in *in vitro*.

There have been a number of studies that have highlighted the role of vascular endothelial cells (ECs) in beta cell biology. During development, dorsal aorta has been shown to induce budding of dorsal pancreas and expression of pancreatic specific factors such as Pdx1, Pax4, Insulin and glucagon [145]. EC secreted factors have also been shown to be important for beta cell proliferation, insulin gene transcription and glucose mediated insulin release [1, 154, 156, 229, 230].

Previous studies have shown that EC derived factors are not only critical in the regulation of beta cell growth, proliferation but also expression of beta cell specific markers and lineage allocation during development [1, 145, 154, 156, 167, 231]. As beta cells are unable to form a basement membrane of their own they recruit ECs to form a basement membrane that contains laminin, collagen type IV and fibronectin [154]. These factors are known to promote insulin gene expression and beta cell proliferation to different extents. A host of other EC derived factors have been shown to be beneficial for the development of beta cells. Connective tissue growth factor (CTGF), an EC secreted factor is important in beta cell proliferation, differentiation and islet morphogenesis [156, 231]. Another vascular derived factor sphingosine-1-phosphate has been shown to stimulate the growth of the pancreas [148]. Hepatocyte growth factor, secreted by ECs has been shown to support beta cell proliferation. Thus, signals mediated by the ECs are critical regulators of the beta cell development and function [163].

Previous studies have shown evidence that isolated islets in co-culture with ECs show better survival, integration and functionality [159, 161-164]. A study by Adame *et al.* showed that co-culture of mES derived EBs with ECs led to an increased expression of PDX1, Ngn3, Nkx6.1, Proinsulin, GLUT-2 and Pax4 [167]. This study provided evidence that ECs enhanced the differentiation of EBs into pancreatic progenitor cells. However, no studies have been published regarding the effects of IECs on IPC development in *in vitro* conditions. As IECs form a vascular niche for the pancreatic development [154, 165], their presence might have a positive impact on the IPC differentiation efficiencies and in obtaining mature glucose sensing beta cells.

Recently, a study by Lau *et al.* showed that highly perfused islets had superior beta cell proliferation, function and gene expression [163]. It has been shown previously that blood flow in islets is heterogenous [232], with some islets receiving more blood flow than others and this heterogeneity is maintained over time [233]. Interestingly, EphrinA5 was significantly up regulated in highly perfused islets compared to islets having lesser flow [163]. Ephrin A5, a ligand present on beta cells has been shown to mediate glucose stimulated insulin secretion [205].

Ephrins are the ligands of Eph receptors, the largest family of tyrosine receptor kinases [234] and have been shown to play an important role in cell cell signaling [205, 235]. Beta cells are known to communicate with each other through EphAs and EphrinAs [205], where EphA forward signaling inhibits insulin secretion, whereas Ephrin-A reverse signaling stimulates insulin secretion [205]. Although it was believed that EphrinA class ligands only react with EphA receptors, a study by Himanen *et al*., showed that Ephrin A5 binds EphB2 with great affinity [236]. EphB2 is a protein that is

expressed by endothelial cells and is important during angiogenesis [237]. As ECs play an important role in beta cell development, it will be interesting to examine such an interaction occur in *in vitro* conditions, if ECs are co-cultured with IPCs.

Thus, in the presented study, mES derived IPCs were cultured in 3D collagen gel system to characterize their function in 3D compared to a traditional 2D culture. Optimization studies were performed to improve survival and function of the IPCs. In order to address the diffusion limitations that 3D tissues present, perfusion flow was applied to the 3D tissues using a previously developed perfusion flow bioreactor [238]. The study also describes the co-culture of IPCs with ECs, which were derived from mES cells (mESC-ECs). The details of the derivation and characterization of these cells are presented in chapter 4. The co-culture gels were cultured under static and flow conditions for five days and were analyzed for survivability. A detailed gene expression analysis was performed on the monoculture and co-culture gels and the expression of beta cell specific genes were studied. The presented study reports preliminary studies in deriving a 3D tissue using stem cell derived IPCs, which can be extended further to the development of a unique platform for improved function and maturation of IPCs *in vitro.*

3.2 Materials and Methods

3.2.1 Preparation of IPC Clusters for 3D Tissues

IPC clusters were differentiated from mES cells and isolated as described in Chapter 2 section 2.2. Figure 3.2 shows a simple schematic of the gel preparation process. After being stained positive with DTZ, IPC clusters were manually handpicked using a fine bent tip forceps from the differentiation plate. The IPC clusters were briefly stored in

FBS in a microcentrifuge tube and then washed 3x with PBS. The typical size of differentiated IPC clusters was 380 um, which is much larger than a mouse islet which is approximately 150 um [2]. Thus to obtain IPC clusters with sizes that are comparable to physiologic mouse islets, IPC clusters were manually pipetted to dissociate them into smaller clusters. To break the clusters into smaller pieces, a 22G needle attached to a 3 ml plastic syringe (Fisher) was used. Repeated pipetting was necessary to achieve smaller IPC clusters. Alternatively, the clusters can be broken down by a blunt plastic canula (Fisher) mounted on top of a 200ul pipette tip attached to a pipetteman.

Once pipetted, the IPCs in culture medium were strained using a 40μm cell strainer (BD Falcon) to remove cell fragments and debris from the manual disturbance. Only the IPC clusters were collected in a petri dish and then transferred into a microcentrifuge tube. Clusters were then allowed to settle down in a conical tube for ten minutes. Supernatant was slowly removed without disturbing the IPCs and discarded. Collected IPCs were used for incorporation into collagen gels as described in detail in Section 3.2.2.

3.2.2 Preparation of Static Collagen Tissues Containing IPC Clusters

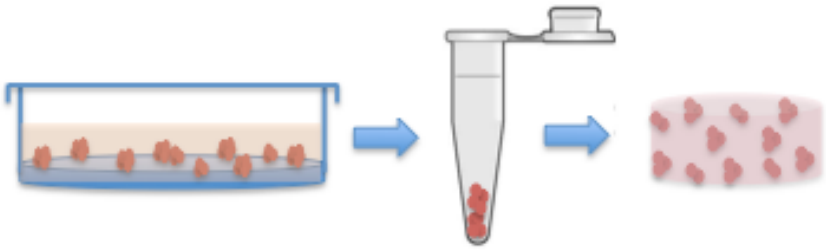

Figure 3.2 Schematic of the Gel Preparation Process. IPCs were harvested from differentiation culture (Day 33) in a microcentrifuge tube containing FBS using a sterile fine bent tip forceps. After 3X PBS wash, the IPC clusters were broken down manually by passing 5-10 times through a plastic canula. The IPC suspension was then passed through a 40 µm cell strainer to remove dead cells and debris before being suspended inside 3D collagen gels.

Rat tail collagen type I (BD Biosciences), 10X DMEM (Sigma Aldrich) and 10X reconstitution buffer (0.05 N NaOH with 0.16 M HEPES and 0.25 M $NaHCO_3$) were mixed on ice in the ratio of 80:10:10 to form collagen solution. The final concentration of collagen was 3 mg/ml. The pH was adjusted to 7.2-7.4 by adding 1N NaOH until the mixture appeared salmon pink in color. 24 IPC clusters were suspended in 55 µl of the collagen solution prepared above and added to the wells of a 96 well plate. This process is demonstrated schematically in Figure 3.2. The collagen gel solution was incubated for 30 minutes at 37 °C to allow polymerization. Once polymerized, differentiation medium was added to collagen gel with IPC clusters and culture medium was changed every other day.

3.2.3 Preparation of Flow Collagen tissues Containing IPC Clusters

A custom made bioreactor set up was used for the application of flow to the collagen tissues containing IPC clusters [238]. A flow bioreactor is capable of applying constant perfusion to the tissues/cells housed within. The purpose of using the flow bioreactor was to provide flow or shear mediated cues that cells receive physiologically. The effect of flow on the tissues was studied by comparing flow collagen tissues to statically cultured tissues.

The collagen IPC mix was pipetted onto a polyethylene terephthalate (PET) membrane glued onto a PDMS ring placed on the inside edge of the bottom piece of the flow bioreactor. This porous membrane supported the gel during the experiment. To reduce the resistance to flow created by the membrane, 15-20 holes were punched into it using a 30-gauge needle as has been previously described. After the gel was added to the membrane, the bioreactor was placed inside a 50 ml conical tube and allowed to polymerize for 2 hours at 37 °C. After 2 hours, the bioreactor was brought back to the laminar flow hood where it was fully assembled. The top piece was fastened and 3-way stopcock valves (Smith Medicals) were attached on either side of the bioreactor using connectors (Cole Parmer). Poly tetra fluoro ethylene (PTFE) tape was wrapped around the threads of the connectors to make the assembly leak proof. LS'13 tubing was used to connect the bioreactor assembly with a medium reservoir. Syringe ports (Baxter) were attached on stopcock valves and used for filling the inlet and the outlet tubing with medium. The bioreactor was connected to a peristaltic pump (Cole Parmer) and the flow was started at 0.5ml/min and continued for up to 5 days.

3.2.4 Creating 3D co-culture tissues

3D collagen gels were created by a sandwich method, which contains two layers of cells prepared in between three layers of collagen. A schematic of the process is shown in Figure. 3.3. To form 3D collagen gels, collagen solution was prepared as described in Section 3.2.4 and was first poured into tissue culture plates and incubated at 37°C for 30 minutes to allow polymerization before mESC-ECs suspended in MCDB complete medium were added on top. These mESC-ECs were allowed to spread out for 4 hours. In the meantime DTZ staining was performed on end stage beta cell differentiation plate i.e., Day 33 of differentiation as described in Chapter 2 Section 2.3.

The IPC clusters thus identified by DTZ staining were used for making an IPC embedded gel. This gel was added on top of the first layer of mESC-ECs after medium removal. The gel was allowed to polymerize for 30 minutes and then another layer of mESC-ECs was added on top and allowed to spread out. After 4 hours, medium was carefully removed and a final layer of cold collagen gel solution was poured on top of the cell layer. This process yielded a collagen gel with one layer of IPC cluster embedded gel sandwiched between two layers of mESC-ECs. The gel was cultured for 3-5 days and medium was changed every other day.

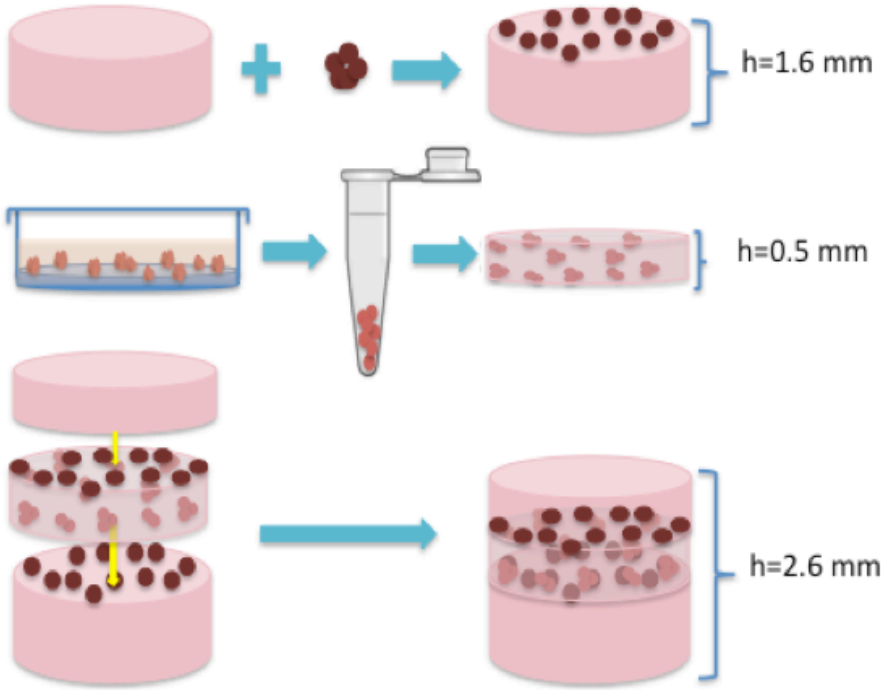

Figure 3.3 Schematic for Co-culture Gel Preparation. First a layer of mESC-ECs was added on a layer of collagen, allowed to spread for 4 hours and then DTZ+ IPC clusters were suspended inside a 0.5mm thick collagen layer that was cast directly on top. After 30 minutes medium, a layer of mESC-ECs was added, allowed to spread out for 4 hours before a final layer of collagen gel was added on top. The gel was cultured for 3-5 days under static and flow conditions.

3.2.5 Live Dead Staining

Live/Dead viability/cytotoxicity assay (Invitrogen) was used to determine the viability of IPC cells in 3D collagen monoculture and co-culture tissues. After five days in culture, collagen tissues subjected to flow were transferred from the flow bioreactor into a 96 well plate using sterile fine tip forceps. Static collagen tissues were processed directly in the 96 well plates where they were being cultured. Calcein AM (2 μM) and Ethidium homodimer-1 (4 μM) were added to stain live and dead cells, respectively. Stock

solutions were diluted as per the manufacturer's instructions using sterile PBS. Tissues were incubated at 37 °C for 30 minutes while being protected from light. Samples were imaged on a glass coverslip without washing off the staining solution using an inverted fluorescence microscope (IX81 DSU, Olympus).

3.2.6 Immunofluorescence Studies

After five days in culture, both static and flow collagen tissues were fixed with 4% PFA overnight at room temperature. In case of flow collagen tissues, they were removed from the bioreactor and placed in a petri dish prior to fixation. Gels were then washed 3X with PBS and blocked for 4 hours with 10% goat serum (Sigma) in PBS at room temperature. Primary antibodies mouse anti Insulin/Proinsulin (Abcam, 1:1000) and rabbit anti glucagon (Santa Cruz, 1:200) were added to the samples and incubated overnight at 4 °C on a rocker. Samples were then washed 3X with PBS on a rocker and goat anti-mouse pAb-Rhodamine (1:2000, Abcam) and goat anti-rabbit pAb-Texas Red (Santa Cruz, 1:200) were added and incubated for 1 hr. at room temperature. Samples were washed again with 3X PBS and counterstained with DAPI to visualize the nuclei. Samples were imaged using a confocal fluorescent microscope (C1si, Nikon). Images were analyzed using the EZC 1 software.

3.2.7 Glucose Challenge

After five days in culture, both monoculture and co-culture collagen tissues under static and flow culture conditions were collected and washed 3x with PBS. Differentiation medium prepared separately without insulin was added to the gels 24 hr. prior to the glucose challenge. For the gels cultured under flow, they were transferred from the bioreactors into petri dishes containing differentiation medium without insulin. After 24

hours, samples were washed with PBS, and were incubated with solutions containing two different concentrations of glucose consecutively. First, the tissues were incubated with 2.5mM glucose supplemented Krebs Ringer Bicarbonate Hepes (KRBH, See Appendix for details) for 90 minutes. The supernatant was collected prior to the incubation with higher concentration of glucose. KRBH buffer supplemented with 27.7 mM glucose was added and the samples were incubated for additional 2 hours. Supernatants were again collected at the end of the incubations, aliquoted in 200 µl tubes and stored at -20 °C for performing an insulin ELISA.

3.2.8 Real time PCR studies

After five days in culture, both monoculture and co-culture collagen tissues under static and flow culture conditions were frozen down for RNA isolation. RNA isolation and cDNA synthesis were performed as described previously in Chapter 2, section 2.2.9 and RT PCR studies were performed as described in Chapter 2, Section 2.12.

3.2.9 Real Time PCR Data Analysis

Real time PCR data was exported from the SDS software (Life technologies) to an Excel sheet (Microsoft Office 2011 for Mac). The C_T values were averaged for all the samples and were normalized to GAPDH. The C_T (cycle threshold) is defined as the number of cycles required for the fluorescent signal to cross the threshold (i.e., exceed background level) so that it can be detected [239]. Relative gene expression analysis was performed using the Livak method or the $\Delta\Delta C_T$ method [9]. The Livak method includes three steps: (i) Normalizing the C_T of the target gene to the reference gene (GAPDH) (ii) Normalizing the ΔC_T of the test sample to the ΔC_T of the calibrator sample and (iii) calculating the expression ratio or the fold change.

3.2.10 Statistical Analysis

Results are presented as mean± standard deviation. A one-way paired student T-test was used to determine the statistical significance between two data sets and a one way ANOVA test was performed to analyze the interaction between the culture conditions. Statistical significance was accepted for $p<0.05$.

3.3 Results

3.3.1 IPC Survival in 3D Collagen Tissues

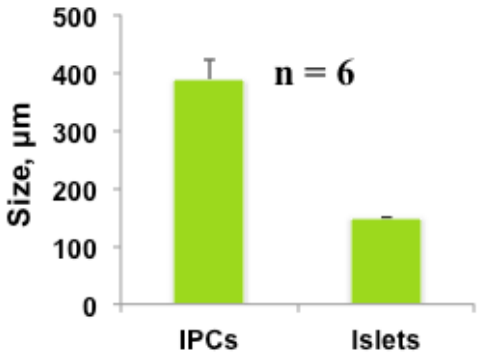

Figure 3.4 Size Comparison of IPC Clusters vs. Native Mouse Islets. The average size of differentiated IPC clusters was approximately 380 µm in diameter (n=6), whereas the native islets are in a size range 50-250 µm [2].

IPCs were obtained by manual isolation from differentiation plates at Day 33, using a pair of sterile bent tip forceps. It is shown that our differentiated IPC clusters were much bigger than the size of isolated native mouse islets (Figure. 3.4). Immediately following the isolation, IPC clusters were plated on 2D surface to first check their viability. Figure.

3.5A shows an IPC cluster plated on a poly-ornithine and laminin coated 2D surface immediately after isolation without any processing. Live dead staining revealed that these clusters consisted of a mixture of living and dead cells.

As the clusters were irregularly sized and had a complex structure, additional steps were performed to break these clusters down into smaller pieces to derive physiologically relevant sized clusters and to minimize diffusion limitation, The IPC clusters were subjected to manual breaking by using either a 22G needle with sharp end or a blunt plastic cannula attached to a syringe. When these processed clusters were embedded in 3D collagen tissues, a large number of dead cells were observed (Figure. 3.5B). While 22G needle method was successful in creating smaller clusters, this method simultaneously resulted in massive cell death. As a comparison, the clusters that were directly embedded in collagen tissues without physical breaking process had fewer dead cells (Figure. 3.5C), although the size was considerably bigger than the ones in Figure. 3.5B.

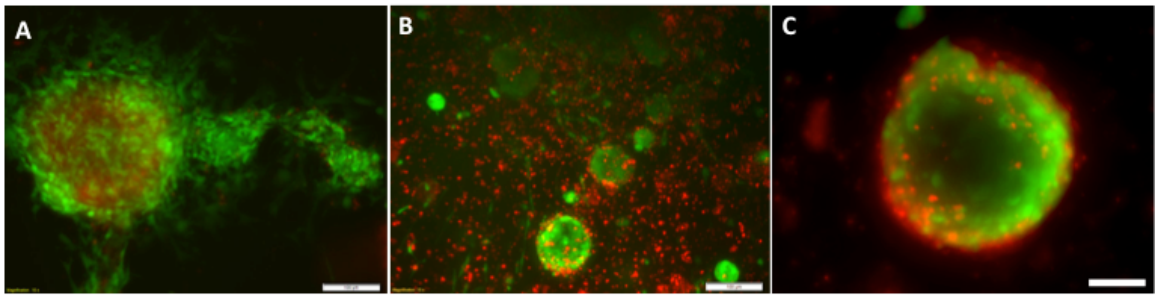

Figure 3.5 Live Dead Staining of IPC Clusters. (A) Live dead staining at Day 1 shows IPC cluster plated on poly-ornithine and laminin coated 2D surface (B) IPC clusters were broken down by passing through a 22G needle and then used for preparing 3D collagen tissues. (C) 3D collagen tissue with control IPC cluster that was not broken prior to embedding. Calcein stains the living cells green and Ethidium bromide stains the dead cells in red. Scale bar: 100 μm.

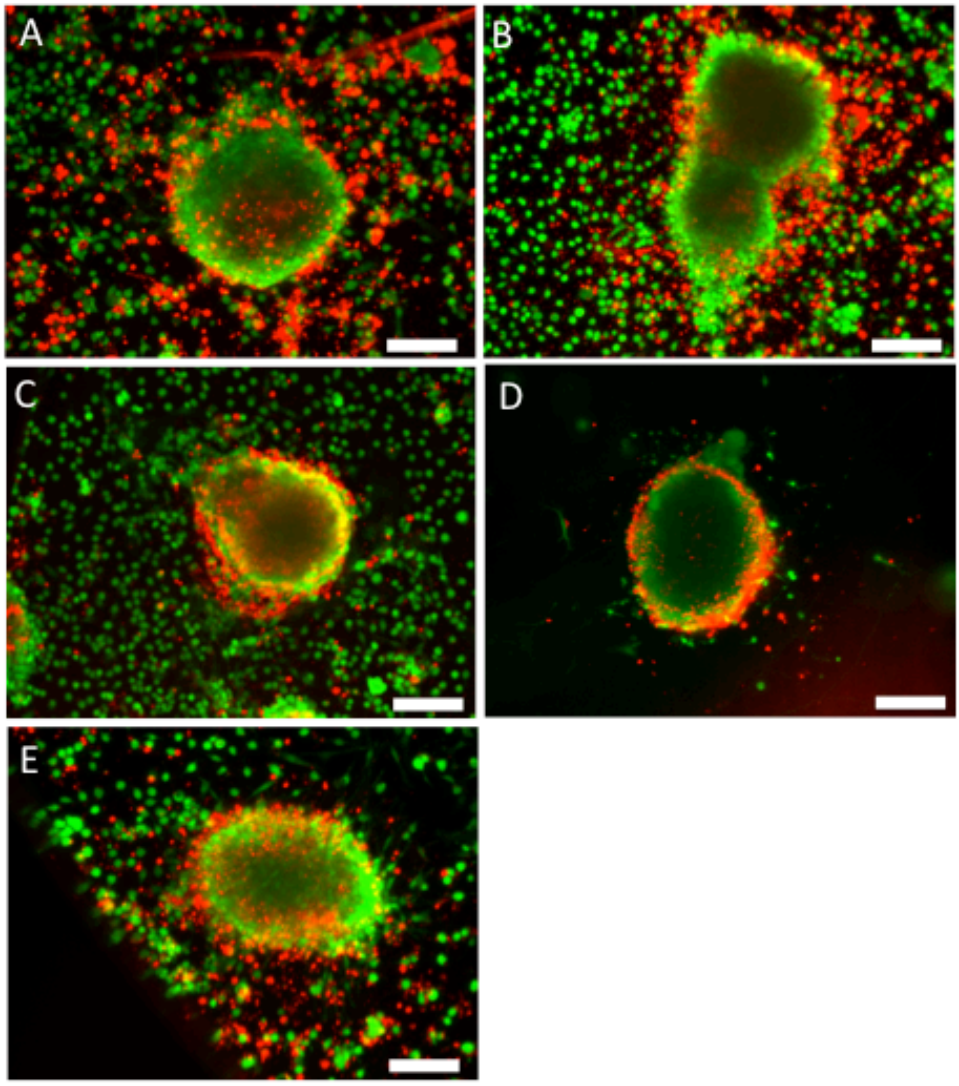

Figure 3.6 Comparison of Various Methods for Removing Dead Cells/debris from IPC Clusters. Live dead staining images show the IPC clusters subjected to preplating for (A) 15 min, (B) 30 min, (C) 60 min still consisted of dead cells. (D) The IPC clusters passed through a cell strainer had the least number of dead cells when compared to all the other methods (E) shows the control, non treated IPC cluster on a 2D surface. Calcein (green) stains the living cells and Ethidium bromide (red) stains the dead cells. Scale bar: 100 μm.

Alternatively, a small blunt plastic canula attached to a pipette tip was used to break the clusters, in order to minimize the damage to the cells. Although this method resulted in a reduced number of dead cells, it did not fully eliminate the presence of dead cells. Since the presence of dead cells can affect other cells in the 3D tissue, additional steps were taken to remove them.

Pre-plating of the cell/clusters was performed to determine whether it can be used to separate dead cells/debris from the IPCs. Once the clusters were manually broken down, the cell/cluster suspension was subjected to 15, 30 or 60 min pre-plating on gelatin coated surface. Our hypothesis was that the dead cells and other debris will not attach to the gelatin coated surface and will remain suspended in medium, while IPCs and single living cells will attach to the surface thus separating the living and dead cell populations. However, as demonstrated in Figure. 3.6, pre-plating for 15-60 min was ineffective in fully separating the living cells from the dead cell populations. As most of the IPCs did not attach even after 60 minutes, the separation was unsuccessful.

The other method was to use a cell strainer. A 40μm cell strainer was used to collect IPC clusters with sizes 40um and bigger on the membrane while removing the unwanted debris and dead cells. The retentate constituted of IPC clusters and was subsequently used for preparing 3D collagen tissues. It was observed that the cell strainer treatment resulted in the least number of dead cells carried over in the culture as shown in Figure. 3.6D.

3.3.2. IPC Cluster Density in a 3D Collagen Tissue

The optimal density of IPC clusters in 3D collagen tissues was determined based on the size of the clusters and cross-sectional area of the tissue. By assuming the diameter of an IPC cluster to be approximately 500μm, the surface area of an average IPC cluster was calculated to be 0.196 mm^2. Thus, for a well within a 96 well plate with the surface area of 32 mm^2, 163 IPC clusters were needed to cover the entire surface of the gel with IPC clusters. Based on the limited yield of the IPC clusters from each batch of differentiation, densities of 10% and 15% were used in our experiments. Thus, for a well of a 96 well plate, 16 and 25 clusters for used for a 10% density gel and 15% density gel, respectively. Figure 3.7 shows an example of 3D collagen gels with 10% and 15% density of IPCs. 15% density gels had a higher number of IPCs embedded compared to the 10% density gels.

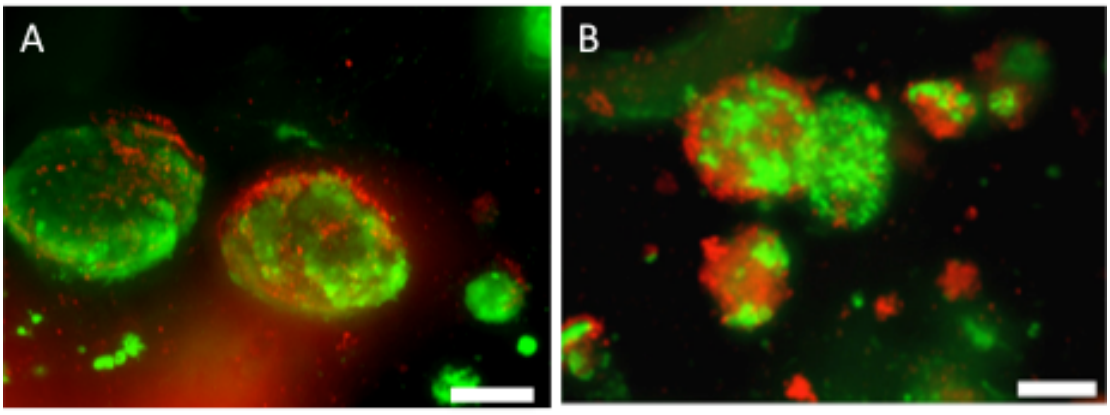

Figure 3.7 IPC Density in 3D Collagen Gel. (A) A collagen tissue with 10% IPC clusters and (B) with 15% IPC clusters. Live cells are shown in green, whereas dead cells are in red. Scale bar: 100μm.

3.3.3 Survival of IPC Clusters in 3D Tissues Under Static and Flow Culture Conditions

Since it is known that tissues with thickness more than 2 mm have diffusion limitations, [240], our 3D collagen tissues were subjected to flow to improve viability of the cells through enhanced perfusion and nutrient diffusion. The bioreactor system had a top and bottom piece that when screwed together formed the housing for the collagen gel.

The bioreactor was connected with a medium reservoir via silicone tubings as depicted in the schematic in Figure 3.8. A peristaltic pump was used for the constant perfusion of medium through the collagen tissues at 0.5 ml/min flowrate. The viability of IPC clusters in IPCs gels cultured under static and flow conditions were compared after 5 days of culture. Live dead staining on these collagen tissues showed that the cell viability was reduced in tissues cultured under flow conditions compared to the ones under static conditions (Figure 3.9).

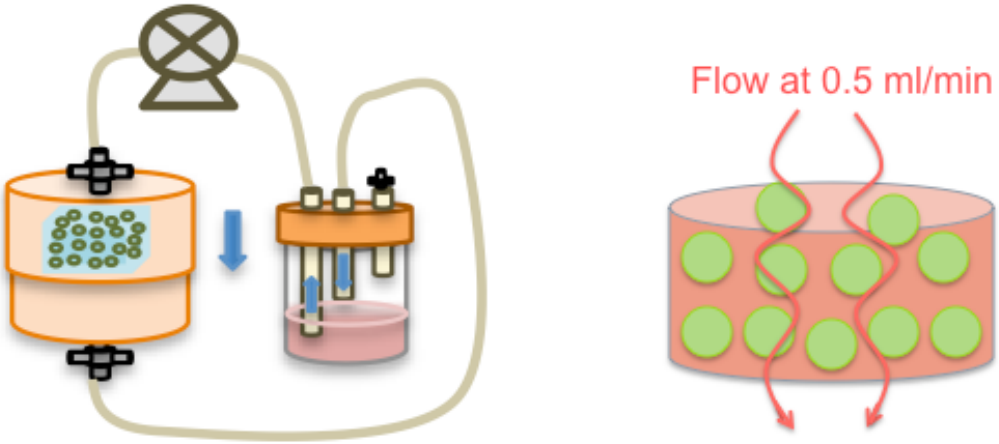

Figure 3.8 Schematic of Flow Bioreactor System. The schematic shows a bioreactor connected to the medium reservoir through tubings and a peristaltic pump. Flow rate of 0.5 ml/min for 5 days was used in our study.

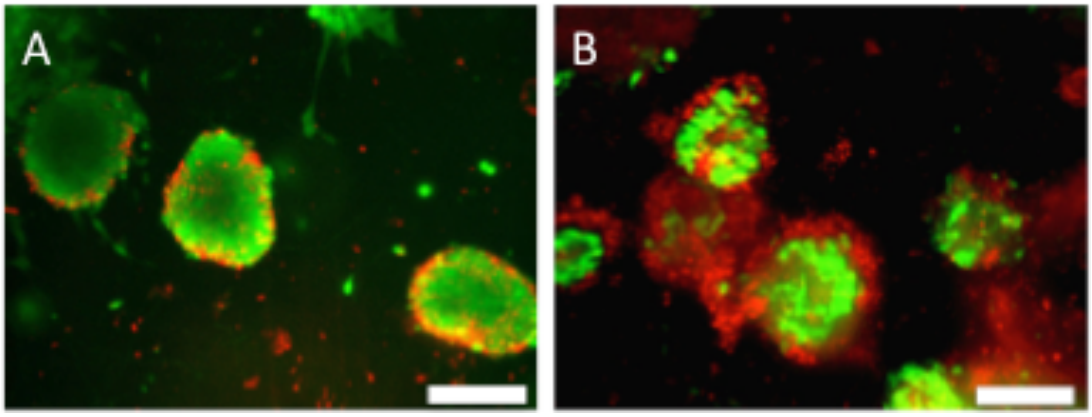

Figure 3.9 Live dead Staining of IPC Embedded Collagen Tissues Under Static and Flow Conditions. At day 5 the (A) statically cultured collagen tissue had fewer dead cells compared to the (B) tissue cultured under flow conditions. Calcein (green) stained the living cells and Ethidium bromide (red) stained the dead cells (n=6). Scale bar: 100 μm.

3.3.4 Survivability of Whole and Dissociated IPC Cluster Gels

In order to examine whether dissociation helps to reduce cell death in our 3D flow system, IPC clusters were dissociated using trypsin and their survival examined in 3D collagen tissue culture. Live dead staining after 5 days revealed the dissociated IPC gels had an improved survivability compared to whole IPC gels both in static and flow conditions (Figure 3.10). While comparing within the dissociated IPC gels, it was found that the static gels had higher viability of IPCs compared to that of flow gels.

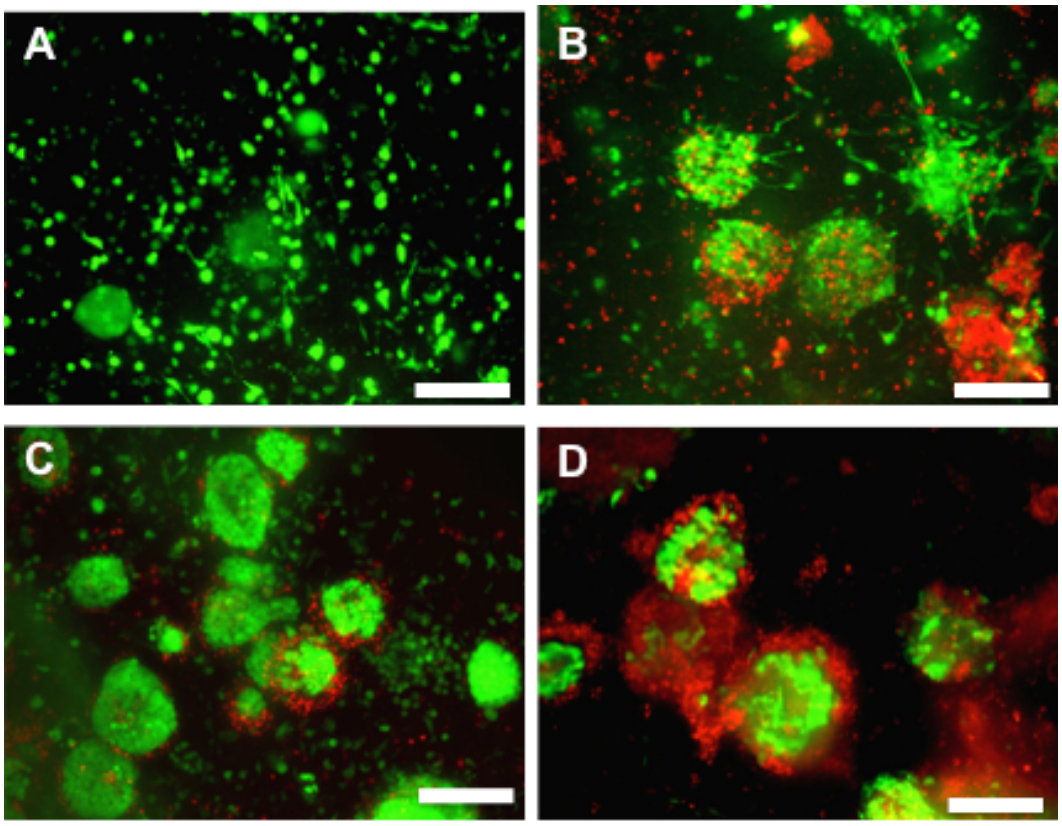

Figure 3.10 Whole and dissociated IPC Clusters in Collagen Tissues. Live dead staining shows the (A) dissociated IPC clusters and (B) whole IPC clusters in statically cultured collagen tissues, respectively, and (C) dissociated IPC clusters and (D) whole IPC clusters under flow condition, respectively. Live cells were stained with calcein (Green), dead cells were stained with Ethidium bromide (Red). Scale bar: 100 μm.

3.3.5 Survival of 3D Co-Culture Tissues Under Static and Flow Culture Conditions

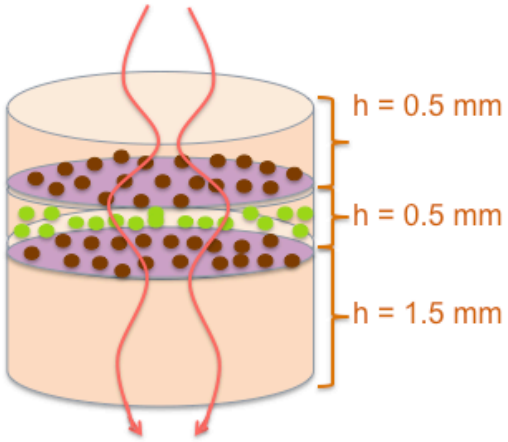

Figure 3.11 Schematic of a Co-culture Gel. A fully assembled co-culture gel had dissociated IPCs (green) embedded in a 0.5 mm thick collagen gel. This IPC gel was sandwiched between two layers of mESC-ECs, which were further sandwiched using a top and a bottom collagen gel layer. Flow was applied directly through the gel using a peristaltic pump using microbore tubing.

A schematic of the co-culture gel setup is shown in Figure 3.11. Live dead staining demonstrated high IPC viability in both static and flow conditions as shown in Figure 3.12.

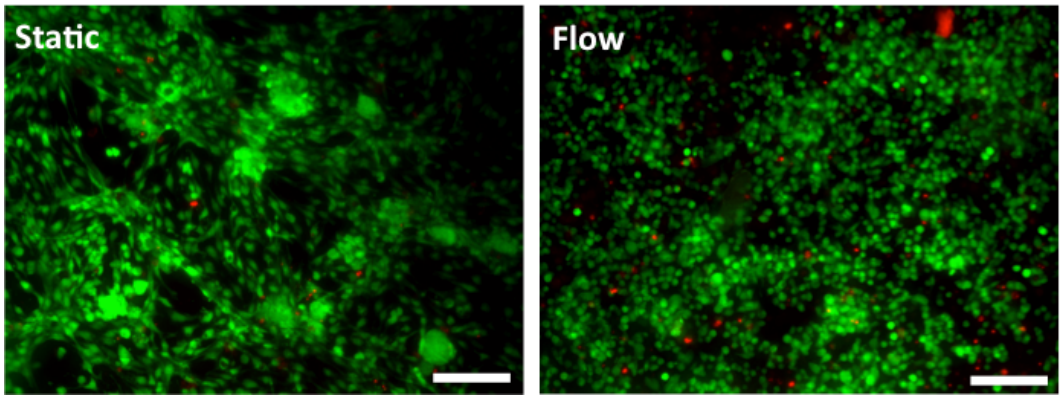

Figure 3.12 Live Dead Staining of 3D Co-culture Tissues. Live dead staining after 5 days of culture showing high viability of IPCs in both static and flow gels. Scale bar: 100μm.

3.3.6 Insulin Expression by IPC clusters in 3D Monoculture Gels

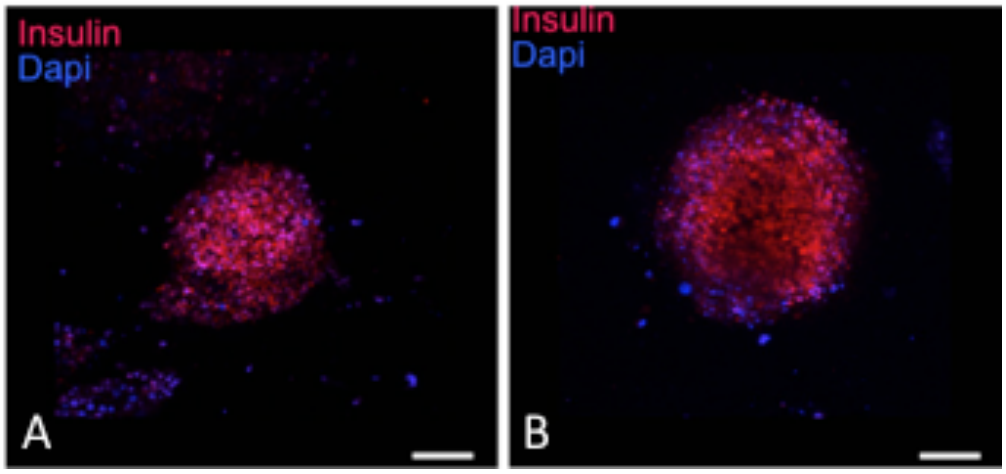

Figure 3.13 Insulin Expression by IPCs in 3D Gels. Immunofluorescence studies showing IPC clusters stained positive for Insulin (red) expression in tissues cultured (A) statically and (B) under flow for 3 days. Nuclei were stained blue using DAPI. Scale bar: 50 μm.

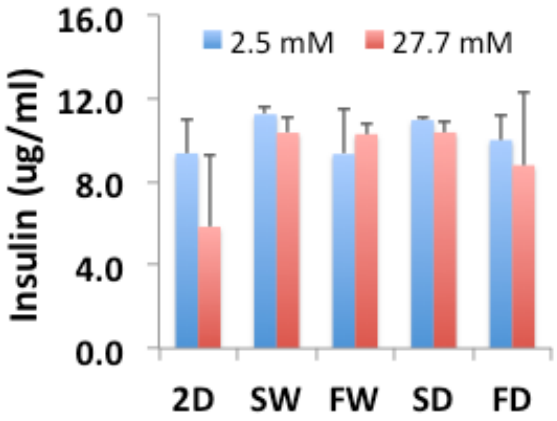

Figure 3.14 Insulin ELISA Assay. An insulin ELISA was performed followed by a glucose challenge on IPCs in 3D collagen gels. (n=4). 2D: IPCs isolated and plated on 2D surface, SW: Static tissue containing whole IPC clusters, FW: Tissue containing whole IPC clusters under flow, SD: Static tissue containing dissociated IPC clusters, FD: Tissue containing dissociated IPC clusters under flow (n=4).

After three days of culture, both the static and flow gels were found to produce insulin as shown in Figure 3.13. The presence of insulin protein was detected using immunofluorescence labeling. This provides evidence that the IPC clusters were able to maintain their capacity to produce insulin in the 3D culture conditions. Further tests were done to check if the IPC clusters were able to upregulate their insulin secretion levels based on the glucose conditions they were exposed in 3D collagen tissues. A glucose challenge was performed on tissues containing whole IPC clusters as well as dissociated IPC clusters. Our results showed that there was no significant effect of culture conditions on the final insulin secreted level, nor the glucose responsiveness of IPCs. Only the

insulin secretion of static tissue containing whole IPC clusters was significantly different from that of 2D culture when exposed to higher glucose concentration (n=4, $p<0.05$).

3.3.7 Glucose Responsiveness of IPCs in 3D Co-culture Tissues

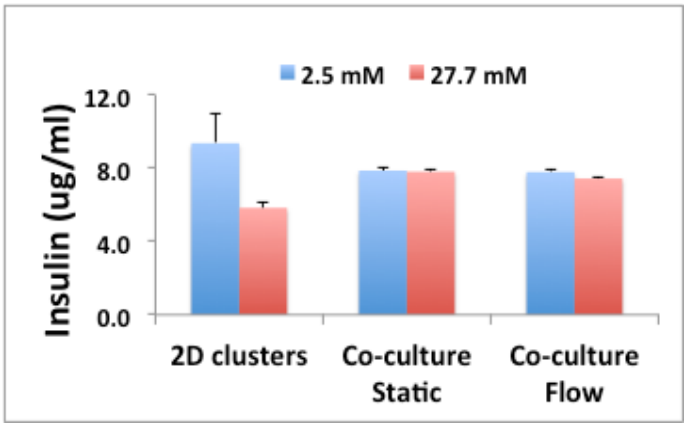

Figure 3.15 Glucose Responsiveness of 3D Co-culture Tissues. An Insulin ELISA assay revealed the insulin secretion from the 3D coculture tissues under static and flow conditions at low and high glucose conditions. Isolated IPCs plated on 2D culture conditions were used as control. (n=4)

A glucose challenge followed by an insulin ELISA demonstrate that there was a significant decrease in insulin secretion in high glucose condition compared to lower glucose condition within the 2D culture group. However, no significant difference was observed in the 3D co-culture conditions in either static or flow conditions as shown in Figure 3.15 indicating that IPCs in 3D co-culture conditions are not glucose responsive.

3.3.8 Gene Expression Analysis of IPC Clusters in Monoculture Gels

In order to characterize gene expression of IPC clusters in 3D culture conditions, RNA was isolated from 3D collagen tissues cultured for 5 days. Freshly isolated IPCs identified by DTZ staining were used as 2D control. Table 3.1 lists all the primer

sequences used and their respective product length. Relative gene quantification was performed using the Livak method. As shown in Figure 3.16, IPCs in 2D as well as 3D culture conditions were found to express genes such as Ins 2, PDX1, Pax4, Nkx6.1, Glut2 and EphrinA5.

Glut 2 expression was found to reduce 0.69 fold and 0.17 fold, respectively for IPC cluster gels cultured under static and flow culture conditions, compared to the 2D culture. In case of the dissociated IPC cluster gels, the Glut 2 expressions reduced 0.184 fold and 0.311 fold for static and flow culture conditions, respectively. A large variability was seen in the insulin gene expression between the different IPC cluster gel samples. The values obtained were not found to be statistically significant.

Nkx6.1 expression in statically cultured whole IPC gels reduced 0.29 fold and 0.47 fold for the ones cultured under flow conditions. The dissociated IPC cluster gels under static conditions had a 1.74 fold increase over the control sample, while the corresponding gel in flow conditions had a 0.33 fold reduced expression of Nkx6.1.

Compared to 2D culture, PDX1 expression was found to reduce 0.45 fold and 0.89 fold, respectively for IPC cluster gels cultured under static and flow culture conditions. In case of the dissociated IPC cluster gels, the PDX1 expression reduced 0.41 fold and 0.36 fold for static and flow culture conditions, respectively.

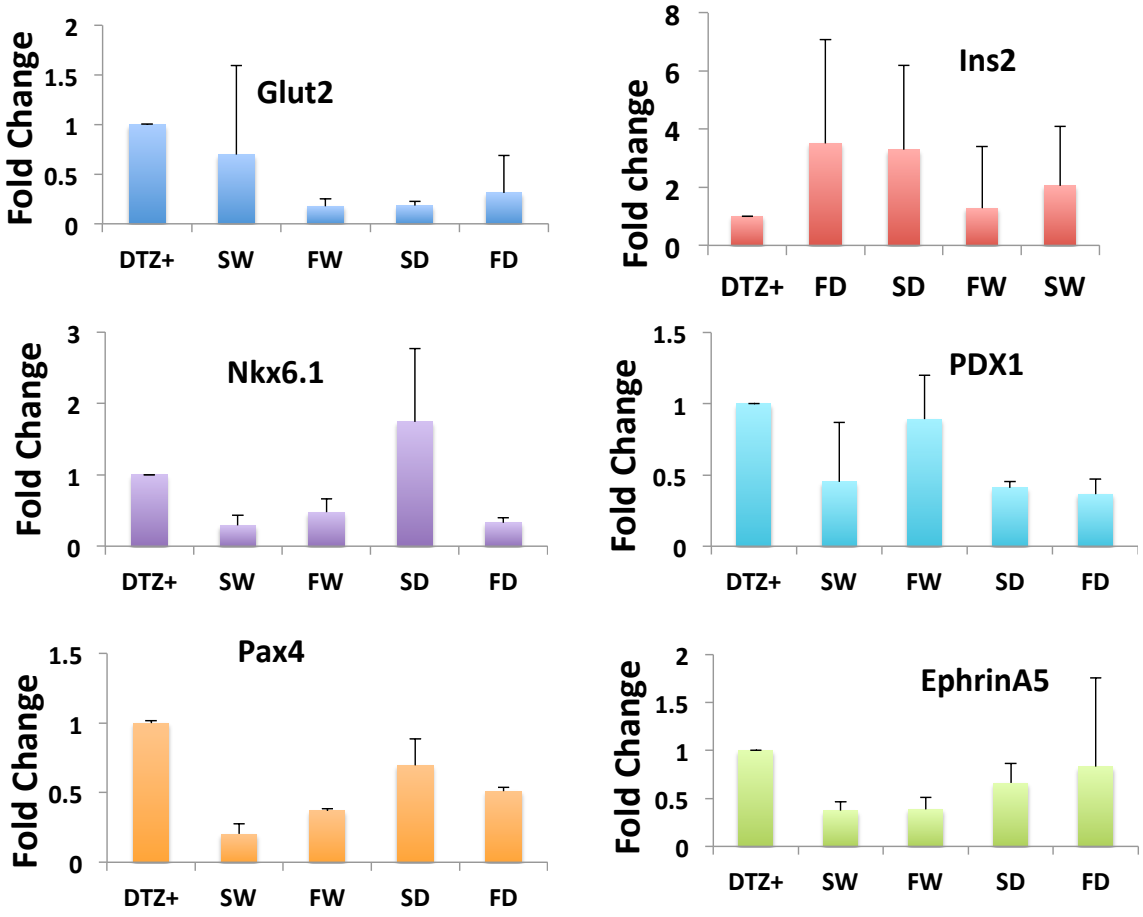

Figure 3.16 Gene Expression Analysis of IPCs Cluster Gels. Whole and dissociated IPC cluster gels cultured under static and flow conditions were used for real time PCR analysis. Relative gene quantification was performed using the Livak method [9]. GAPDH was used as housekeeping control. Freshly isolated IPCs identified by DTZ staining were used as control (n=4). DTZ+:DTZ positive IPC clusters, SW: Whole IPCs in static condition, FW:IPC clusters in flow condition, SD: Dissociated IPCs in Static condition, FD: Dissociated IPCs in flow condition.

It was also found that the Pax4 expression reduced 0.2 fold and 0.37 fold, respectively for IPC cluster gels cultured under static and flow culture conditions compared to 2D culture. The Pax4 expression in case of the dissociated IPC cluster gels reduced 0.69 fold and 0.51 fold for static and flow culture conditions, respectively. EphrinA5 expression was found to reduce 0.37 fold and 0.38 fold, respectively in IPC cluster gels cultured under static and flow culture conditions compared to the 2D culture. In case of the dissociated IPC cluster gels, the PDX1 expression reduced 0.66 fold and 0.83 fold for static and flow culture conditions, respectively.

3.3.9 Gene Expression Analysis of IPC Clusters in Co-Culture Gels

Gene expression analysis on 3D co-culture gels cultured for five days demonstrated that IPCs in 2D as well as 3D co-culture conditions express genes such as Ins 2, PDX1, Pax4, Nkx6.1, Glut2 and EphrinA5.

Insulin gene expression was significantly down regulated under flow compared to static conditions in the 3D culture. Glut2 expression in the 3D co-culture tissues under static and flow conditions had decreased to 0.12 fold and 0.07 fold, respectively, compared to 2D culture. For EphrinA5, the 3D co-culture tissues under static and flow conditions decreased 0.35 fold and 0.12 fold, respectively, while for Nkx6.1 a 0.65 fold and 0.62 fold reduction was observed for 3D co-culture tissues under static and flow conditions. It was found that the PDX1 gene expression in the 3D co-culture tissues under static and flow conditions had decreased to 0.35 fold and 0.32 fold, respectively for Pax4, 0.39 fold and 0.17 fold, respectively. Overall, a down regulation of beta cell specific markers was observed in the 3D co-culture gels under both static and flow culture conditions compared to 2D conditions.

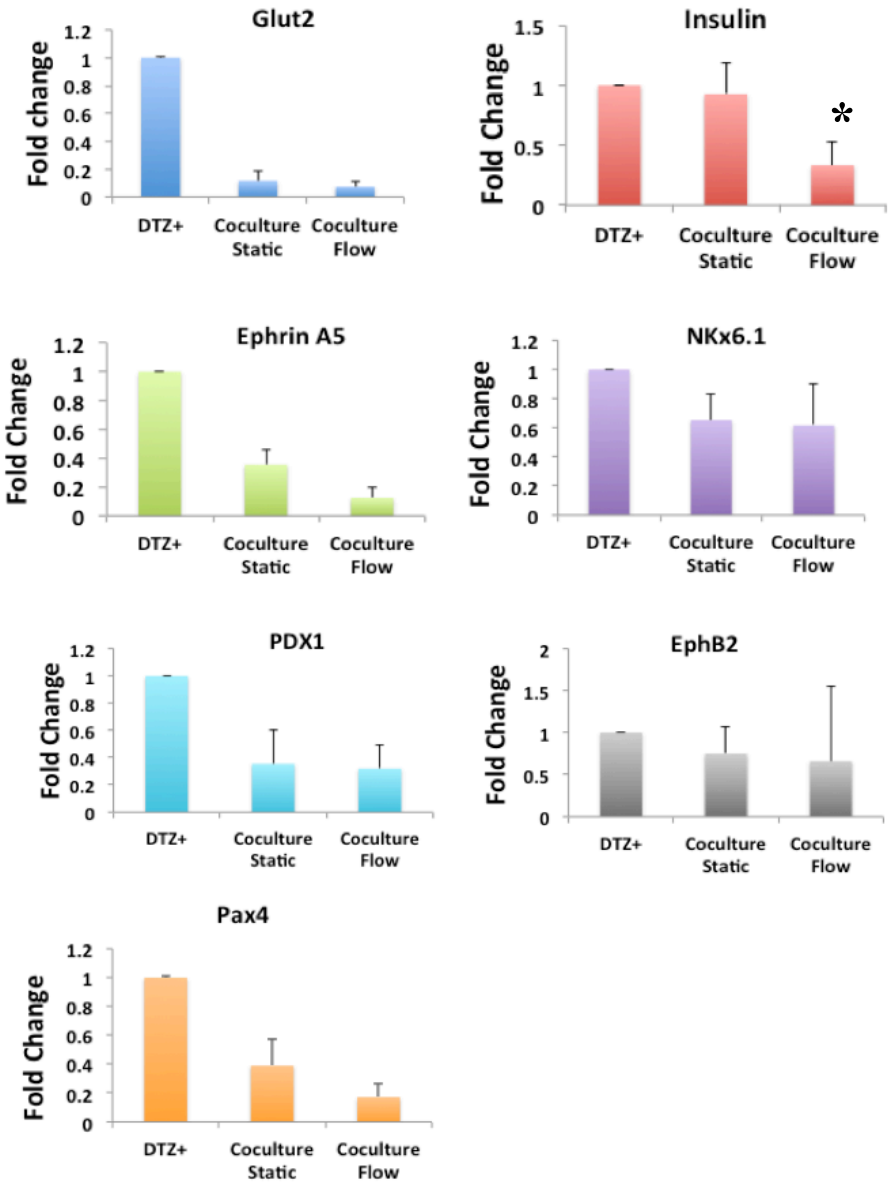

Figure 3.17 Gene Expression Analysis of 3D Co-culture Tissues. Real time PCR analysis was done to study the gene expression levels of various genes of interest such as Glut2, insulin, Pax4, PDX1, Nkx6.1 and EphrinA5. Co-culture tissues under static and flow conditions for five days were used. Relative gene quantification was performed using the Livak method [9]. GAPDH was used as housekeeping control. Freshly isolated IPCs identified by DTZ staining were used as control (n=4, $p<0.05$).

3.4 Discussion

The present study describes preliminary optimization and characterization of differentiated IPC clusters in 3D culture conditions, and their subsequent co-culture in 3D with ECs. While previous studies have shown the beneficial effect of collagen on islet culture [116, 225], studies using 3D collagen with stem cell derived IPCs have not yet been demonstrated. Thus, attempts were done to optimize a few experimental conditions to develop 3D collagen tissues with IPCs. To derive IPC clusters with size physiologically relevant to the islets, cannulas were used to manually break the IPC clusters. While obtaining smaller size IPC clusters, large number of dead cells and debris were also seen in culture. In order to prevent these from carrying forward in culture, various strategies were tried for their removal. It was observed that filtering the IPC cluster suspension through a cell strainer effectively removed most dead cells and debris, when compared to pre-plating method.

Once smaller IPCs were achieved, they were cultured in 3D environment. Our study showed that the majority of the IPC clusters remained viable after embedding in 3D collagen gels. However, an increase in glucose responsiveness was not observed in the 3D culture conditions used in the current study. The final concentration of the gel used in this study was 3 mg/ml., which is shown to have a pore size of ~1.8 μm [241]. However, concentration of the collagen should be further optimized as stiffness of the gel can affect the behavior of IPCs in 3D culture.

To determine whether perfusion flow improves viability of IPCs in 3D collagen tissue, flow was applied to the 3D tissues. Flow rate of 0.5 ml/min was chosen as it has previously been demonstrated that this value corresponds to a shear stress of

approximately 0.71 dyn/cm^2, which has been shown to be in the physiological range in microvessels in *in vivo* conditions [238]. This flow-rate was chosen to minimize gel compaction of the 3D tissues due to high velocity of flow. Our studies with endothelial cells (Chapter 4) demonstrated that the cell seeded collagen gels underwent significant compactions when exposed to 2 ml/min flowrate. This compaction was reduced upon changing the flowrate to 0.5 ml/min.

Upon live dead staining, it was found that the IPC cluster viability was higher in static culture conditions compared to the flow culture conditions. Dead cells were found on the outer edges of the IPC clusters. This was not expected as islets in perifusion studies that are exposed to higher flow rates ranging from 130 µl/min to 1 ml/min survive without a problem [141, 242]. Further studies are required to examine the effect of lower flow rate as well as shorter culture period on IPC function in 3D culture. The difference is the duration of exposure. Perifusion can last from a few min to a few hours whereas our study continued for 5 days. 3D collagen gels were cultured for 5 days to detect any changes in gene expression, which may not be reflected in short term studies. Since individual rat islets *in vivo* are normally exposed to a flowrate of 2 x 10^{-5} ml/min of blood [142, 243], it is possible that much lower flow rate needs to be tested. It is not clear from the study whether similar cell death will occur at lower flow rates or shorter culture period. Thus, more experiments are required to better understand the effects of flow on IPC clusters.

It was observed that the IPC clusters lose their glucose responsiveness once they are isolated out of the differentiation plate. Isolated IPCs plated on 2D surface as well as the ones incorporated in 3D collagen gels cultured under static and flow culture

conditions displayed this lack of glucose responsiveness. Prior to isolation of IPCs, IPCs were glucose responsive. Past studies have reported evidence that exposure to high glucose medium de-sensitized rat and human islets and impaired their function in response to a glucose challenge [221, 244, 245]. The medium used in this study contained about 17.5 mM of glucose and as this is considerably high, it is possible that the cells were rendered glucose unresponsive because of exposure to the medium. Assady e*t al.* in their ground breaking study that described the first derivation of IPCs by hES cells, suggested that the high glucose conditions of the differentiation medium might make the IPCs unresponsive to glucose [76]. It was suggested by this group that switching differentiating cells to a low glucose medium during the last stage of differentiation might be able to restore the glucose responsiveness [76]. Thus, whether this is due to desensitization of IPCs in high glucose containing culture medium awaits further studies.

Prior to the gel preparation, IPC clusters were manually handpicked from their environment in the differentiation culture, which caused separation of IPCs from the basement membrane proteins as well as from the neighboring cells. Since, laminin and collagen type IV are produced by cells in our culture and they are known to be important in insulin gene regulation and support glucose stimulated insulin release [246], it is plausibe that the loss of these basement membrane proteins may have led to the loss of glucose responsiveness for the IPC clusters when they were transferred in collagen gels or plated in 2D culture conditions. In fact, previous studies have indicated that a combination of collagen and Matrigel can help maintain insulin gene expression of islets in culture [221, 225]. Future studies exploring a combination of collagen with other

ECM proteins such as laminin or Matrigel are needed to determine their effects on IPC function in 3D *in vitro* conditions.

It is also possible that the IPCs may have undergone transdifferentiation in culture [247]. Although studies have shown that collagen provides a permissive environment for islet organization and helps maintain islets in culture for a longer time [221], there have also been a few reports that have shown that islets embedded inside collagen gels transdifferentiated into duct like cells [248, 249]. Further studies are needed to verify whether transdifferentiation has occurred by examining the expression of ductal cell markers such as cytokeratin 7,19 and 20 [250].

Past studies have highlighted the beneficial effect of endothelial cells on islet culture. Endothelial cell secreted factors improve insulin gene expression, beta cell proliferation and growth [1, 145, 150, 151, 154, 165, 205, 251, 252]. In the present study, we used ECs and IPCs derived from mES cells to develop 3D co-culture gel tissues. These co-culture tissues were cultured up to 5 days in static and flow culture conditions. Live dead staining at Day 5 showed that most of the cells in the co-culture maintained their viability after five days of culture. Although the insulin gene expression levels were comparable to that of 2D clusters, the 3D co-culture gels showed diminished glucose responsiveness. The basal level of insulin expression was about 8 μg/ml when the cells were exposed to low glucose levels. This is about four times higher than the response of DTZ+ clusters in 2D conditions as shown in Chapter 2, section 3.4. In 2D conditions, the cells had secreted less than 2 μg/ml of insulin when exposed to 2.5 mM of glucose and ~8 μg/ml upon exposure to 27.7 mM of glucose. But in 3D condition, the cells secreted 8 μg/ml of insulin when exposed to 2.5 mM of glucose and upon exposure to 27.7 mM

glucose no significant increase in insulin secretion was observed. This presents evidence that the IPC clusters were not responding to glucose levels.

The high level of insulin expression at the low glucose stimuli can be explained by the fact that the 3D co-culture gels had more IPCs packed together compared to the 2D culture and which may have resulted in higher insulin release compared to that in 2D culture condition. This however, does not explain why the cells did not upregulate their insulin levels upon high glucose exposure.

A study by Boyd *et al.* showed that the number of islets plays an important role in determining the end result of a glucose challenge test. In their study, 600, 300, 100, 66, 55and 25 islets were cultured separately. Upon performing a glucose challenge at 3.3mM and 25 mM glucose, only the first two groups i.e., 600 and 300 islets behaved in a glucose responsive manner [88]. When this procedure was repeated using IPC clusters derived from mES cells, similar results were obtained [88]. Therefore further studies are needed to examine whether increasing the number of IPC clusters will have a positive effect on the IPC culture in our study.

In addition, a previous study by Song *et al.*, showed that when cultured with rat endothelial cells, islets were not glucose responsive up to 5 days. However, a difference was noticed between day 7-14 of the co-culture [253], when the islets became glucose responsive. This suggests that the effect of endothelial cell co-culture on islet glucose responsiveness might not be immediate and requires longer time to fully manifest. As our study only lasted for 5 days, it will be interesting to see the impact of a longer duration on the glucose responsiveness of the co-culture tissues.

Gene expression analysis showed that EphrinA5 expression was not increased in flow co-culture conditions as hypothesized. On the contrary, the EphrinA5 expression was found to be higher in static co-culture gels compared to flow co-culture gels. The reason for this was not understood and hence the interaction between the EphB2 and EphrinA5 was not analyzed as initially described in the specific aim III.

Jaramillo *et al.* used a co-culture of ECs while differentiating human embryonic stem cells into IPCs [254]. In this study, the authors showed that the direct co-culture of endothelial cells resulted in higher insulin expression when compared to transwell cultures and exposure to conditioned medium from endothelial cells [254]. It is noteworthy that the IPCs were differentiating while they were exposed to ECs, which is a different condition compared to the presented study where the differentiated IPCs were co-cultured with ECs. Whether the ECs have a more beneficial effect during or after the differentiation process is not clear.

Previous studies have also highlighted the role ECs play in the development of diabetes type I. ECs can get activated by cytokines and then make large quantities of NO, that can cause beta cell death [255]. An interesting study by Steiner *et al.*, showed that in co-culture of islet endothelial cells and islet cells, the endothelial cells acted as effector cells and were able to mediate strong to complete lysis of islet cells [256]. Such lysis is preceded by DNA strand breaks with no morphological evidence of apoptosis [256-258]. Although extensive cell death was not observed in the co-culture system in the presented study, there was however a downregulation of key beta cell markers in the co-culture environment in both static and flow culture conditions. Measuring the NO levels in the co-culture experiments and checking the DNA strands for signs of breakage can give an

insight into the cell-to-cell interactions between the IPCs and mESC-ECs. NO levels can be measured by performing an NOS ELISA assay, but was not performed in the interest of time. Checking DNA strands for breakage was beyond the scope of this work and hence was not performed.

The presented chapter describes strategies for 3D encapsulation of IPC clusters and their detailed characterization. It also describes useful strategies to prepare 3D co-culture gels using IPCs and mESC-ECs. Although the survival rate was high in the monoculture and co-culture gels, an improvement in the glucose responsiveness was not observed. Further, a downregulation of key beta cell markers was seen in the 3D culture conditions. Further studies with different culture conditions will need to be performed to collect more evidence on the effects of 3D environment and flow on the survival and functionality of IPC clusters in *in vitro* conditions. Longer duration of culture and a switch to low glucose conditions during the final stages of differentiation might improve the outcomes of the co-culture. Rigorous optimizations will be required to improve the glucose responsiveness and genetic profile of the co-culture tissues before they can be used for any therapeutic applications.

CHAPTER 4

DIFFERENTIATION OF MOUSE EMBRYONIC STEM CELLS INTO ISLET ENDOTHELIAL CELLS

4.1 Introduction

Several efforts have recently been made to differentiate pluripotent stem cells into endothelial progenitor cells or endothelial cells using various strategies (2,10,17,38,66). These pluripotent stem cell derived endothelial cells can provide an abundant cell source for tissue engineering applications as well as more personalized medical treatments. Levenberg *et al.* reported the derivation of endothelial cells from human embryonic stem cells (hESCs) and Blancas *et al.* demonstrated a chemically defined protocol to differentiate mouse embryonic stem cells (mESC) into endothelial cells (9,10). Other groups have shown that fluid shear stress can promote an endothelial-like phenotype from early embryonic stem cell differentiation (31,65) and the role of matrix stiffness has also been explored for endothelial differentiation (16,71). Recently, Nolan *et al.* established a library of molecular signatures of tissue-specific microvascular endothelial cells. They demonstrated that when murine embryonic stem cell-derived endothelial cells were transplanted into animal models, the generic endothelial cells acquired the specific characteristics of the tissues in which they were transplanted (46). Notably, endothelial cells are recognized as a heterogeneous cell population in their structure and function based on the location in the body (3). However, protocols for *in vitro* stem cell differentiation into organ-specific endothelial lineages are not yet available

Endothelial cells found in pancreatic islets, known as islet endothelial cells (IEC) are being increasingly appreciated as an important contributing factor in pancreatic islet development and maturation (28,67), as pancreatic islets have a very dense capillary network *in vivo*. IECs are known to exhibit a unique phenotype and markers that distinguish them from neighboring endothelial cell populations. It has previously been reported that isolated human IECs have more fenestrations than endothelial cells found within the exocrine part of the pancreas (20,47,68,69). In addition to classical endothelial cell makers such as von Willbrand factor, platelet endothelial cell adhesion molecule (PECAM1), and uptake of acetylated- low density lipoprotein (LDL), IECs are shown to express unique markers including nephrin and alpha1-antitrypsin (AAT) (43,69). Other studies have shown that rat IECs constitutively express endothelial nitric oxide synthase (eNOS) and the expression of eNOS is glucose-dependent unlike other endothelial cells (56,68,69). These unique properties of IECs contribute to normal development of beta cells in the pancreas. IECs secrete various molecules such as collagen type IV (29), laminin (26,45,61), connective tissue growth factor (CTGF) (14) and hepatocyte growth factor (HGF) (27) that are important for insulin secretion, beta cell proliferation, differentiation and endocrine lineage specification. Recent studies have also highlighted the role of IECs in the revascularization and stabilization of transplanted islets in the host tissue (11). Mattsson *et al.* showed that the expression of angiogenic and inhibitory factors by IECs varied at different time points post transplantation (44). However, due to difficulty in isolating a pure population of IECs and expanding in *in vitro* culture, the information on IECs is still relatively limited.

In the current study, we report the first demonstration of endothelial cells exhibiting IEC markers differentiated from mESC. This population of IECs appeared as a side-product in the differentiation culture of mESC into pancreatic beta cells. A pure population of endothelial cells was successfully isolated from the vicinity of insulin-producing cells and expanded in *in vitro* culture for further characterization. These highly purified endothelial cells with islet specific characteristics will further enhance our understanding of tissue-specific endothelial cell function. Moreover, studies investigating the interaction between neighboring insulin-producing beta cells and IECs can lead to a significant step in formulating new therapeutic angiogenic approaches for diabetes.

4.2 Materials and Methods

4.2.1 Identification and Isolation of mESC-Derived Endothelial Cells (mESC-ECs)

MESC were used to derive insulin producing cells (IPCs) of the pancreatic beta lineage as described in Chapter 2 Section 2.2. During various stages of mESC differentiation into pancreatic beta cells, acetylated Dio-LDL (Biomedical Technologies Inc., Stoughton, MA) was used to identify a mature endothelial cell population in the culture. LDL working solution was prepared by diluting LDL 1:10 in culture medium in the dark. Medium was removed from cells, LDL was added and the dishes were wrapped in aluminum foil and incubated for 4 hours at 37 °C. LDL positive cells were detected as stained green under an inverted florescence microscope (IX81 DSU, Olympus).

At the end of the differentiation process, i.e.,, Day 33, LDL positive cells in culture were selectively isolated from the rest of the population using sterile cloning discs (Capitol Scientific, Austin, TX). Dishes were washed 2X with warm PBS to remove

traces of medium. The sterile cloning discs were treated for ten minutes with UV light to further sterilize them. Using a fine tip forceps, 1-2 cloning discs were added to an aliquot of 0.25% trypsin and pre-treated for 5-10 minutes. They were then added carefully on previously marked areas with a large subpopulation of LDL positive cells and incubated for 3 min at 37°C. At the end of the incubation, the discs were gently lifted from the top and placed in a new dish coated with 0.1% gelatin and were initially cultured in the pancreatic differentiation medium supplemented with 10% FBS. After a few passages, culture medium was replaced with MCDB complete endothelial growth media containing 10% FBS, 1% penicillin-streptomycin (Sigma Aldrich), and Endogro, an endothelial cell growth supplement from VEC Technologies. Cells were passaged at 70-80% confluence and the cell culture medium was exchanged every 2-3 days.

4.2.2 FACS Analysis of mESC-ECs

Fluorescence-activated flow cytometry (FACS) was used to confirm the phenotype and the purity of the isolated cell population. For FACS analysis, cells were fixed with 4% PFA for 30 min and then washed 3X with PBS. Cells were then permeabilized with 0.25% Triton-X for 5 min. at room temperature. Cells were centrifuged to remove Triton-X and re suspended in ice cold FACS buffer. After incubation at 4 °C for ten minutes, cells were incubated with a polyclonal rabbit anti-PECAM1 (1:20, Santa Cruz) in FACS buffer (PBS with 1% BSA and 2 mM EDTA) for 30 minutes at 4 °C. Cells were then washed three times with cold PBS and secondary donkey anti-rabbit APC (1:20, Fisher Scientific) was added and incubated for 30 minutes at 4 °C. Cells were again washed three times with cold PBS. Cells were analyzed using a FC500 Flow cytometer (Beckman

Coulter, Pasadena, CA) and FlowJo software at the FACS facility at Rutgers Medical School.

4.2.3 Western Blot Characterization of mESC-ECs

A detailed characterization of cell phenotype was performed using western blotting analysis. For making cell lysates, cells were washed twice with ice cold PBS, and then incubated with cell lysis buffer (See Appendix B for details) for 20 min at 4 °C. The cells were then gently scraped off using a cell scraper (USA scientific) and then added to a microcentrifuge tube. Tissue lysates were made by first grinding the tissue over dry ice, making sure that it remains frozen throughout the process. The powdered tissue was then transferred to a microcentrifuge tube with the lysis buffer and incubated at 4 °C for 20 min. The lysates were centrifuged at 4 °C for 30 min at 14,000 rpm in a microcentrifuge. The supernatant was transferred into a fresh tube and used for protein quantification using the Bradford or DC assay (See Appendix X for details). The results were read using the Smart Spec Spectrophotometer (BioRad). Cell lysates were diluted (1:1) in Laemmli buffer (Bio-Rad, Hercules, CA) containing 5% mercaptoethanol and 2% sodium dodecyl sulfate (SDS). The lysates were stored in 25-30 μg aliquots and stored at -20 °C till ready for use.

2D gel electrophoresis was performed using Miniprotean TGX precast gels (BioRad). Dual color precision plus protein standard (BioRad) was used as a protein marker. The gels were transferred on Immunoblot PVDF membranes (BioRad) at 100 V for 90 minutes at 4 °C. For immunoblotting, primary antibodies used were a polyclonal rabbit anti-PECAM1 (1:200, Santa Cruz), a monoclonal mouse anti-thrombomodulin (1:200, Abcam), a monoclonal mouse anti-ICAM1 (1:500 Abcam), a polyclonal rabbit

anti-eNOS (1:200, Abcam), a polyclonal rabbit anti-EphB2 (1:200, Santa Cruz), a polyclonal goat anti-EphB4 (1:200, Santa Cruz), a polyclonal rabbit anti-Notch-1 (1:100, Santa Cruz), a polyclonal rabbit anti-Nephrin (1:250, Abcam) and a monoclonal mouse anti-β actin (1:2000, Sigma). After three washes with TBS-Tween buffer, blots were incubated with a secondary goat anti-rabbit IgG HRP, a goat anti-mouse IgG HRP antibodies or a goat anti-donkey IgG HRP antibody (1:2000, Santa Cruz) for 1 hour at room temperature. After three washes with TBS-Tween buffer and one wash with TBS buffer, the blots were developed using a Supersignal chemiluminescent substrate (Thermoscientific, Rockford, IL). Blots were incubated with 3 mls of 1:1 ratio of the Supersignal substrate solution and Supersignal enhancer solution in the dark. Blots were then exposed to UV and developed using a Chemidoc XRS (BioRad). Fresh rat aortic tissue homogenates and low passage of cultured rat aortic endothelial cells (RAEC) lysates were used as controls. mESC-EC lysates from passages 6-16 were used.

4.2.4 Deposition of ECM Proteins by mESC-ECs

To determine whether mESC-ECs deposit basement membrane proteins in culture, cells were cultured on glass slides for 5-7 days for immunohistological evaluation. Cells were fixed for 30 minutes at room temperature using 4% PFA (Boston Bioproducts) and then washed three times with PBS. Cells were then blocked with 10% horse serum in PBS with 0.1% Tween-20 for 30 minutes followed by an overnight incubation with primary antibodies at 4 °C. Primary antibodies used were a polyclonal goat anti-laminin (1:200, Santa Cruz), a polyclonal rabbit anti-collagen type IV (1:200, Santa Cruz) and a polyclonal rabbit anti-fibronectin (1:200, Santa Cruz). Cells were washed 3X with PBS and then incubated with secondary donkey anti-goat (1:200, Santa Cruz) and goat anti-

rabbit (1:200, Santa Cruz) for 30 minutes. Cells were counterstained with hematoxylin (Boston Bioproducts, Ashland, MA), and mounted using Permount (Fisher Scientific, Hampton, NH). Cells were imaged using an inverted microscope with a color camera (Nikon Eclipse Ti-S, Japan).

4.2.5 Immunofluorescence Characterization

To determine the expression of FLK1 by mESC-ECs, immunofluorescence analysis was performed. Cells were fixed for 30 minutes at room temperature using 4% PFA (Boston Bioproducts) and then washed 3X with PBS. Cells were then blocked with 10% goat serum in PBS with 0.1% Tween-20 for 1 hr. followed by an overnight incubation with a polyclonal rabbit anti-Flk-1 (1:1000, Abcam) at 4°C. Cells were washed 3X with PBS and then incubated with secondary goat anti-mouse (1:2000, Abcam) for 1 hour. Cells were stained with DAPI to visualize the nuclei and were imaged using a confocal microscope (IX81 DSU, Olympus, Somerset, NJ).

4.2.6 Endothelial Nitric Oxide Synthase (eNOS) Expression by mESC-ECs

ENOS Enzyme linked immunosorbent assay (ELISA) kit (R&D systems, Minneapolis, MN) was used to quantify eNOS expression by cultured mESC-ECs. Cells cultured in MCDB complete endothelial growth media containing 17.5 mM of glucose were first examined. Cells were then exposed to culture medium containing higher glucose concentrations of either 25 mM or 35 mM of glucose for 24 hours to investigate whether eNOS expression by mESC-ECs was dependent on glucose concentrations. The cells were lysed and the lysates were collected to be analyzed by ELISA. The ELISA results were read using an Emax microplate reader (Molecular Devices, Sunnyvale, CA) at the

wavelength of 570 nm. A student T-Test was performed to check whether the data was statistically significant.

4.2.7 Vascular Endothelial Growth Factor (VEGF) Expression by Cells During Pancreatic Differentiation Process

VEGF concentration in the culture medium during the pancreatic differentiation process was quantified using a VEGF ELISA kit, following manufacture's instruction (R&D systems, Minneapolis, MN). Culture medium was collected at various time points, including day 20, 26 and 32 of pancreatic differentiation. In addition, culture medium was collected from mESC-ECs culture, to determine VEGF expression by endothelial cells. Fresh differentiation medium was used as a control. The ELISA results were read using an Emax microplate reader (Molecular Devices, Sunnyvale, CA) at the wavelength of 570 nm. A student T-Test was performed to check whether the data was statistically significant.

4.2.8 Matrigel Assay

A 0.8 mm thick layer of Matrigel (BD Biosciences, San Jose, CA) was prepared by adding Matrigel diluted in ice-cold DMEM (1:1) into a well of a 12 well plate. $1.5x10^4$ mESC-ECs were seeded onto the layer of Matrigel and cultured for up to 48 hours. Cord formation by mESC-ECs was imaged using a microscope with a color camera (Nikon Eclipse Ti-S, Japan).

4.2.9 Preparation of a Sandwiched Collagen Gels Using mESC-ECs

3D Collagen gels were constructed using a modification of the sandwich method previously described [259] as shown in Figure 4.12. The original method describes the

preparation of a collagen gel with one layer of cells sandwiched between two gel layers. The method was modified to include up to three layers of cells embedded in between the collagen gel layers. Further modification was done to reduce the gel preparation time from 72 hours to 9 hours. Rat tail collagen type I (BD Biosciences), 10X DMEM (Sigma Aldrich) and 10X reconstitution buffer (0.05 N NaOH with 0.16 M HEPES and 0.25 M $NaHCO_3$) were mixed to form a collagen solution with final concentration of 3 mg/ml. To form 3D collagen gels, collagen solution was first poured into tissue culture plates and incubated at 37°C for 30 minutes to allow polymerization before mESC-ECs suspended in MCDB complete medium were added on top. After 3 hours, medium was carefully removed and another layer of cold collagen gel solution was added on top of the cell layer. This process was repeated to obtain in total two layers of cells sandwiched between three layers of collagen gel. Medium was changed every other day. After 3-5 days in culture, collagen gels were fixed overnight in 4% PFA at room temperature.

4.2.10 Lumen Formation in mESC-EC Seeded Collagen Gels

Fixed collagen gel samples were paraffin-embedded and histological sections were prepared for immunofluorescent analysis (Core histology Lab, Rutgers Medical School). The samples were de-paraffinized by a series of washes (See Appendix X for details). The sections were incubated with an antigen retrieval buffer (10 mM citric acid, pH = 6) at 95 °C for 25 minutes and then allowed to cool down for 20 min. They were incubated with 10% goat serum and 0.1% Triton-X in PBS for 1 hour for blocking followed by incubation with a polyclonal rabbit anti-PECAM1 (1:200, Santa Cruz) at 4 °C overnight. After 3x wash with PBS, collagen gel sections were incubated with a secondary donkey anti-rabbit (1:200, Santa Cruz) for 1 hour at room temperature over a rocker. DAPI

(Vector labs) was used to stain the nuclei. Images were acquired using a confocal microscope (IX81 DSU, Olympus, Somerset, NJ) and were merged using Image J software (NIH).

4.2.11 Effect of VEGF Inhibitor on mESC-ECs Yield

To determine whether the presence of VEGF is one of the critical factors contributing to the appearance of mESC-ECs in pancreatic differentiation culture, Thalidomide (Sigma), which is known as a potent inhibitor of angiogenesis [260] was added to the differentiation culture on day 15 at a final concentration of either 10 μM or 20 μM in the culture medium. At the end of the differentiation (Day 33), cells were incubated with LDL as previously described and monitored under a florescence microscope.

4.2.12 Application of Flow to mESC-EC Seeded Collagen Gel

A custom made bioreactor set up was used for this study [238]. The collagen mESC-EC mix was pipetted onto a polyethylene terephthalate (PET) membrane glued on a PDMS ring placed on the inside edge of the bottom piece of the flow bioreactor. This porous membrane supported the gel during the experiment. To prevent the gel from moving and undergoing contraction by cellular action, six 27G needle pins were inserted around the periphery of the PDMS ring. To reduce the resistance to flow created by the membrane, 15-20 holes were punched into it using a 30 gauge needle. During the gel preparation when subsequent layers were being added to the gel, it was placed inside a small sterile plastic container (Nalgene) in the incubator. Once all the gel layers were added, the bioreactor was fully assembled inside the laminar flow hood. First a PDMS ring was placed on top of the gel and pushed down upon the needle pins. This was done carefully without disturbing the gel beneath. This ring formed a flow orifice in the system and

forced the medium to flow through the gel. It prevented the medium from taking the path of least resistance and flowing around the gel. Medium was added to the gel so that the bottom piece was completely full of medium. The bioreactor was assembled as described in Chapter 3. Once the bioreactor was fully assembled, it was connected to a peristaltic pump (Cole Parmer) via cartridges. Flow-rate and flow direction were set and the flow was started at 0.5 ml/min. Flow was continued for 1-10 days.

4.2.13 Actin Staining

Fixed collagen gels were stained with Rhodamine Actin Phalloidin (Life technologies) diluted 1:20 with PBS in the dark for 2 hrs on a rocker. Afterwards, the gels were washed 3x with PBS on a rocker. Samples were stained with DAPI to visualize the nuclei and mounted with a coverslip for imaging. A DSU unit attached to an inverted fluorescence microscope (Olympus) was used to take z-sections of the gels. Cell sens software was used to combine the z-sections to acquire a 3D image of the gel samples. Deconvolution was performed using the Image J software (NIH).

4.2.14 ECM Protein Staining in Differentiation Culture

This was done to demonstrate whether the mESC-ECs were capable of depositing basement membrane proteins in the differentiation culture, prior to their isolation. DTZ positive clusters were marked in a differentiation plate and the plates were fixed for 4 hours with 4% PFA. After 3X washing with PBS, the cells were blocked with 10% goat serum and 0.1% Triton-X 100 in PBS for 1 hour at room temperature. Primary antibodies polyclonal goat anti-laminin (1:200, Santa Cruz), a polyclonal rabbit anti-collagen type IV (1:200, Santa Cruz) were added for overnight incubation at 4 °C. Cells were washed 3X with PBS and then incubated with secondary donkey anti-goat (1:200, Santa Cruz)

and goat anti-rabbit (1:200, Santa Cruz) for 30 minutes. Cells were counterstained with hematoxylin (Boston Bioproducts, Ashland, MA) to visualize the nuclei.

4.2.15 Addition of VEGF to Promote Angiogenesis

Lyopholized recombinant VEGF powder (R&D systems) was resuspended in sterile PBS containing 0.1% BSA (Bovine serum albumin) to make a 100 μg/ml stock solution. This solution was then aliquoted and stored at -20 °C. In order to obtain a more interconnected and dense vasculature, recombinant VEGF was added to the medium at 5 ng/ml. VEGF was directly added to the medium and mixed up and down by pipetting.

4.2.16 Statistical Analysis

Results are presented as mean± standard deviation. A one-way paired student T-test was performed. Statistical significance was accepted for $p<0.05$.

4.3 Results

4.3.1 Identification of mESC-ECs

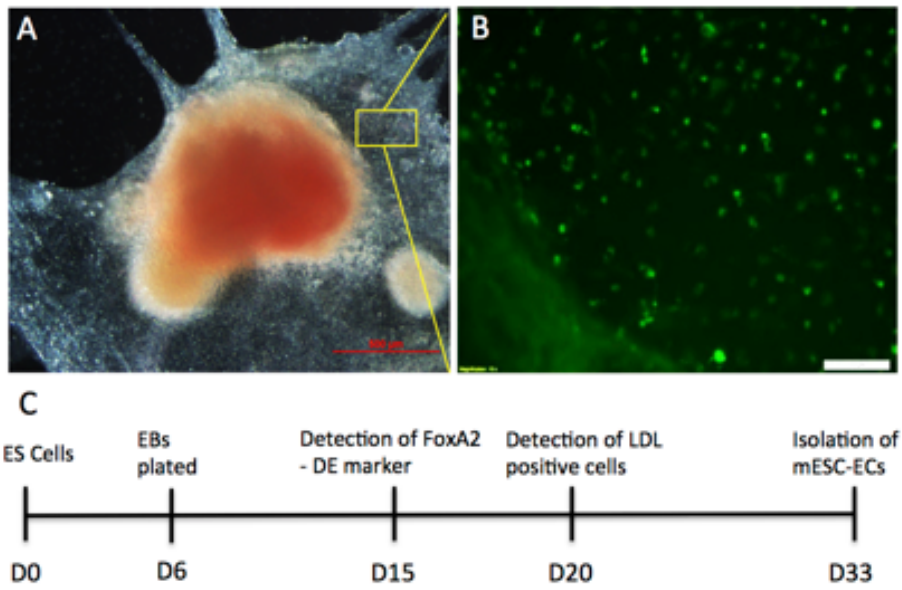

Figure 4.1 Identification of Mouse Embryonic Stem Cell-Derived Endothelial Cells (mESC-ECs). **(**A) A brightfield image of insulin-producing cell cluster stained with Dithizone (DTZ) is shown in red. (B) Cells surrounding DTZ positive cell cluster are stained green by the uptake of acetylated Dio-LDL. Scale bar, 100 µm. (C) A time line with important milestone marks during differentiation of mESC into pancreatic beta cells. Embryoid bodies (EBs) formed by a hanging drop method were plated at day 6. A definitive endoderm marker, FoxA2, was first detected at day 15. LDL positive cells started to appear at day 20. The mESC-ECs were isolated on day 33, which corresponds to the end of pancreatic differentiation. Scale bar: 100µm.

IPCs were obtained successfully from mESC using a previously established protocol [73], as described in detail in Chapter 2. Insulin-producing cell clusters were identified after 33 days of differentiation by staining with DTZ as shown in Figure 4.1A. Interestingly, in the vicinity of DTZ positive cell clusters, we have detected a population of cells that uptake LDL (Figure 4.1B). By examining the differentiation culture at various time

points, we found that the LDL positive cells start to appear as early as day 20 of differentiation (Figure 4.1C). It was also found that the number of LDL positive cells progressively increases, reaching approximately 6.3±0.9% of the total number of cells on the final day of differentiation, day 33 as shown in the Figure 4.2.

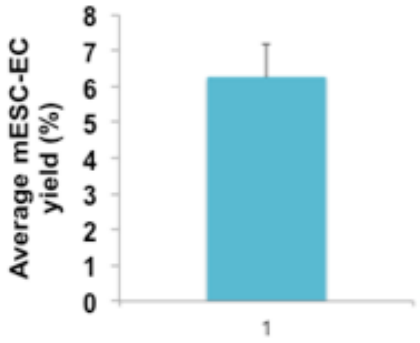

Figure 4.2 Yield of mESC-ECs. The average yield of mESC-ECs was ~6.3% (n=3). This was calculated by counting the LDL positive cells and the total number of cells in a well.

4.3.2 Characterization of mESC-ECs

Isolated mESC-ECs positive for LDL were expanded and cultured for up to 15 passages. Cultured mESC-ECs exhibited a cobblestone morphology as shown in Figure 4.3A. To determine whether these cells express an endothelial cell adhesion marker, PECAM1, a western blot analysis was performed on cells at various stages of differentiation. It was found that while undifferentiated mESCs and cells differentiated for up to 15 days do not express PECAM1, only isolated and cultured mESC-ECs express PECAM1 (Figure 4.3B). In order to determine the purity of the cultured cell population, a FACS analysis using PECAM1 was performed. Figure 4.3C shows that 99% of mESC-ECs express

PECAM1, confirming that the isolated cell population is a pure endothelial cell population.

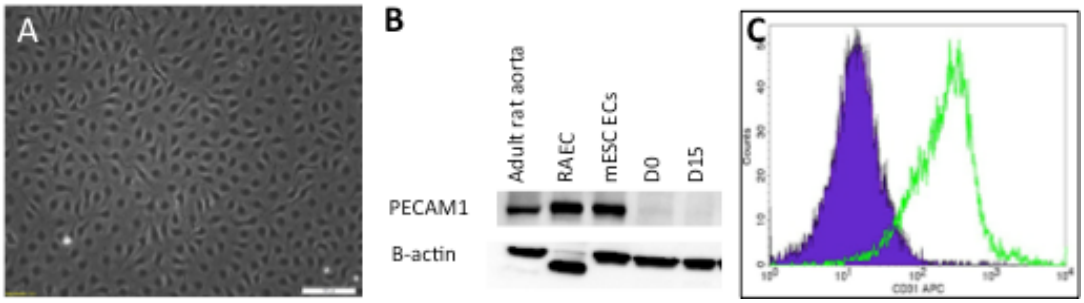

Figure 4.3 Characterization of mESC-ECs. (A) A representative phase contrast image showing mESC-ECs (Passage 7) exhibiting cobblestone morphology in culture. Scale bar: 100 µm. (B) Western blot analysis showing PECAM1 expression only by isolated mESC-ECs, and not by undifferentiated mESC or mESC at earlier time points of differentiation i.e before day 15. Rat aortic tissue lysate and primary RAECs served as positive controls and beta actin served as a loading control. (C) FACS histogram demonstrating a complete shift of peak for PECAM1 positive mESC-ECs (green) compared to isotype control (purple).

Moreover, immunohistochemistry results revealed that these cells express basement membrane proteins such as collagen type IV, laminin and fibronectin in culture (Figure 4.4 A, B and C, respectively), although difference in the protein expression level at various culture times was not observed.

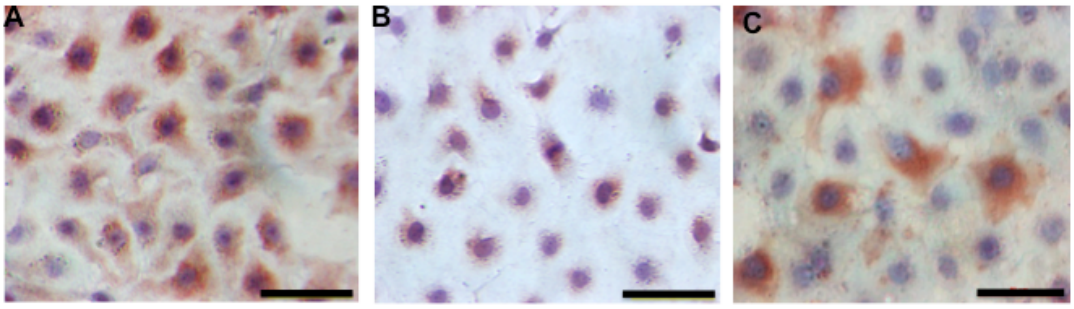

Figure 4.4 Basement Membrane Protein Expression by mESC-ECs. Representative immunohistochemical micrographs demonstrating the deposition of (A) collagen type IV, (B) fibronectin and (C) laminin by cultured mESC-ECs. Scale bar : 100 μm.

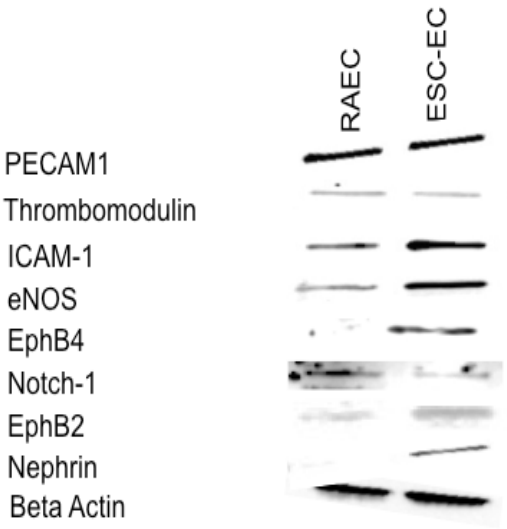

Figure 4.5 Western Blot Characterization of mESC-ECs. Western blot analysis showing PECAM1 expression only by isolated mESC-ECs, and not by undifferentiated mESC or mESC at earlier time points of differentiation i.e., Day 15. Rat aortic tissue lysate and primary rat aortic endothelial cells served as positive controls and Beta actin served as a loading control.

Figure 4.5 demonstrates that cultured mESC-ECs express classical endothelial markers such as thrombomodulin, eNOS and ICAM-1 in addition to PECAM1 and EphB2. Unlike RAECs that only express an arterial marker, Notch-1, mESC-ECs express both venous and arterial markers, EphB4 and Notch-1, respectively. More importantly mESC-ECs express nephrin, which is known as one of the islet endothelial cell specific markers.

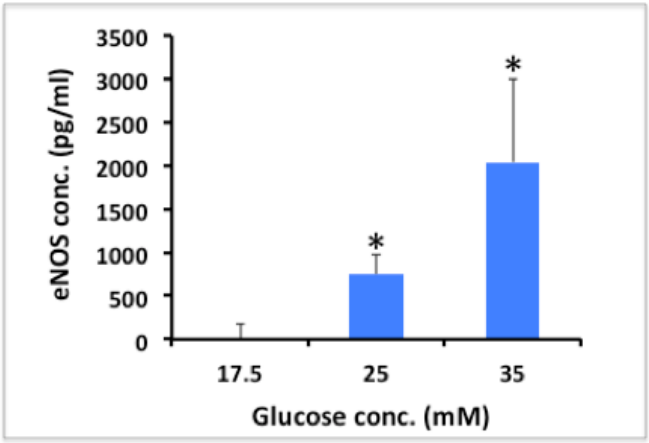

Figure 4.6. eNOS Expression in mES Cell Derived ECs. Expression of endothelial nitric oxide synthases (eNOS) expression by mESC-ECs exposed to different glucose levels (25mM and 35mM) in the medium. Significant increase in eNOS expression by mESC-ECs was observed when exposed to higher glucose concentration, demonstrating glucose-dependent eNOS expression. The DMEM/F12 culture medium containing 17.5 mM of glucose served as a control ($n=3$, $p<0.05$).

To determine whether eNOS expression by mESC-ECs is glucose-dependent, cells were subjected to different glucose concentrations. Negligible amount of eNOS was detected in the culture medium, which contains 17.5 mM glucose (Figure 4.6). However,

when the cells were exposed to higher glucose concentration of either 25 mM or 35 mM, eNOS expression was significantly upregulated ($n=5$, $p < 0.05$). Since the cells were cultured in medium containing 17.5 mM glucose, it was considered as a baseline glucose level and 25 mM and 35 mM concentrations were chosen. However, it is important to culture cells in low glucose containing medium to further examine the effects of glucose concentration on eNOS expression.

As the number of mESC-ECs progressively increased in the differentiation culture, VEGF ELISA was performed to examine the presence of VEGF in the culture, and to determine whether VEGF plays a role in the appearance of the endothelial cell. Culture medium was collected from various time points during the differentiation, and fresh medium was used as a control. Culture medium used to culture mESC-EC was also tested to identify the origin of VEGF. The VEGF ELISA results showed a significant increase in VEGF concentrations at day 20 of differentiation compared to that of fresh culture medium (Figure 4.7). This day 20 of differentiation coincides with when LDL positive cells were first detected in the culture. It was also observed that the VEGF concentration is significantly higher in culture medium at day 33 compared to day 20 of

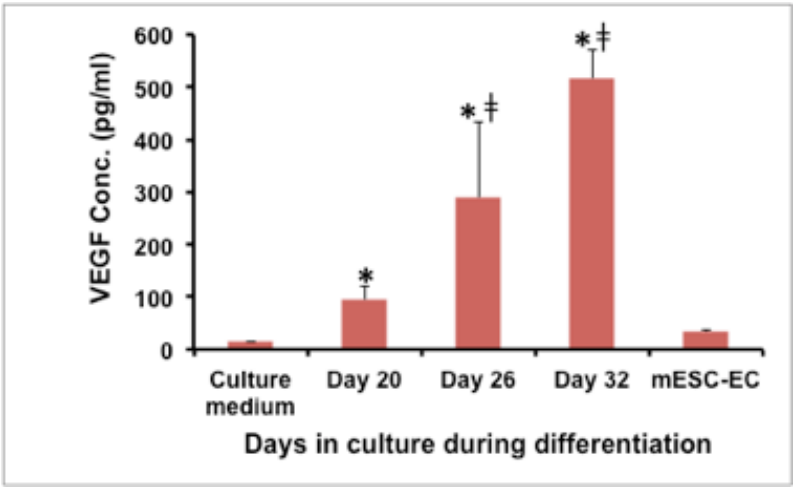

Figure 4.7 VEGF Expression in Differentiation Culture. VEGF concentrations in culture medium measured at various time points (day 20, 26, and 32) during differentiation. VEGF was significantly higher in measured time points compared to that of fresh culture medium. Increasing trend of VEGF with more days in culture was observed ($n=3$, $p<0.05$).

differentiation. The increase of VEGF expression in culture correlates to the increasing number of endothelial cells as the differentiation progresses. However, since it was found that cultured mESC-EC do not produce significant amounts of VEGF in culture, insulin positive cells are likely to be the main source of VEGF in the differentiation culture. Moreover, the addition of either 10 μM or 20 μM of Thalidomide, an angiogenesis inhibitor in the culture for 18 days resulted in a significantly less number of LDL positive endothelial cells at the end of the differentiation as shown in Figure 4.8, indicating that VEGF is necessary for mESC-EC formation.

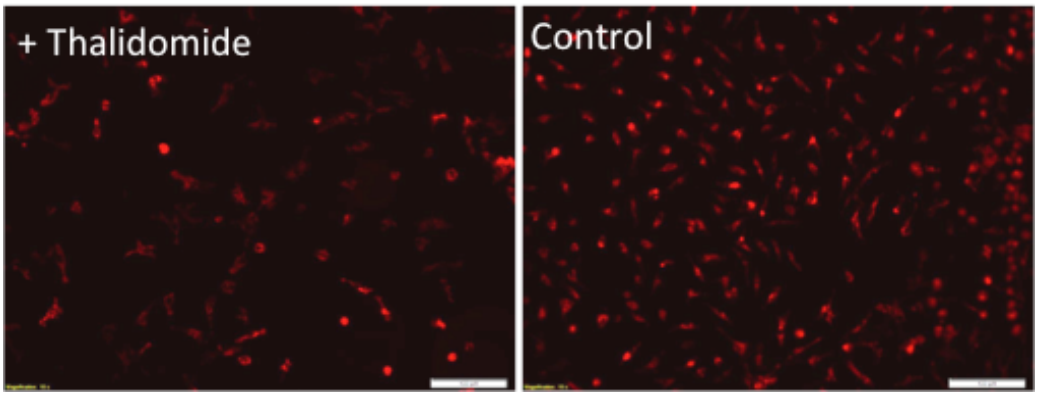

Figure 4.8. Effect of Thalidomide on mESC-EC Yield. mESC-ECs exposed to Thalidomide had reduced numbers of cells that were positive for LDL uptake (Red) compared to the control samples (Scale bar: 100 μm).

Previous studies have suggested that beta cells are unable to form a basement membrane on their own and hence they recruit endothelial cells to deposit basement membrane proteins for them [154]. In order to check if the mESC-ECs were capable of depositing basement membrane proteins in the pancreatic differentiation culture, the dishes with DTZ positive clusters were fixed and stained with basement membrane proteins such as laminin and collagen type IV. It was observed that the cells surrounding the DTZ+ clusters stained positive suggesting that the endothelial cells were capable of depositing the ECM proteins in the differentiating culture (Figure 4.9). This also reinforces the interplay of signaling that happens between the developing beta cells and the endothelial cells.

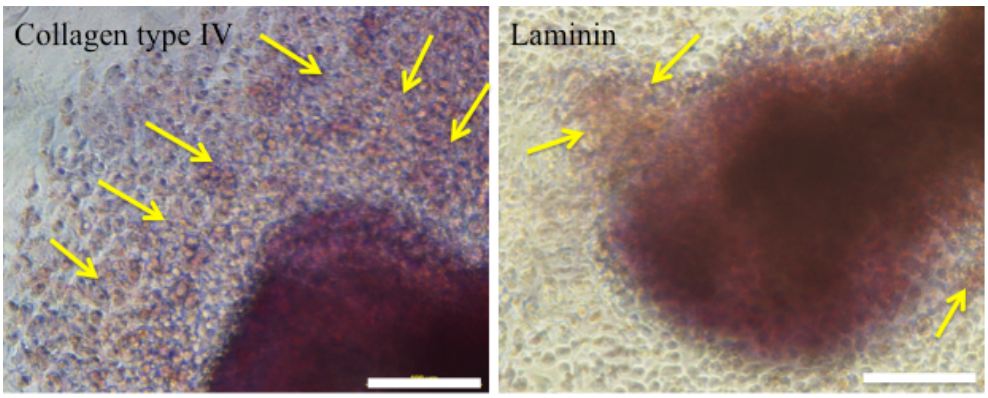

Figure 4.9 Basement Membrane Protein Staining in Differentiation Culture. Immunohistochemical staining demonstrated expression of collagen type IV and laminin by the cells surrounding DTZ+ clusters as shown by yellow arrows. The cells were counterstained with Hematoxylin. Scale bar: 100um.

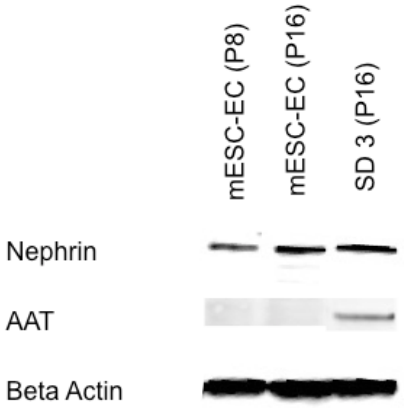

Figure 4.10 Expression of Islet Endothelial Specific Marker by mESC-ECs at Higher Passage. A western blot analysis demonstrated the presence of islet endothelial specific markers such as Nephrin and AAT on mESC-ECs at Passage 8, passage 16 and in 3D collagen gels made with mESC-EC (P16) and cultured for 3 days under static conditions. Beta actin was used as a loading control.

In order to test whether the mES derived endothelial cells were capable of maintaining their islet endothelial specific marker even after repeated passaging, a western blot analysis was performed on cells from passage 16. It was found that the cells continued to express islet endothelial specific markers such as Nephrin and AAT (Figure 4.10).

4.3.3 Angiogenic Capacity of mESC-ECs.

When mESC-ECs were cultured on a layer of Matrigel, they were able to spontaneously organize into cord-like structures, which were maintained for up to 48 hours as shown in Figure 4.11. This *in vitro* Matrigel angiogenesis assay demonstrates the angiogenic capacity of mESC-ECs, consistent with known characteristics of endothelial cells [261].

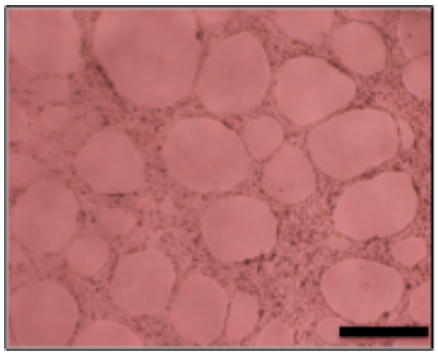

Figure 4.11. Angiogenic Capacity of mESC-ECs. mESC-ECs plated on Matrigel formed tube-like structures 12 hours after plating (Scale bar: 500 μm).

Furthermore, to examine mESC-EC behavior in a 3D environment, collagen gels were created by a sandwich method, which contained two layers of cells prepared in between three layers of collagen. The method was modified to include up to three layers of cells embedded between the collagen gel layers. Further modifications reduced the gel

preparation time from 72 hours to 9 hours. A schematic of the gel preparation method has been shown in Figure 4.12 and a schematic with the final dimensions of the multilayered sandwich gel has been shown in Figure 4.13.

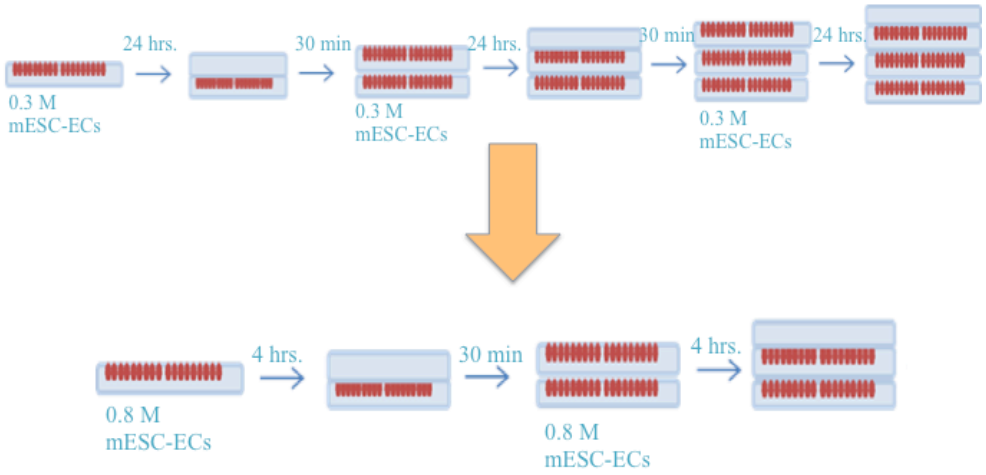

Figure 4.12. Schematic of the multi layered sandwich gel making procedure. The top figure shows the previous method that was used for making multi-decked gels. mESC-ECs were plated on a layer of collagen gel and allowed to spread out for 24 hours, before another layer of collagen was added on top. This layer was allowed to incubate for 30 minutes before adding a second layer of mESC-ECs on top. Again, the cells were allowed to spread out for 24 hours and a third layer of collagen was added. A total of three cell layers were added following the same procedure. After the final layer of collagen was added the gel assembly was allowed to incubate for 30 minutes and then medium was added. This method was optimized to decrease total gel preparation time. The modified method had only two cell layers sandwiched between three layers of collagen gel. Further, the cell layer was allowed to spread out for about 4 hours before another layer of collagen gel was added on top. This reduced the gel preparation time from 72 hours to 9 hours.

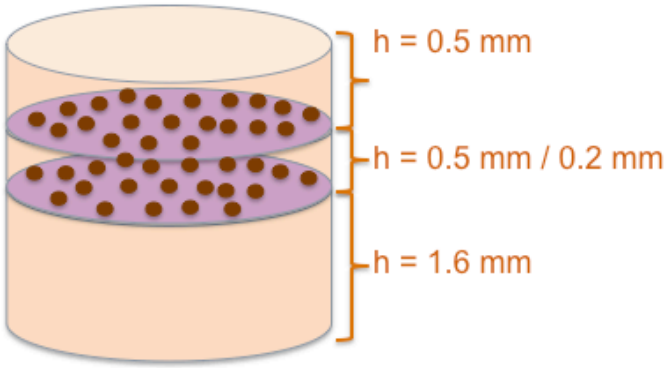

Figure 4.13. Schematic of the mESC-EC Multilayered Sandwich Collagen Gel. The sandwich gel had two cell layers sandwiched in between the three gel layers. The gel layers were 0.5mm, 0.2 mm/0.5 mm and 1.6 mm thick from top to bottom. 0.8 million cells were added in each layer of the gel.

Cells within each layer were spread out and formed networks with the neighboring cells after 5 days in culture, as demonstrated by F-actin staining (Figure 4.14A). Although connections between cells across two separate layers were not observed, cells within the layer formed lumen like structures in the 3D collagen gels. This was apparent in cross-sections of gels stained with Hematoxylin & Eosin (H&E) (Figure 4.14B). A representative immunofluorescence image further confirmed that the lumens were lined with PECAM1 positive mESC-ECs (Figure 4.14C).

To check if the distance between the mESC layers will impact the formation of lumens, gels with 0.2 mm and 0.5 mm distance between the cell layers were made. Interestingly, it was observed that the number of lumens seemed to increase when the distance between the mESC layers was reduced from 0.5 mm to 0.2 mm, as shown in Figure 4.15.

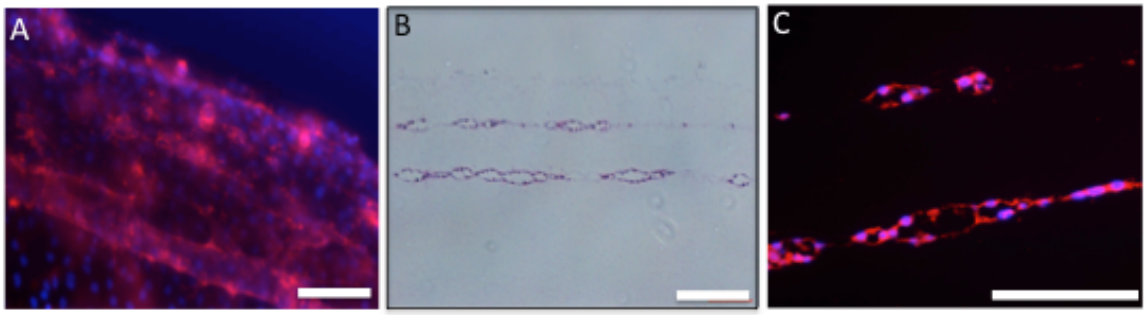

Figure 4.14 mESC-EC Behavior Inside Collagen Gels. (A) Rhodamine-phalloidin conjugated F-Actin staining revealed formation of lumen-like structures by mESC-ECs cultured in a sandwiched 3D collagen gel. Scale bar: 100 μm (B) A cross-sectional Hematoxylin and eosin (H&E) micrograph demonstrating lumen like structures in both cell layers. Scale bar: 100 μm (C) Immunofluorescence image confirming the presence of lumens lined by PECAM1 positive endothelial cells (shown by yellow arrows). Scale bar: 50 μm

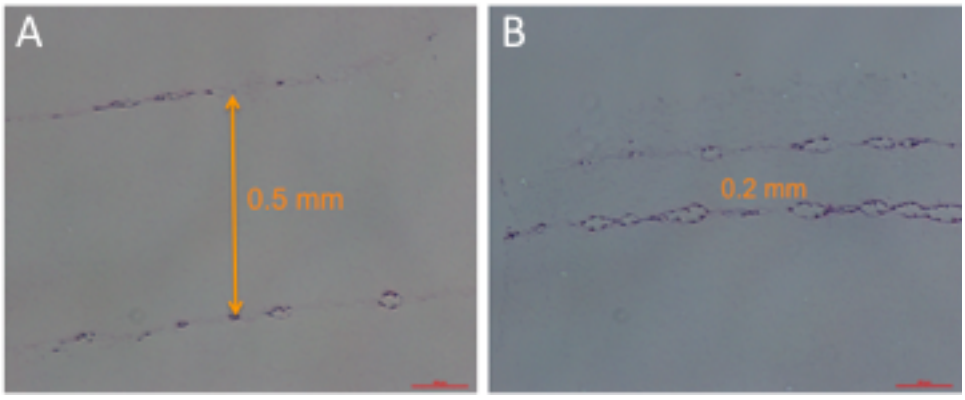

Figure 4.15 Lumen Formation in Static Gels. Lumen formation was observed in the histology sections of the statically cultured mESC-EC gels. (A) shows the two mESC-EC layer in the sandwich gel with the distance between the two cell layers being 0.5 mm while (B) shows the gel with the separating distance as 0.2 mm. The right panel displayed an increased number of lumens compared to the left panel. Scale bar: 100 μm.

Although lumen formation was observed in the collagen gels cultured, no interaction was detected to occur between the two cell layers within the collagen gels. In an effort to induce interaction between endothelial cell layers flow was applied to the collagen gels using a previously described perfusion bioreactor setup [238]. The most noticeable difference in the statically cultured gels and flow-cultured gels was the thickness of the samples. When flow was initially applied to the collagen gels at the rate of 2 ml/min, a significant compaction of the gel was observed. Collagen gels with a range of initial thickness from 11 mm to 3.5 mm were tested and it was found that the final thickness became less than 1 mm at the end of five days of flow as shown in Figure 4.16. The flowrate was reduced to 0.5 ml/min to reduce the compaction and erosion of the gel under the higher flowrate. Even with the application of flow no interbridging of the cell layers was observed as shown in Figure 4.17.

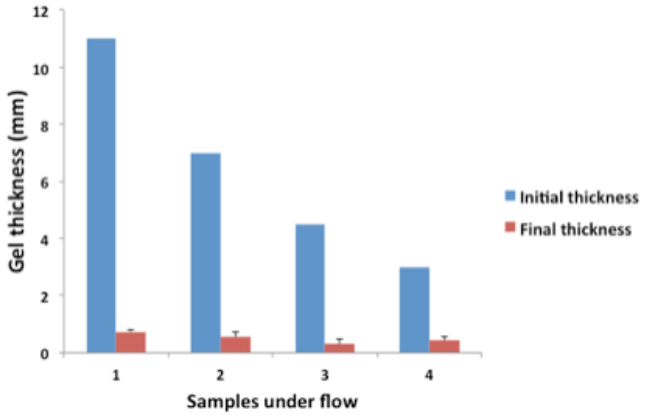

Figure 4.16 Multi Layered Sandwich Collagen Gel Compaction Under Flow. Collagen gels seeded with mESC experienced considerable compaction under flow. The initial thicknesses tested ranged from 11 mm to 3.5 mm. After 5 days of flow, considerable compaction was observed and the final thickness came down to less than 1 mm.

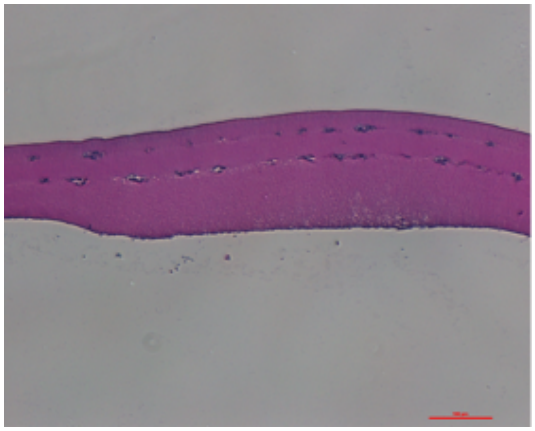

Figure 4.17 mESC-EC Behavior inside Collagen Gels Under Flow. A cross-sectional Hematoxylin and eosin (H&E) micrograph of a collagen gel cultured under flow demonstrated lumen like structures in both cell layers. However, no inter bridging was observed between the two cell layers Scale bar: 100 μm.

The expression pattern of AAT was analyzed in static and flow culture conditions. Interestingly, it was found that while mESC-ECs in a traditional 2D culture do not express AAT, they expressed AAT when cultured in a 3D collagen gel environment, both under static and flow culture conditions as shown in Figure 4.18.

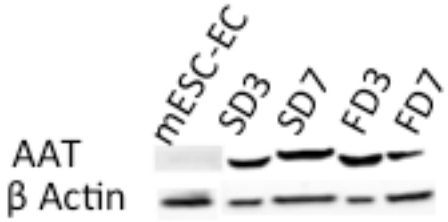

Figure 4.18 AAT Expression by mESC-ECs in 3D Culture System. Western blot analysis shows the expression of AAT by mESC-ECs in collagen gels after 3 and 7 days of static as well as flow culture but not by mESC-ECs cultured in a 2D condition. Beta actin served as a loading control. SD= mESC-EC collagen gel under static conditions for Days 3/7, FD = mESC-EC collagen gel under flow for Days 3/7.

Past studies have shown that VEGF promotes sprouting angiogenesis and has been used by several groups to create vasculature in various culture systems. VEGF was added in the culture medium at 5 ng/ml concentration and was used for culturing collagen gels seeded with mESC-ECs in both static and flow culture conditions. Actin staining for VEGF supplemented gels at Day 5 in static and flow culture conditions is shown in Figure 4.19. A western blot performed on the VEGF supplemented gels and the control gels showed the expression of eNOS by mESC-ECs in 3D culture conditions in static or flow conditions (Figure 4.20).

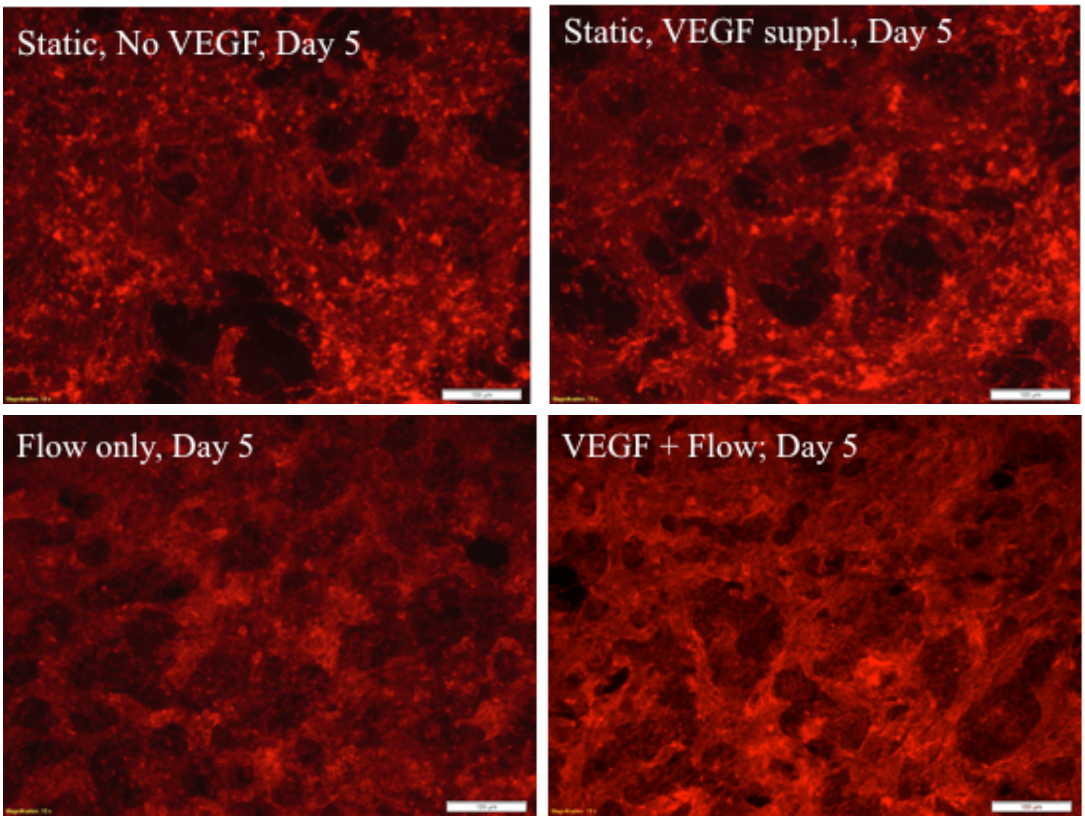

Figure 4.19 Actin Staining on VEGF Supplemented mESC-EC Collagen Gels. Multilayered sandwich collagen gels were cultured under static and flow culture condition with or without the addition of VEGF for 5 dyas before being fixed and stained with rhodamine-phalloidin conjugated f-actin (red). Scale bar: 100 μm.

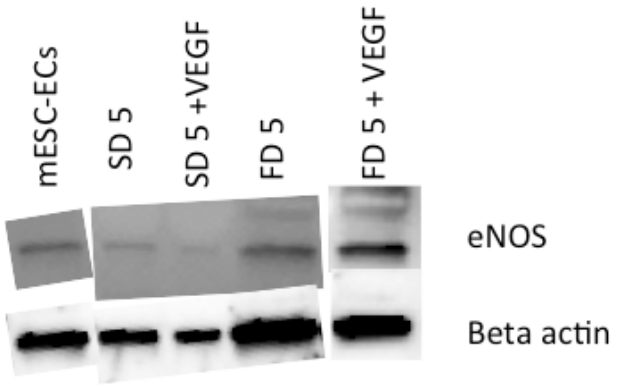

Figure 4.20 eNOS Expression in VEGF Supplemented Collagen Gels. A western blot analysis shows the expression of eNOS in the VEGF supplemented gels cultured in static and flow conditions at Day 5. Beta actin was used as a loading control.

4.4 Discussion

In this study, we describe the identification, isolation and characterization of a pure endothelial cell population exhibiting islet microvascular endothelial cell phenotype derived from mESC. These cells appeared as a side-product in mESC differentiation into pancreatic beta cell culture following a previously established protocol [73]. This is a unique finding, as differentiation was not achieved through a conventional direct differentiation method, which uses successive maturation steps to derive endothelial cells. While endothelial cells are recognized as a highly heterogeneous population exhibiting different phenotypes and functions depending on the location of the endothelium within the body [262], tissue-specific endothelial cell populations, especially derived from pluripotent stem cells *in vitro* have not been demonstrated. Thus, to the best of our knowledge, this is the first report on stem cell derived islet specific endothelial cells.

The isolated mESC-EC population incorporates Dio-ac-LDL, which is a hallmark of mature endothelial cells. In addition, they exhibit classical endothelial-specific markers such as PECAM1, eNOS and thrombomodulin, which are essential to endothelial adhesion and vascular network formation even at high passage numbers ($p \geq 15$). mESC-ECs also express EphB2, which is known to play an important role in sprouting angiogenesis [263, 264]. Unlike a previous study that showed expression of PECAM1 by mESC [261], our results demonstrated that neither our mESC nor cells during early differentiation periods express PECAM1. Only cells selectively isolated from the differentiation culture exhibited expression of PECAM1, indicating a pure population of isolated endothelial cells. Endothelial cells are generally considered to exhibit cobblestone morphology in culture; however these cells can vary in thickness, aspect ratio, and orientation *in vivo*. In the presented study, the mESC-ECs initially had more of an elongated morphology when first detected near insulin-producing cells, which is consistent with previous reports on primary human and rat IECs [265]. Upon culturing in endothelial cell medium, however, they progressed more towards a cobblestone like morphology. As information on mouse IECs is currently lacking due to difficulty in deriving purified IECs, whether the morphological changes induced any functional changes needs further studies. However, detailed characterization of these cells was performed on cultured mESC-ECs with cobblestone morphology and as the cells possessed properties of islet specific endothelial cells, significant functional difference due to morphological changes was not expected.

Pancreatic beta cells are unable to form a basement membrane in the absence of IECs [154]. Instead, endothelial cells secrete proteins that are known to promote insulin

producing cell proliferation and insulin regulation [118, 154, 205]. IEC secreted collagen type IV is shown to potentiate insulin secretion via interaction with integrin α1β1 on beta cells [266]. Likewise, laminin has been shown to up-regulate insulin gene expression and secretion and induce beta cell differentiation and proliferation [154, 155, 267]. Through immunohistochemical analysis, it was found that mESC-ECs in close proximity to insulin positive cells deposit collagen type IV and laminin during differentiation culture. Isolated mESC-ECs in culture also secret ECM proteins such as fibronectin, laminin, and collagen type IV. This further confirms their endothelial cell phenotype and provides additional evidence for possible interactions of mESC-ECs with the pancreatic beta cell populations.

Although the cells formed lumens in 3D collagen gels, cell branching between the two layers was not observed. Application of flow and addition of VEGF was hypothesized to induce the cell branching. Actin staining in the flow gels and the VEGF supplemented gels revealed a more tortuous structure of cell networks but histological sections did not reveal connections between the two cell layers (data not shown).

It has previously been shown that VEGF plays an important role in recruitment of endothelial cells and formation of IEC fenestrations [149, 268-270]. Our results demonstrate the presence of VEGF in the culture medium during differentiation, which progressively increases with more days in culture. This increased concentration of VEGF coincided with the increased number of mESC-ECs. As our populations of endothelial cells were detected in the vicinity of insulin-producing cells, it is plausible that the signals originating from endodermal pancreatic cells induced formation and growth of endothelial cell population in the differentiation culture. Since it was found that mESC-ECs do not produce significant amounts of VEGF in culture and pancreatic beta cells are

known to constitutively secrete VEGF to recruit endothelial cells [154], it is likely that VEGF is mostly originated from insulin producing beta cells in our culture. Moreover, as IECs are known to constitutively express VEGF-R1 (Flk-1) [271-273] enabling them to bind to VEGF, the expression of FLK1 by our isolated mESC-ECs further supports the hypothesis that pancreatic beta cells plays an important role in endothelial cell growth although the exact mechanisms involved needs to be further elucidated. Addition of Thalidomide, an angiogenesis inhibitor [260] substantially suppressed the formation of mESC-ECs in our culture. Future studies with addition of VEGF receptor antagonists in the culture medium will be necessary to ascertain the role of VEGF in mediating the formation of mESC-ECs in the differentiation culture.

In addition to classical endothelial cell phenotype, mESC-ECs exhibit distinct functional characteristics of IECs that are manifested by unique markers that can aid in their identification. mESC-ECs express nephrin, which is considered one of the specific IEC marker as shown by Zanone *et al*. [265]. While nephrin is expressed by other cell types including podocytes in kidneys [274], some parts of the central nervous system in mice [275, 276] and by the Sertoli cells where it forms the blood-testis barrier [277], other tissue-specific endothelial cells have not been shown to express nephrin. The precise function of nephrin on IECs however, remains unknown. Studies have also shown that AAT is another IEC specific marker that is not expressed by endothelial cells in surrounding tissues [278]. A study by Zhang *et al.* showed that AAT significantly reduces cytokine and streptozotocin induced pancreatic beta cell apoptosis [279]. Additionally, the administration of clinical grade AAT after islet transplantation has been shown to improve the graft survival in mice [280, 281]. While our mESC-ECs cultured in traditional 2D

condition do not express AAT, it is important to note that mESC-ECs cultured in a 3D collagen gel environment express AAT. As endothelial cells may lose some of their phenotypical characteristics when maintained in a 2D culture condition, it is possible that mESC-ECs cultured in a 3D condition regained their AAT expression, which was originally down-regulated from long-term 2D culture. This indicates the need for a physiological microenvironment to maintain phenotype and function of cells *in vitro*.

Moreover, IECs are known to produce a host of vasodilators including nitric oxide (NO) [143]. NO is generated by NO synthase (NOS) and eNOS is the major NOS isoform predominantly expressed in endothelium. Both constitutive and cytokine induced eNOS are present in pancreatic islets, although the role of constitutive eNOS in beta cell physiology has been controversial [282]. Studies using islet cells and beta cell lines have reported that the constitutive eNOS either stimulates [283-288] or inhibits [289-295] the insulin release. Unlike other endothelium, constitutive and cytokine inducible eNOS in islets is specifically upregulated depending on glucose levels [282]. Thus, the fact that our mESC-ECs express eNOS, which is regulated by glucose levels of 25-35 mM in the culture medium, further demonstrates their behavior as IECs. However, eNOS expression was not significantly upregulated in culture medium containing 17.5 mM of glucose, which is much higher than physiological glucose levels for endothelial cells at 4mM-6mM [167, 296, 297]. Since mESC-ECs were cultured using medium containing 17.5 mM of glucose, it is plausible that cells have become insensitivity to that glucose level from being exposed for prolonged time. Thus, additional stimuli such as cytokines may be required to induce cells to produce eNOS at that level.

Given the increasing interest in tissue-specific endothelial cell populations, the availability of an unlimited source of IECs derived from pluripotent stem cells provide a promising source of cells for both research and clinical use. Although primary endothelial cells are widely used in *in vitro* studies, stem cell-derived endothelial cells, especially organ-specific endothelial cells, provide the opportunity to further study their specific functions in *in vitro* conditions. Better understanding of mESC-EC function and their interaction with their neighboring pancreatic beta cells can lead to significant advancements in the development of therapeutic strategies for diabetes treatment.

CHAPTER 5

SUMMARY AND FUTURE DIRECTIONS

In summary, this thesis describes methods to develop 3D engineered tissue system as an *in vitro* model to enhance survival and function of IPCs derived from mES cells. First of all, IPCs were successfully derived from mouse embryonic stem cells. Not only did the differentiated IPCs expressed beta cell specific markers such as FoxA2, Sox17, Pdx1, Insulin, C-peptide, Pax4, Nkx6.1, Glut2 and EphrinA5, but they also displayed glucose responsiveness when exposed to low and high concentrations of glucose. The differentiation yield of the IPCs was however only 5.76%, suggesting that further optimization to the protocol is needed to improve the efficiencies. It was further observed that the yield increased significantly upon increasing the duration of culture by additional 7 days suggesting that culture duration was an important factor governing the differentiation yield. It is also critical to identify other cell types that are present in the culture as they may play a supporting role in the development of IPCs. Tumor formation was not observed in the cultures in *in vitro* condition but the possibility of tumor formation in *in vivo* condition needs to be examined.

Secondly, simple 3D engineered tissues were developed to mimic the native environment that the islet cells reside in. The 3D collagen tissue environment allowed better maintenance of IPC viability for up to 5 days compared to IPCs on a poly-ornithine and laminin coated surface. However, IPCs lost their glucose responsiveness in 3D condition. Their basal insulin level was 10 μg/ml, but this level did not increase when exposed to a high glucose condition. There are several possible factors that may attribute

to this functional change. When IPCs are selectively picked from the culture to form 3D tissues, they are being removed from the other cell types in the differentiated culture as well as from basement membrane proteins deposited by other cells. The presence of other cell types and ECM proteins not only play a supporting role in the development of the IPCs but also, may be instrumental in the maintenance of beta cell specific characteristics. In addition, as islet ECM is richly populated with laminins, collagen type IV and several proteoglycans, collagen gel supplemented or immobilized with ECM proteins may improve the glucose responsiveness of isolated IPCs in 3D tissue environment. Another factor that may have contributed to the loss of glucose responsiveness is the glucose concentration of the culture medium used. Past studies have reported evidence that exposure to high glucose medium de-sensitized rat and human islets and impaired their function in response to a glucose challenge [221, 244, 245]. The medium used in this study contained about 17.5 mM of glucose and as this is considerably higher than the physiological level of 4-6 mM, it is possible that the cells were rendered glucose unresponsive because of exposure to the medium used. Transition to low glucose conditions during final stages of differentiation can also be employed to improve glucose responsiveness as has been previously [76].

It has also been suggested that during development mesenchymal cells surround the budding pancreas and their loss impairs the development and proliferation of insulin producing beta cells [298] because the pancreatic mesenchyme and the innervating neural cells govern important aspects of the pancreas organogenesis [298-300]. Beta-cell phenotype is easily lost upon removal from their native environment [301, 302]. Identification of this supporting cell population in the differentiation culture will be an

important step in making the IPCs glucose responsive. If this cell population is identified it can be used for potential co-culture with IPCs to improve their outcome in 3D culture systems.

To facilitate nutrient diffusion and gas exchange on IPCs in 3D collagen tissues, perfusion flow was applied for 5 days in culture. A flowrate of 0.5 ml/min was chosen for our study. Although this flowrate translates in the microvasculature to a shear stress of ~0.71 dyne/cm^2 [238], it is considerably higher than the flowrate in rat islets i.e., 2 x 10^{-5} ml/min [142, 243]. Higher cell death was observed in tissues exposed to flow compared to statically cultured tissues. The outcome with a lower flow-rate or shorter culture duration might be very different. It is also possible that IPCs inherently do not have a favorable response to flow application. Studies have provided evidence of the detrimental behavior of epithelial cells to flow exposure [303]. As beta cells are of epithelial origin, it is possible that they behave poorly under flow culture condition. Thus, various parameters including different flowrates, stiffness of the tissue, cell concentrations, etc. need to be carefully examined and optimized to decide the most suitable culture condition.

Since islet beta cells are in close relation to vascular endothelial cells, mES derived IPCs were co-cultured with ECs in 3D collagen tissues to provide a more physiological environment to the IPCs. It was found that the co-culture with mESC-ECs improved survival of the IPCs in both static and flow culture condition. However, the co-culture tissue was not glucose responsive from 5 days in culture. A similar behavior was observed for co-culture gels under flow condition. Extending the co-culture duration to 14 days might improve the glucose responsiveness, as longer culture duration increased

the glucose, responsiveness in a previously reported study [304]. Although the ECs appeared spread out in the co-culture tissues as visualized through live dead staining, advanced characterization of the co-culture tissue to assess the degree of vascularization is required. Histological sectioning of the co-culture tissue and further staining for cell specific markers will be important to study the interactions between IPCs and ECs.

It was found that the mESC derived IPCs and ECs expressed EphrinA5 and EphB2, respectively. EphB2 is expressed by ECs and EphrinA5 is present on beta cells and it has been shown that these proteins interact with each other with high affinity [236]. EphB2 was found highly upregulated in mESC-ECs when they were plated on Matrigel suggesting that it might play a role in vasculogenesis. EphrinA5 expression was observed in IPCs in all different culture conditions and did not show significant changes upon application of flow. The interaction between these two proteins was not analyzed. As EphrinA5 is important in beta cell-to-cell communication and in glucose sensing it will be interesting to see how its expression changes at different culture conditions and whether the presence of ECs can enhance the expression of EphrinA5.

Thirdly, mESC-ECs were identified in close vicinity of IPCs and isolated from the IPC differentiation culture. The isolated and cultured mESC-EC population was found to be highly pure. These cells exhibited characteristics unique to the islet endothelium with the expression of nephrin, Flk-1 and AAT in addition to the expression of classical endothelial cell markers. Moreover, these cells regulate their eNOS levels based on glucose levels. The mESC-ECs also showed cord formation on Matrigel and upon embedding inside collagen gels, which is a classic behavior of endothelial cells. An increasing VEGF gradient with days in culture corresponded with increased number of

mESC-ECs, suggesting that VEGF might play a role in the derivation of ECs. Upon addition of thalidomide, a potent angiogenesis inhibitor, the number of ECs was greatly reduced in culture. This is the first demonstration of a tissue specific endothelial cell type derivation from mES cells and is completely novel. The derivation of such specialized endothelial cells creates exciting opportunities to study their function in *in vitro* conditions as well as their interactions with the tissue specific cells – beta cells in this case.

It is important to note that there are some inherent limitations of the culture system. The total cell population in the co-culture tissues is formed by IPCs and mESC-ECs, while the 2D culture was formed entirely of IPCs. Hence, gene expression of beta cell specific markers appears lower than its actual value in the co-culture samples. To accurately compare the gene expression levels in both the conditions a 2D co-culture of mES derived IPCs and ECs is required. This can be effective in teasing apart the specific effects of co-culture and 2D vs. 3D environment. Gene expression analysis studies revealed that insulin gene expression was significantly higher in the co-culture in static condition compared to flow condition. Further studies are needed to determine the effects of culture conditions and application of flow on beta cell specific gene expression. Moreover, additional studies are needed to determine whether IPCs can gain glucose responsiveness upon transplantation in concurrence with previous studies [95, 172].

In conclusion, the presented study demonstrates useful strategies to develop a 3D insulin producing tissue using mES cells. While no significant improvements were seen in the glucose responsiveness in 3D culture conditions in static or flow culture conditions, this study describes includes preliminary design considerations that can be further

extended in developing functional 3D insulin-producing tissues, and ultimately establishing a long-term clinically relevant strategy. The presented approach will need to be optimized to develop a clinically relevant cell therapy for diabetes in the future.

APPENDIX A

CELL CULTURE MEDIUM RECIPES

The following appendix has the culture medium recipes used for all the presented studies. All mediums were prepared in volumes of 500 ml-1000 ml and were stored at 4 °C. Mediums were prepared in sterile glass bottles and were used within 2-3 months of preparation.

Mouse embryonic fibroblast (MEF) culture medium:

DMEM (High Glucose)	500 ml, Life Technologies, 11965-084
FBS	58 ml, Life Technologies, 16000044
100 X L-Glutamine	5.8 ml, Life Technologies, 25030
100 X Pen./Strep.	5.8 ml, Life Technologies, 15140
100 X NEAA	5.8 ml, Life Technologies, 11140
100X Na-pyruvate	5.8 ml, Life Technologies, 11360

Mouse embryonic stem cell culture medium

DMEM (High Glucose)	500 ml, Life Technologies 11965-084
Knock Out Serum Replacement	90 ml, Life Technologies 10828
100 X L-Glutamine	6 ml, Life Technologies ,25030
100 X Pen./Strep.	6 ml, Life Technologies, 15140
100 X NEAA	6 ml, Life Technologies,11140
100X Na-pyruvate	6 ml, Life Technologies, 11360
2-Mercaptoethanol	4.4ul, Sigma, M6250

It is recommended that LIF is freshly thawed out and added to the media just before use (100 ul/ 50 ml of medium).

Differentiation medium #1

IMDM	400 ml, Life Technologies, 12440-061
FBS	100 ml, Life Technologies, 10828
100 X L-Glutamine	5 ml, Life Technologies, 25030
100 X Pen/Strep.	5 ml, Life Technologies, 15140
1-Thioglycerol	3.9 ul, Sigma, M6145

Differentiation Medium #2

DMEM/F 12 medium	1000 mls, 12500-062
Progesterone	10 ul [Stock 2mM; Final conc. 20 nM, Sigma]
Putresciene	100 ul [Stock 1M; Final conc. 100 uM, Sigma]
Laminin	1 ml, Sigma L2020
Nicotinamide	1 ml [Stock : 1M; final conc. 10mM, Sigma]
Insulin	6.25 ml, Life Technologies, 12585-014
Sodium Selenite	100 ul [Stock: 300 uM; Final conc 30 nM, Sigma]
Apo transferrin	50 mg, Sigma T1147
B 27	20 mls, Life Technologies, 17504-044
Penn Strep	10 mls, Life Technologies, 15140

Endothelial cell culture medium

MCDB 131 Medium	1000 ml, Sigma, M8537
FBS	100 ml, Life Technologies, 10828
Penn Strep	10 ml, Life Technologies, 15140
Endogro	4 ml, VEC Technologies

APPENDIX B

REAGENT RECIPES

This appendix describes the recipes for the various reagents used for all the presented studies. All reagents were were stored at 4 °C. Mediums were prepared in sterile glass bottles and were used within 2-3 months of preparation.

Krebs Ringer Bicarbonate Hepes (KRBH) Buffer:

Solution A:	
Sodium Chloride	6.92 gm.
Potassium Chloride	0.36 gm.
Monopotassium Phosphate	0.16 gm.
Calcium Chloride	0.38 gm.
Magnesium Sulfate Heptahydrate	0.3 gm.
De-Ionized (DI) Water	200 mls.

Solution B:	
Sodium Bicarbonate	2.08 gm.
DI Water	160 mls.

Solution A	200 mls.
Solution B	160 mls.
HEPES	2.4 gm.
BSA	2 gm.

All the contents were mixed and the volume was increased to 1 liter by adding DI water. The pH was adjusted to 7.4 and the solution was filtered through a 0.22 μm filter. The KRBH buffer was then stored at 4°C.

All the reagents were purchased from Sigma unless otherwise stated.

Blocking Buffer for Western Blot Applications

A 5% BSA solution was prepared using TBS-Tween buffer (Boston Bioproducts). The solution was placed on a magnetic stir plate till the BSA was completely in solution. The solution was stored at 4 °C.

Blocking Buffer for Immunofluorescence and Immunohistochemistry

A 10% goat serum solution was made in PBS. This solution was made and used fresh.

Lysis Buffer Cell Lysate Preparation

RIPA Buffer	500 µl
Protease Inhibitor	5 µl
Triton-X 100	5 µl

APPENDIX C

PROTEIN ASSAY PROTOCOLS

This appendix describes the protocol used to the protein quantification using Bradford assay and DC assay.

Bradford Protein Assay:

Bradford reagent will be needed to perform this assay.

1. Prepare and label the correct number of cuvettes: # of your sample + 1 blank + 7 BSA standards (0.125mg/mL, 0.25 mg/mL, 0.5 mg/mL, 0.75 mg/mL, 1 mg/mL, 1.5 mg/mL, 2 mg/mL).
2. Add 20ul of each sample, standards or RIPA buffer to the cuvettes.
3. Add 1 ml of Quick Start Bradford Dye Reagent, warmed to room temperature, into each cuvette. Pipette well to mix. At this point a color change will be observed.
4. Incubate 5 minutes a room temperature before further processing.
5. Start up the BioRad smart Spec plus Spectrophotometer.
6. Measure the absorption values and the concentration of the sample.

DC Protein Assay:

A DC Assay kit will be needed to perform this assay.

1. Add 20 µl of reagent S to each ml of reagent A that will be needed for the run. This is called working reagent A'.
2. Prepare and label the correct number of cuvettes: # of your sample + 1 blank + 7 BSA standards (0.125mg/mL, 0.25 mg/mL, 0.5 mg/mL, 0.75 mg/mL, 1 mg/mL, 1.5 mg/mL, 2 mg/mL).
3. Pipet 20 µl of standards and samples into cuvettes.
4. Add 100 µl of reagent A or A' into each tube.
5. Add 800 µl of reagent B into each test tube and vortex immediately.
6. After 15 min incubation, absorbance can be read at 750 nm.

APPENDIX D

MISCELLANEOUS PROTOCOLS

The following protocol to remove the paraffin coating from histology slides before they were used for immuostaining purposes. It also describes the FACS staining protocol.

De-paraffinization protocol:

1. Wash slides 2X in Xylene for 5 min each.
2. Wash slides 1X in 100% ethanol for 5 min.
3. Wash slides 1X in 95% ethanol for 5 min.
4. Wash slides 1X in 80% ethanol for 5 min.
5. Wash slides 1X in 70% ethanol for 5 min.
6. Wash slides 1X in 50% ethanol for 5 min.
7. Wash slides 2X in DI water for 5 min each.
8. Proceed to permeabilization and staining.

FACS Protocol :

1. Trypsinize and count cells. Use $5x10^5$ to $1x10^6$ cells per 5 ml polystyrene round-bottom tube.
2. Centrifuge the cells to remove the medium.
3. Add ice cold 4% PFA to the cells and allow them to sit for 30 min.
4. Centrifuge and remove the PFA, add 1 ml PBS and spin at 1500 rpm. Discard the PBS and repeat the process 3 times.
5. Add 0.25% Triton X and allow to incubate at RT for 5 min. Do not exceed 5 minutes.
6. Add cold PBS and centrifuge at 1500 rpm for 5 min. Drain the supernatant and re-suspend the cells in 100 µl of cold FACS buffer (PBS + 1% BSA+ 2mM EDTA). Avoid any cell clumps.
   NOTE: Include blank and isotype controls. Blank is just the FACS buffer, and isotype control is cells having just the secondary antibody on them. Blank and isotype control are also fixed and permeabilized. This protocol involved fixing and permeabilization, as the antibody was specific to an intracellular epitope.
7. Allow cells to sit at 4 °C for 10 minutes in the FACS solution, which is also the blocking solution.
8. Add primary antibody directly in the cells + FACS buffer. For CD-31; use 5 µl for 100 µl of FACS buffer.
9. Incubate at 4 °C for 30 minutes over ice.
10. Add 1 ml cold PBS to the tube. Centrifuge at 1200 rpm for 7 minutes at 4 °C. Discard supernatant.

11. Resuspend in 1 ml cold PBS. Centrifuge and discard the supernatant.
12. Resuspend in 100 µl FACS buffer.
13. Add secondary antibody directly to the cells + FACS buffer mix. Use 5 µl for 100 µl of FACS buffer
14. Incubate at 4 °C for 30 minutes over ice.
15. Add 1 ml of cold PBS to each tube. Centrifuge and discard the supernatant.
16. Resuspend in 1 ml cold PBS. Centrifuge and discard the supernatant.
17. Resuspend in 0.3 ml PBS (same amount per tube). Keep at 4 °C until ready for FACS analysis. (Use less than 0.3 ml if low cell count).

REFERENCES

1. Eberhard, D., M. Kragl, and E. Lammert, *'Giving and taking': endothelial and beta-cells in the islets of Langerhans.* Trends Endocrinol Metab, 2010. **21**(8): p. 457-63.

2. Nam, K.H., et al., *Size-based separation and collection of mouse pancreatic islets for functional analysis.* Biomed Microdevices, 2010. **12**(5): p. 865-74.

3. Federation, I.D. *International Diabetes Federation*. 2013; Available from: http://www.idf.org/diabetesatlas/. Accessed: Sep 2014

4. Rorsman, P., et al., *The Cell Physiology of Biphasic Insulin Secretion*. Vol. 15. 2000. 72-77.

5. Pokrywczynska, M., et al., *Differentiation of stem cells into insulin-producing cells: current status and challenges.* Archivum immunologiae et therapiae experimentalis, 2013. **61**(2): p. 149-158.

6. Ellis, H., *Anatomy of the pancreas and the spleen.* Surgery (Oxford), 2013. **31**(6): p. 263-266.

7. American Diabetes Association. *National Diabetes Statistics Report*. Sep 2014; Available from: http://www.diabetes.org/diabetes-basics/statistics/.

8. Suckale, J. and M. Solimena, *Pancreas islets in metabolic signaling--focus on the beta-cell.* Front Biosci, 2008. **13**: p. 7156-71.

9. Livak, K.J. and T.D. Schmittgen, *Analysis of relative gene expression data using real-time quantitative PCR and the 2(-Delta Delta C(T)) Method.* Methods, 2001. **25**(4): p. 402-8.

10. Micallef, S.J., et al., *Retinoic acid induces Pdx1-positive endoderm in differentiating mouse embryonic stem cells.* Diabetes, 2005. **54**(2): p. 301-5.

11. Cryer, P.E., *Hypoglycemia, functional brain failure, and brain death.* The Journal of clinical investigation, 2007. **117**(4): p. 868-870.

12. Gaba, R.C., R. Garcia-Roca, and J. Oberholzer, *Pancreatic islet cell transplantation: An update for interventional radiologists.* Journal of Vascular and Interventional Radiology, 2012. **23**(5): p. 583-594.

13. Beck, J., et al., *Islet encapsulation: strategies to enhance islet cell functions.* Tissue engineering, 2007. **13**(3): p. 589-599.

14. Teramura, Y., Y. Kaneda, and H. Iwata, *Islet-encapsulation in ultra-thin layer-by-layer membranes of poly (vinyl alcohol) anchored to poly (ethylene glycol)–lipids in the cell membrane.* Biomaterials, 2007. **28**(32): p. 4818-4825.

15. Shapiro, A.M.J., et al., *International Trial of the Edmonton Protocol for Islet Transplantation.* New England Journal of Medicine, 2006. **355**(13): p. 1318-1330.

16. Carlsson, P.-O., et al., *Markedly decreased oxygen tension in transplanted rat pancreatic islets irrespective of the implantation site.* Diabetes, 2001. **50**(3): p. 489-495.

17. Barshes, N.R., S. Wyllie, and J.A. Goss, *Inflammation-mediated dysfunction and apoptosis in pancreatic islet transplantation: implications for intrahepatic grafts.* Journal of Leukocyte Biology, 2005. **77**(5): p. 587-597.

18. Alberti, K.G.M.M. and P.Z. Zimmet, *Definition, diagnosis and classification of diabetes mellitus and its complications. Part 1: diagnosis and classification of diabetes mellitus. Provisional report of a WHO Consultation.* Diabetic Medicine, 1998. **15**(7): p. 539-553.

19. *WHO Expert Committee on Diabetes Mellitus: second report.* World Health Organ Tech Rep Ser, 1980. **646**: p. 1-80.

20. Verge, C.F., et al., *Prediction of type I diabetes in first-degree relatives using a combination of insulin, GAD, and ICA512bdc/IA-2 autoantibodies.* Diabetes, 1996. **45**(7): p. 926-933.

21. Betterle, C., et al., *Clinical and subclinical organ-specific autoimmune manifestations in type 1 (insulin-dependent) diabetic patients and their first-degree relatives.* Diabetologia, 1984. **26**(6): p. 431-436.

22. Piñero-Piloña, A., et al., *Idiopathic Type 1 Diabetes in Dallas, Texas: A 5-year experience.* Diabetes Care, 2001. **24**(6): p. 1014-1018.

23. Imagawa, A., et al., *A novel subtype of type 1 diabetes mellitus characterized by a rapid onset and an absence of diabetes-related antibodies.* New England journal of medicine, 2000. **342**(5): p. 301-307.

24. Ahrén, B. and C. Corrigan, *Intermittent need for insulin in a subgroup of diabetic patients in Tanzania.* Diabetic medicine: a journal of the British Diabetic Association, 1985. **2**(4): p. 262-264.

25. Ryan, E.A., et al., *Five-Year Follow-Up After Clinical Islet Transplantation.* Diabetes, 2005. **54**(7): p. 2060-2069.

26. Bennet, W., et al., *Incompatibility between human blood and isolated islets of Langerhans: a finding with implications for clinical intraportal islet transplantation?* Diabetes, 1999. **48**(10): p. 1907-1914.

27. Ozmen, L., et al., *Inhibition of thrombin abrogates the instant blood-mediated inflammatory reaction triggered by isolated human islets: possible application of the thrombin inhibitor melagatran in clinical islet transplantation.* Diabetes, 2002. **51**(6): p. 1779-1784.

28. Rabinovitch, A. and W.L. Suarez-Pinzon, *Cytokines and their roles in pancreatic islet β-cell destruction and insulin-dependent diabetes mellitus.* Biochemical pharmacology, 1998. **55**(8): p. 1139-1149.

29. DeFronzo, R.A., R.C. Bonadonna, and E. Ferrannini, *Pathogenesis of NIDDM: a balanced overview.* Diabetes care, 1992. **15**(3): p. 318-368.

30. Lillioja, S., et al., *Insulin resistance and insulin secretory dysfunction as precursors of non-insulin-dependent diabetes mellitus: prospective studies of Pima Indians.* New England Journal of Medicine, 1993. **329**(27): p. 1988-1992.

31. Mooy, J.M., et al., *Prevalence and determinants of glucose intolerance in a Dutch Caucasian population: the Hoorn Study.* Diabetes care, 1995. **18**(9): p. 1270-1273.

32. Harris, M.I., *Undiagnosed NIDDM: clinical and public health issues.* Diabetes care, 1993. **16**(4): p. 642-652.

33. Simonson, D.C., et al., *Mechanism of improvement in glucose metabolism after chronic glyburide therapy.* Diabetes, 1984. **33**(9): p. 838-845.

34. Wing, R.R., et al., *Caloric restriction per se is a significant factor in improvements in glycemic control and insulin sensitivity during weight loss in obese NIDDM patients.* Diabetes care, 1994. **17**(1): p. 30-36.

35. Zimmet, P.Z., *Kelly West Lecture 1991 challenges in diabetes epidemiology—from West to the rest.* Diabetes care, 1992. **15**(2): p. 232-252.

36. Harris, M.I., *Diabetes in America*. 1995, Elsevier.

37. Valle, T., J. Tuomilehto, and J. Eriksson, *Epidemiology of NIDDM in Europids.* International textbook of diabetes mellitus, 1997. **2**: p. 125-42.

38. De Courten, M., et al., *Epidemiology of NIDDM in non-Europids.* International Textbook of Diabetes Mellitus. 2nd edn. Chichester: John Wiley, 1997. **143**: p. 70.

39. Knowler, W.C., et al., *Determinants of diabetes mellitus in the Pima Indians.* Diabetes Care, 1993. **16**(1): p. 216-227.

40. Group, D.P.P.R., *Reduction in the incidence of type 2 diabetes with lifestyle intervention or metformin.* The New England journal of medicine, 2002. **346**(6): p. 393.

41. Ratner, R.E., *Type 2 diabetes mellitus: the grand overview.* DIABETIC MEDICINE-CHICHESTER-, 1998. **15**: p. S4-S7.

42. Moses, S. Pancreas 2012; Available from: http://www.fpnotebook.com/legacy/GI/Anatomy/PncrsAntmy.htm. Accessed: Sep 2014

43. Taylor, T. *Pancreas*. Endocrine system 1999 [cited 2014; Available from: http://www.innerbody.com/image/endo03.html. Accessed: Sep 2014

44. Weir, G.C. and S. Bonner-Weir, *Islets of Langerhans: the puzzle of intraislet interactions and their relevance to diabetes.* Journal of Clinical Investigation, 1990. **85**(4): p. 983.

45. Lifson, N., et al., *Blood flow to the rabbit pancreas with special reference to the islets of Langerhans.* Gastroenterology, 1980. **79**(3): p. 466-73.

46. Orci, L. and R.H. Unger, *Functional subdivision of islets of Langerhans and possible role of D cells.* Lancet, 1975. **2**(7947): p. 1243-4.

47. Samols, E., S. Bonner-Weir, and G.C. Weir, *Intra-islet insulin-glucagon-somatostatin relationships.* Clin Endocrinol Metab, 1986. **15**(1): p. 33-58.

48. Yukawa, M., et al., *Proportions of various endocrine cells in the pancreatic islets of wood mice (Apodemus speciosus).* Anat Histol Embryol, 1999. **28**(1): p. 13-6.

49. Wieczorek, G., A. Pospischil, and E. Perentes, *A comparative immunohistochemical study of pancreatic islets in laboratory animals (rats, dogs, minipigs, nonhuman primates).* Exp Toxicol Pathol, 1998. **50**(3): p. 151-72.

50. Sujatha, S.R., A. Pulimood, and S. Gunasekaran, *Comparative immunocytochemistry of isolated rat & monkey pancreatic islet cell types.* Indian J Med Res, 2004. **119**(1): p. 38-44.

51. Cabrera, O., et al., *The unique cytoarchitecture of human pancreatic islets has implications for islet cell function.* Proceedings of the National Academy of Sciences of the United States of America, 2006. **103**(7): p. 2334-2339.

52. Bonner-Weir, S. and T.D. O'Brien, *Islets in Type 2 Diabetes: In Honor of Dr. Robert C. Turner.* Diabetes, 2008. **57**(11): p. 2899-2904.

53. Bosco, D., et al., *Expression and secretion of alpha1-proteinase inhibitor are regulated by proinflammatory cytokines in human pancreatic islet cells.* Diabetologia, 2005. **48**(8): p. 1523-1533.

54. Brissova, M., et al., *Assessment of human pancreatic islet architecture and composition by laser scanning confocal microscopy.* Journal of Histochemistry & Cytochemistry, 2005. **53**(9): p. 1087-1097.

55. Newgard, C.B. and J.D. McGarry, *Metabolic coupling factors in pancreatic beta-cell signal transduction.* Annu Rev Biochem, 1995. **64**: p. 689-719.

56. Iynedjian, P.B., *Mammalian glucokinase and its gene.* Biochemical Journal, 1993. **293**(Pt 1): p. 1-13.

57. De Vos, A., et al., *Human and rat beta cells differ in glucose transporter but not in glucokinase gene expression.* Journal of Clinical Investigation, 1995. **96**(5): p. 2489-2495.

58. Dean, P.M. and E.K. Matthews, *Glucose-induced electrical activity in pancreatic islet cells.* The Journal of Physiology, 1970. **210**(2): p. 255-264.

59. Curry, D.L., L.L. Bennett, and G.M. Grodsky, *Requirement for calcium ion in insulin secretion by the perfused rat pancreas.* Am J Physiol, 1968. **214**(1): p. 174-8.

60. Gerich, J.E., et al., *Characterization of the glucagon response to hypoglycemia in man.* The Journal of Clinical Endocrinology & Metabolism, 1974. **38**(1): p. 77-82.

61. Aronoff, S.L., et al., *Glucose Metabolism and Regulation: Beyond Insulin and Glucagon.* Diabetes Spectrum, 2004. **17**(3): p. 183-190.

62. Cryer, P.E. and K. Polonsky, *Glucose homeostasis and hypoglycemia.* Williams textbook of endocrinology, 11th ed. Philadelphia: Saunders, an imprint of Elsevier, Inc, 2008: p. 1503-1533.

63. Moore, C.X. and G.J.S. Cooper, *Co-secretion of amylin and insulin from cultured islet β-cells: Modulation by nutrient secretagogues, islet hormones and hypoglycemic agents.* Biochemical and Biophysical Research Communications, 1991. **179**(1): p. 1-9.

64. Cooper, G., et al., *Purification and characterization of a peptide from amyloid-rich pancreases of type 2 diabetic patients.* Proceedings of the National Academy of Sciences, 1987. **84**(23): p. 8628-8632.

65. Ogawa, A., et al., *Amylin secretion from the rat pancreas and its selective loss after streptozotocin treatment.* Journal of Clinical Investigation, 1990. **85**(3): p. 973.

66. Gedulin, B.R., T.J. Rink, and A.A. Young, *Dose-response for glucagonostatic effect of amylin in rats.* Metabolism, 1997. **46**(1): p. 67-70.

67. Weyer, C., et al., *Amylin replacement with pramlintide as an adjunct to insulin therapy in type 1 and type 2 diabetes mellitus: a physiological approach toward improved metabolic control.* Current pharmaceutical design, 2001. **7**(14): p. 1353-1373.

68. Heise, T., et al., *Effect of pramlintide on symptom, catecholamine, and glucagon responses to hypoglycemia in healthy subjects.* Metabolism, 2004. **53**(9): p. 1227-1232.

69. Samsom, M., et al., *Pramlintide, an amylin analog, selectively delays gastric emptying: potential role of vagal inhibition.* American Journal of Physiology-Gastrointestinal and Liver Physiology, 2000. **278**(6): p. G946-G951.

70. Unger, R., *Glucagon physiology and pathophysiology.* The New England journal of medicine, 1971. **285**(8): p. 443-449.

71. Orci, L., et al., *Cell contacts in human islets of Langerhans.* The Journal of Clinical Endocrinology & Metabolism, 1975. **41**(5): p. 841-844.

72. Gerich, J., et al., *Hormonal mechanisms of recovery from insulin-induced hypoglycemia in man.* Am J Physiol, 1979. **236**(4): p. E380-E385.

73. Schroeder, I.S., et al., *Differentiation of mouse embryonic stem cells to insulin-producing cells.* Nat Protoc, 2006. **1**(2): p. 495-507.

74. Blyszczuk, P., et al., *Expression of Pax4 in embryonic stem cells promotes differentiation of nestin-positive progenitor and insulin-producing cells.* Proceedings of the National Academy of Sciences, 2003. **100**(3): p. 998-1003.

75. Miyazaki, S., E. Yamato, and J.-i. Miyazaki, *Regulated expression of pdx-1 promotes in vitro differentiation of insulin-producing cells from embryonic stem cells.* Diabetes, 2004. **53**(4): p. 1030-1037.

76. Assady, S., et al., *Insulin production by human embryonic stem cells.* Diabetes, 2001. **50**(8): p. 1691-7.

77. Rajagopal, J., et al., *Insulin Staining of ES Cell Progeny from Insulin Uptake.* Science, 2003. **299**(5605): p. 363.

78. Blyszczuk, P., et al., *Embryonic stem cells differentiate into insulin-producing cells without selection of nestin-expressing cells.* Int J Dev Biol, 2004. **48**(10): p. 1095-104.

79. Miyazaki, S., E. Yamato, and J. Miyazaki, *Regulated expression of pdx-1 promotes in vitro differentiation of insulin-producing cells from embryonic stem cells.* Diabetes, 2004. **53**(4): p. 1030-7.

80. Segev, H., et al., *Differentiation of human embryonic stem cells into insulin-producing clusters.* Stem Cells, 2004. **22**(3): p. 265-74.

81. Lavon, N., O. Yanuka, and N. Benvenisty, *The effect of overexpression of Pdx1 and Foxa2 on the differentiation of human embryonic stem cells into pancreatic cells.* Stem Cells, 2006. **24**(8): p. 1923-30.

82. Xu, X., et al., *Endoderm and pancreatic islet lineage differentiation from human embryonic stem cells.* Cloning Stem Cells, 2006. **8**(2): p. 96-107.

83. Soria, B., et al., *Insulin-secreting cells derived from embryonic stem cells normalize glycemia in streptozotocin-induced diabetic mice.* Diabetes, 2000. **49**(2): p. 157-162.

84. Lumelsky, N., et al., *Differentiation of Embryonic Stem Cells to Insulin-Secreting Structures Similar to Pancreatic Islets.* Science, 2001. **292**(5520): p. 1389-1394.

85. Hori, Y., et al., *Growth inhibitors promote differentiation of insulin-producing tissue from embryonic stem cells.* Proceedings of the National Academy of Sciences, 2002. **99**(25): p. 16105-16110.

86. Sipione, S., et al., *Insulin expressing cells from differentiated embryonic stem cells are not beta cells.* Diabetologia, 2004. **47**(3): p. 499-508.

87. Hansson, M., et al., *Artifactual insulin release from differentiated embryonic stem cells.* Diabetes, 2004. **53**(10): p. 2603-9.

88. Boyd, A.S., et al., *A comparison of protocols used to generate insulin-producing cell clusters from mouse embryonic stem cells.* Stem Cells, 2008. **26**(5): p. 1128-37.

89. Blyszczuk, P., et al., *Expression of Pax4 in embryonic stem cells promotes differentiation of nestin-positive progenitor and insulin-producing cells.* Proc Natl Acad Sci U S A, 2003. **100**(3): p. 998-1003.

90. Moritoh, Y., et al., *Analysis of insulin-producing cells during in vitro differentiation from feeder-free embryonic stem cells.* Diabetes, 2003. **52**(5): p. 1163-8.

91. Baharvand, H., et al., *Generation of insulin-secreting cells from human embryonic stem cells.* Dev Growth Differ, 2006. **48**(5): p. 323-32.

92. Yue, F., et al., *Glucagon-like peptide-1 differentiation of primate embryonic stem cells into insulin-producing cells.* Tissue Eng, 2006. **12**(8): p. 2105-16.

93. Yue, F., et al., *Glucagon-like peptide-1 differentiation of primate embryonic stem cells into insulin-producing cells.* Tissue engineering, 2006. **12**(8): p. 2105-2116.

94. D'Amour, K.A., et al., *Production of pancreatic hormone–expressing endocrine cells from human embryonic stem cells.* Nature biotechnology, 2006. **24**(11): p. 1392-1401.

95. Kroon, E., et al., *Pancreatic endoderm derived from human embryonic stem cells generates glucose-responsive insulin-secreting cells in vivo.* Nat Biotechnol, 2008. **26**(4): p. 443-52.

96. Borowiak, M., et al., *Small molecules efficiently direct endodermal differentiation of mouse and human embryonic stem cells.* Cell stem cell, 2009. **4**(4): p. 348-358.

97. Takenaga, M., M. Fukumoto, and Y. Hori, *Regulated Nodal signaling promotes differentiation of the definitive endoderm and mesoderm from ES cells.* Journal of cell science, 2007. **120**(12): p. 2078-2090.

98. Strubing, C., et al., *Differentiation of pluripotent embryonic stem cells into the neuronal lineage in vitro gives rise to mature inhibitory and excitatory neurons.* Mech Dev, 1995. **53**(2): p. 275-87.

99. Wobus, A.M., et al., *Retinoic acid accelerates embryonic stem cell-derived cardiac differentiation and enhances development of ventricular cardiomyocytes.* J Mol Cell Cardiol, 1997. **29**(6): p. 1525-39.

100. Drab, M., et al., *From totipotent embryonic stem cells to spontaneously contracting smooth muscle cells: a retinoic acid and db-cAMP in vitro differentiation model.* FASEB J, 1997. **11**(11): p. 905-15.

101. Shi, Y., et al., *Inducing embryonic stem cells to differentiate into pancreatic beta cells by a novel three-step approach with activin A and all-trans retinoic acid.* Stem Cells, 2005. **23**(5): p. 656-62.

102. Vaca, P., et al., *Induction of Differentiation of Embryonic Stem Cells into Insulin-Secreting Cells by Fetal Soluble Factors.* Stem Cells, 2006. **24**(2): p. 258-265.

103. Pagliuca, Felicia W., et al., *Generation of Functional Human Pancreatic β Cells In Vitro.* Cell, 2014. **159**(2): p. 428-439.

104. Karnieli, O., et al., *Generation of insulin-producing cells from human bone marrow mesenchymal stem cells by genetic manipulation.* Stem Cells, 2007. **25**(11): p. 2837-44.

105. Timper, K., et al., *Human adipose tissue-derived mesenchymal stem cells differentiate into insulin, somatostatin, and glucagon expressing cells.* Biochemical and biophysical research communications, 2006. **341**(4): p. 1135-1140.

106. Wang, Y., et al., *Application of microfluidic technology to pancreatic islet research: first decade of endeavor.* Bioanalysis, 2010. **2**(10): p. 1729-1744.

107. Schmied, B.M., et al., *Transdifferentiation of Human Islet Cells in a Long-term Culture.* Pancreas, 2001. **23**(2): p. 157-171.

108. Gingerich, R.L., et al., *Insulin and Glucagon Secretion from Rat Islets Maintained in a Tissue Culture-Perifusion System.* Diabetes, 1979. **28**(4): p. 276-281.

109. Schuppin, G., et al., *Replication of adult pancreatic-beta cells cultured on bovine corneal endothelial cell extracellular matrix.* In Vitro Cellular & Developmental Biology-Animal, 1993. **29**(4): p. 339-344.

110. Perfetti, R., et al., *Insulin release and insulin mRNA levels in rat islets of Langerhans cultured on extracellular matrix.* Pancreas, 1996. **13**(1): p. 47-54.

111. Oberg-Welsh, C., *Long-term culture in matrigel enhances the insulin secretion of fetal porcine islet-like cell clusters in vitro.* Pancreas, 2001. **22**(2): p. 157-63.

112. Ris, F., et al., *Impact of integrin-matrix matching and inhibition of apoptosis on the survival of purified human beta-cells in vitro.* Diabetologia, 2002. **45**(6): p. 841-850.

113. Edamura, K., et al., *Brief Communication: Effect of Adhesion or Collagen Molecules on Cell Attachment, Insulin Secretion, and Glucose Responsiveness in the Cultured Adult Porcine Endocrine Pancreas: A Preliminary Study.* Cell transplantation, 2003. **12**(4): p. 439-446.

114. Woods, T.C., et al., *Activation of EphB2 and Its Ligands Promotes Vascular Smooth Muscle Cell Proliferation.* Journal of Biological Chemistry, 2002. **277**(3): p. 1924-1927.

115. Knight, K.R., et al., *Vascularized tissue-engineered chambers promote survival and function of transplanted islets and improve glycemic control.* FASEB journal: official publication of the Federation of American Societies for Experimental Biology, 2006. **20**(3): p. 565-567.

116. Nagata, N., et al., *Co-culture of extracellular matrix suppresses the cell death of rat pancreatic islets.* Journal of Biomaterials Science -- Polymer Edition, 2002. **13**(5): p. 579-590.

117. Kaido, T., et al., *αv-Integrin utilization in human β-cell adhesion, spreading, and motility.* Journal of Biological Chemistry, 2004. **279**(17): p. 17731-17737.

118. Kaido, T., et al., *Regulation of human beta-cell adhesion, motility, and insulin secretion by collagen IV and its receptor alpha1beta1*. J Biol Chem, 2004. **279**(51): p. 53762-9.

119. Wang, R.N. and L. Rosenberg, *Maintenance of beta-cell function and survival following islet isolation requires re-establishment of the islet-matrix relationship.* J Endocrinol, 1999. **163**(2): p. 181-90.

120. Kaiser, N., et al., *Monolayer culture of adult rat pancreatic islets on extracellular matrix: long term maintenance of differentiated B-cell function.* Endocrinology, 1988. **123**(2): p. 834-40.

121. BEATTIE, G.M., et al., *Functional Impact of Attachment and Purification in the Short Term Culture of Human Pancreatic Islets*.* The Journal of Clinical Endocrinology & Metabolism, 1991. **73**(1): p. 93-98.

122. Bosco, D., et al., *Importance of cell-matrix interactions in rat islet beta-cell secretion in vitro: role of alpha6beta1 integrin.* Diabetes, 2000. **49**(2): p. 233-43.

123. Bosco, D., et al., *Increased intracellular calcium is required for spreading of rat islet β-cells on extracellular matrix.* Diabetes, 2001. **50**(5): p. 1039-1046.

124. Lacy, P., et al., *Maintenance of normoglycemia in diabetic mice by subcutaneous xenografts of encapsulated islets.* Science, 1991. **254**(5039): p. 1782-1784.

125. O'Shea, G.M. and A. Sun, *Encapsulation of rat islets of Langerhans prolongs xenograft survival in diabetic mice.* Diabetes, 1986. **35**(8): p. 943-946.

126. Fan, M.-Y., et al., *Reversal of diabetes in BB rats by transplantation of encapsulated pancreatic islets.* Diabetes, 1990. **39**(4): p. 519-522.

127. O'Shea, G.M., M.F. Goosen, and A.M. Sun, *Prolonged survival of transplanted islets of Langerhans encapsulated in a biocompatible membrane.* Biochimica et Biophysica Acta (BBA)-Molecular Cell Research, 1984. **804**(1): p. 133-136.

128. Wang, T., et al., *An encapsulation system for the immunoisolation of pancreatic islets.* Nature biotechnology, 1997. **15**(4): p. 358-362.

129. Brendel, M., et al., *Improved functional survival of human islets of Langerhans in three-dimensional matrix culture.* Cell transplantation, 1993. **3**(5): p. 427-435.

130. Daoud, J.T., et al., *Long-term in vitro human pancreatic islet culture using three-dimensional microfabricated scaffolds.* Biomaterials, 2011. **32**(6): p. 1536-1542.

131. Chao, S., et al., *Entrapment of cultured pancreas islets in three-dimensional collagen matrices.* Cell transplantation, 1991. **1**(1): p. 51-60.

132. Mohammed, J.S., et al., *Microfluidic device for multimodal characterization of pancreatic islets.* Lab on a Chip, 2009. **9**(1): p. 97-106.

133. Sankar, K.S., et al., *Culturing Pancreatic Islets in Microfluidic Flow Enhances Morphology of the Associated Endothelial Cells.* PLoS ONE, 2011. **6**(9): p. e24904.

134. Nunemaker, C.S., et al., *Glucose metabolism, islet architecture, and genetic homogeneity in imprinting of [Ca2+] i and insulin rhythms in mouse islets.* PloS one, 2009. **4**(12): p. e8428.

135. Dishinger, J.F., K.R. Reid, and R.T. Kennedy, *Quantitative monitoring of insulin secretion from single islets of Langerhans in parallel on a microfluidic chip.* Analytical chemistry, 2009. **81**(8): p. 3119-3127.

136. Dishinger, J.F. and R.T. Kennedy, *Serial immunoassays in parallel on a microfluidic chip for monitoring hormone secretion from living cells.* Analytical chemistry, 2007. **79**(3): p. 947-954.

137. Zhang, X. and M.G. Roper, *Microfluidic perfusion system for automated delivery of temporal gradients to islets of Langerhans.* Analytical chemistry, 2008. **81**(3): p. 1162-1168.

138. Zhang, X., et al., *Microfluidic system for generation of sinusoidal glucose waveforms for entrainment of islets of Langerhans.* Analytical chemistry, 2010. **82**(15): p. 6704-6711.

139. Easley, C.J., et al., *Quantitative measurement of zinc secretion from pancreatic islets with high temporal resolution using droplet-based microfluidics.* Analytical chemistry, 2009. **81**(21): p. 9086-9095.

140. Rocheleau, J.V. and D.W. Piston, *Combining microfluidics and quantitative fluorescence microscopy to examine pancreatic islet molecular physiology.* Methods in cell biology, 2008. **89**: p. 71-92.

141. Adewola, A.F., et al., *Microfluidic perifusion and imaging device for multi-parametric islet function assessment.* Biomed Microdevices, 2010. **12**(3): p. 409-17.

142. Lifson, N., C.V. Lassa, and P.K. Dixit, *Relation between blood flow and morphology in islet organ of rat pancreas.* Am J Physiol, 1985. **249**(1 Pt 1): p. E43-E48.

143. Jansson, L. and P.O. Carlsson, *Graft vascular function after transplantation of pancreatic islets.* Diabetologia, 2002. **45**(6): p. 749-63.

144. Carlsson, P.-O., et al., *Islet capillary blood pressure increase mediated by hyperglycemia in NIDDM GK rats.* Diabetes, 1997. **46**(6): p. 947-952.

145. Lammert, E., O. Cleaver, and D. Melton, *Induction of pancreatic differentiation by signals from blood vessels.* Science, 2001. **294**(5542): p. 564-7.

146. Yoshitomi, H. and K.S. Zaret, *Endothelial cell interactions initiate dorsal pancreas development by selectively inducing the transcription factor Ptf1a.* Development, 2004. **131**(4): p. 807-17.

147. Jacquemin, P., et al., *An endothelial–mesenchymal relay pathway regulates early phases of pancreas development.* Developmental biology, 2006. **290**(1): p. 189-199.

148. Edsbagge, J., et al., *Vascular function and sphingosine-1-phosphate regulate development of the dorsal pancreatic mesenchyme.* Development, 2005. **132**(5): p. 1085-92.

149. Brissova, M., et al., *Pancreatic islet production of vascular endothelial growth factor--a is essential for islet vascularization, revascularization, and function.* Diabetes, 2006. **55**(11): p. 2974-85.

150. Lammert, E., et al., *Role of VEGF-A in vascularization of pancreatic islets.* Current Biology, 2003. **13**(12): p. 1070-1074.

151. Jabs, N., et al., *Reduced insulin secretion and content in VEGF-a deficient mouse pancreatic islets.* Experimental and clinical endocrinology & diabetes, 2008. **116**(S 01): p. S46-S49.

152. Iwashita, N., et al., *Impaired insulin secretion in vivo but enhanced insulin secretion from isolated islets in pancreatic beta cell-specific vascular endothelial growth factor-A knock-out mice.* Diabetologia, 2007. **50**(2): p. 380-389.

153. Brindle, N.P., P. Saharinen, and K. Alitalo, *Signaling and functions of angiopoietin-1 in vascular protection.* Circulation Research, 2006. **98**(8): p. 1014-1023.

154. Nikolova, G., et al., *The vascular basement membrane: a niche for insulin gene expression and Beta cell proliferation.* Dev Cell, 2006. **10**(3): p. 397-405.

155. Jiang, F.X., et al., *Laminin-1 promotes differentiation of fetal mouse pancreatic beta-cells.* Diabetes, 1999. **48**(4): p. 722-30.

156. Crawford, L.A., et al., *Connective tissue growth factor (CTGF) inactivation leads to defects in islet cell lineage allocation and beta-cell proliferation during embryogenesis.* Mol Endocrinol, 2009. **23**(3): p. 324-36.

157. Sachdeva, M.M. and D.A. Stoffers, *Minireview: meeting the demand for insulin: molecular mechanisms of adaptive postnatal ß-cell mass expansion.* Molecular Endocrinology, 2009. **23**(6): p. 747-758.

158. Kamba, T., et al., *VEGF-dependent plasticity of fenestrated capillaries in the normal adult microvasculature.* American Journal of Physiology-Heart and Circulatory Physiology, 2006. **290**(2): p. H560-H576.

159. Johansson, M., et al., *Perinatal development of the pancreatic islet microvasculature in rats.* Journal of Anatomy, 2006. **208**(2): p. 191-196.

160. Ham, J.N., et al., *Exendin-4 normalizes islet vascularity in intrauterine growth restricted rats: potential role of VEGF.* Pediatric research, 2009. **66**(1): p. 42-46.

161. Kaufman-Francis, K., et al., *Engineered Vascular Beds Provide Key Signals to Pancreatic Hormone-Producing Cells.* PLoS ONE, 2012. **7**(7): p. e40741.

162. Ranjan, A.K., M.V. Joglekar, and A.A. Hardikar, *Endothelial cells in pancreatic islet development and function.* Islets, 2009. **1**(1): p. 2-9.

163. Lau, J., et al., *Superior beta cell proliferation, function and gene expression in a subpopulation of rat islets identified by high blood perfusion.* Diabetologia, 2012. **55**(5): p. 1390-9.

164. Johansson, M., et al., *Islet endothelial cells and pancreatic beta-cell proliferation: studies in vitro and during pregnancy in adult rats.* Endocrinology, 2006. **147**(5): p. 2315-24.

165. Nikolova, G., B. Strilic, and E. Lammert, *The vascular niche and its basement membrane.* Trends Cell Biol, 2007. **17**(1): p. 19-25.

166. Kragl, M. and E. Lammert, *Basement membrane in pancreatic islet function*, in *The Islets of Langerhans*. 2010, Springer. p. 217-234.

167. Talavera-Adame, D., et al., *Endothelial cells in co-culture enhance embryonic stem cell differentiation to pancreatic progenitors and insulin-producing cells through BMP signaling.* Stem Cell Rev, 2011. **7**(3): p. 532-43.

168. Jiang, W., et al., *In vitro derivation of functional insulin-producing cells from human embryonic stem cells.* Cell research, 2007. **17**(4): p. 333-344.

169. Turitto, V.T., *Blood viscosity, mass transport, and thrombogenesis.* Prog Hemost Thromb, 1982. **6**: p. 139-77.

170. Xu, X., V.L. Browning, and J.S. Odorico, *Activin, BMP and FGF pathways cooperate to promote endoderm and pancreatic lineage cell differentiation from human embryonic stem cells.* Mech Dev, 2011. **128**(7-10): p. 412-27.

171. Segev, H., et al., *Differentiation of human embryonic stem cells into insulin-producing clusters.* Stem cells, 2004. **22**(3): p. 265-274.

172. Blyszczuk, P., et al., *Embryonic stem cells differentiate into insulin-producing cells without selection of nestin-expressing cells.* Int J Dev Biol, 2004. **48**(10): p. 1095-1104.

173. Lendahl, U., L.B. Zimmerman, and R.D. McKay, *CNS stem cells express a new class of intermediate filament protein.* Cell, 1990. **60**(4): p. 585-595.

174. Zulewski, H., et al., *Multipotential Nestin-Positive Stem Cells Isolated From Adult Pancreatic Islets Differentiate Ex Vivo Into Pancreatic Endocrine, Exocrine, and Hepatic Phenotypes.* Diabetes, 2001. **50**(3): p. 521-533.

175. Lee, S.-H., et al., *Efficient generation of midbrain and hindbrain neurons from mouse embryonic stem cells.* Nature biotechnology, 2000. **18**(6): p. 675-679.

176. Bouwens, L., *Cytokeratins and cell differentiation in the pancreas.* The Journal of pathology, 1998. **184**(3): p. 234-239.

177. Brembeck, F.H., et al., *The keratin 19 promoter is potent for cell-specific targeting of genes in transgenic mice.* Gastroenterology, 2001. **120**(7): p. 1720-1728.

178. Bouwens, L., W. Lu, and R. De Krijger, *Proliferation and differentiation in the human fetal endocrine pancreas.* Diabetologia, 1997. **40**(4): p. 398-404.

179. Vaca, P., et al., *Induction of Differentiation of Embryonic Stem Cells into Insulin-Secreting Cells by Fetal Soluble Factors.* Stem cells, 2006. **24**(2): p. 258-265.

180. Omer, A., et al., *Survival and maturation of microencapsulated porcine neonatal pancreatic cell clusters transplanted into immunocompetent diabetic mice.* Diabetes, 2003. **52**(1): p. 69-75.

181. Nishimura, W., et al., *A switch from MafB to MafA expression accompanies differentiation to pancreatic beta-cells.* Dev Biol, 2006. **293**(2): p. 526-39.

182. Shiroi, A., et al., *Identification of insulin-producing cells derived from embryonic stem cells by zinc-chelating dithizone.* Stem Cells, 2002. **20**(4): p. 284-92.

183. Besnard, V., et al., *Immunohistochemical localization of Foxa1 and Foxa2 in mouse embryos and adult tissues.* Gene Expression Patterns, 2004. **5**(2): p. 193-208.

184. Emdin, S.O., et al., *Role of zinc in insulin biosynthesis. Some possible zinc-insulin interactions in the pancreatic B-cell.* Diabetologia, 1980. **19**(3): p. 174-82.

185. Figlewicz, D.P., et al., *Kinetics of 65zinc uptake and distribution in fractions from cultured rat islets of langerhans.* Diabetes, 1980. **29**(10): p. 767-73.

186. Sasaki, H. and B.L. Hogan, *Differential expression of multiple fork head related genes during gastrulation and axial pattern formation in the mouse embryo.* Development, 1993. **118**(1): p. 47-59.

187. Ang, S.L., et al., *The formation and maintenance of the definitive endoderm lineage in the mouse: involvement of HNF3/forkhead proteins.* Development, 1993. **119**(4): p. 1301-15.

188. Monaghan, A.P., et al., *Postimplantation expression patterns indicate a role for the mouse forkhead/HNF-3 alpha, beta and gamma genes in determination of the definitive endoderm, chordamesoderm and neuroectoderm.* Development, 1993. **119**(3): p. 567-78.

189. Kanai-Azuma, M., et al., *Depletion of definitive gut endoderm in Sox17-null mutant mice.* Development, 2002. **129**(10): p. 2367-79.

190. Blum, M., et al., *Gastrulation in the mouse: the role of the homeobox gene goosecoid.* Cell, 1992. **69**(7): p. 1097-106.

191. Gao, T., et al., *Pdx1 maintains β cell identity and function by repressing an α cell program.* Cell metabolism, 2014. **19**(2): p. 259-271.

192. Seufert, J., G.C. Weir, and J.F. Habener, *Differential expression of the insulin gene transcriptional repressor CCAAT/enhancer-binding protein beta and transactivator islet duodenum homeobox-1 in rat pancreatic beta cells during the development of diabetes mellitus.* Journal of Clinical Investigation, 1998. **101**(11): p. 2528.

193. Kulkarni, R.N., et al., *PDX-1 haploinsufficiency limits the compensatory islet hyperplasia that occurs in response to insulin resistance.* Journal of Clinical Investigation, 2004. **114**(6): p. 828-836.

194. Schaffer, A.E., et al., *Nkx6.1 controls a gene regulatory network required for establishing and maintaining pancreatic Beta cell identity.* PLoS Genet, 2013. **9**(1): p. e1003274.

195. Schisler, J.C., et al., *The Nkx6. 1 homeodomain transcription factor suppresses glucagon expression and regulates glucose-stimulated insulin secretion in islet beta cells.* Proceedings of the National Academy of Sciences of the United States of America, 2005. **102**(20): p. 7297-7302.

196. Schisler, J.C., et al., *Stimulation of human and rat islet β-cell proliferation with retention of function by the homeodomain transcription factor Nkx6. 1.* Molecular and cellular biology, 2008. **28**(10): p. 3465-3476.

197. Taylor, Brandon L., F.-F. Liu, and M. Sander, *Nkx6.1 Is Essential for Maintaining the Functional State of Pancreatic Beta Cells.* Cell Reports. **4**(6): p. 1262-1275.

198. Brun, T., et al., *The diabetes-linked transcription factor PAX4 promotes β-cell proliferation and survival in rat and human islets.* The Journal of cell biology, 2004. **167**(6): p. 1123-1135.

199. Sosa-Pineda, B., et al., *The Pax4 gene is essential for differentiation of insulin-producing [beta] cells in the mammalian pancreas.* Nature, 1997. **386**(6623): p. 399-402.

200. *GLUT2*. GeneCards 2014; Available from: http://www.genecards.org/cgi-bin/carddisp.pl?gene=SLC2A2. Accessed: Sep 2014

201. McCulloch, L.J., et al., *GLUT2 (SLC2A2) is not the principal glucose transporter in human pancreatic beta cells: implications for understanding genetic association signals at this locus.* Mol Genet Metab, 2011. **104**(4): p. 648-53.

202. Flanagan, J.G. and P. Vanderhaeghen, *The ephrins and Eph receptors in neural development.* Annu Rev Neurosci, 1998. **21**: p. 309-45.

203. Kullander, K. and R. Klein, *Mechanisms and functions of Eph and ephrin signalling.* Nature Reviews Molecular Cell Biology, 2002. **3**(7): p. 475-486.

204. Pasquale, E.B., *Eph receptor signalling casts a wide net on cell behaviour.* Nat Rev Mol Cell Biol, 2005. **6**(6): p. 462-75.

205. Konstantinova, I., et al., *EphA-Ephrin-A-Mediated ² Cell Communication Regulates Insulin Secretion from Pancreatic Islets.* Cell, 2007. **129**(2): p. 359-370.

206. Moynihan, K.A., et al., *Increased dosage of mammalian Sir2 in pancreatic β cells enhances glucose-stimulated insulin secretion in mice.* Cell Metabolism, 2005. **2**(2): p. 105-117.

207. Rerup, C. and I. Lundquist, *Blood Glucose Level In Mice.* Acta Endocrinologica, 1966. **52**(3): p. 357-367.

208. Barbosa, R.M., et al., *Control of pulsatile 5-HT/insulin secretion from single mouse pancreatic islets by intracellular calcium dynamics.* J Physiol, 1998. **510 (Pt 1)**: p. 135-43.

209. Ashcroft, F.M. and S.J. Ashcroft, *Insulin: molecular biology to pathology*. 1992: Oxford University Press, USA.

210. PREMDAS, F.H., et al., *Electrical activity, cAMP concentration, and insulin release in mouse islets of Langerhans.* 1985.

211. Ma, Y.H., et al., *Differences in insulin secretion between the rat and mouse: role of cAMP.* European journal of endocrinology, 1995. **132**(3): p. 370-376.

212. Gao, F., et al., *< i> In vitro</i> cultivation of islet-like cell clusters from human umbilical cord blood-derived mesenchymal stem cells.* Translational Research, 2008. **151**(6): p. 293-302.

213. Sun, Y., et al., *Differentiation of bone marrow-derived mesenchymal stem cells from diabetic patients into insulin-producing cells in vitro.* Chinese Medical Journal-Beijing-English Edition-, 2007. **120**(9): p. 771.

214. Xu, G., et al., *Exendin-4 stimulates both beta-cell replication and neogenesis, resulting in increased beta-cell mass and improved glucose tolerance in diabetic rats.* Diabetes, 1999. **48**(12): p. 2270-2276.

215. Gannon, M., et al., *Persistent expression of HNF6 in islet endocrine cells causes disrupted islet architecture and loss of beta cell function.* Development, 2000. **127**(13): p. 2883-2895.

216. Bosco, D., L. Orci, and P. Meda, *Homologous but not heterologous contact increases the insulin secretion of individual pancreatic B-cells.* Experimental cell research, 1989. **184**(1): p. 72-80.

217. Samols, E. and J.I. Stagner, *Islet somatostatin-microvascular, paracrine, and pulsatile regulation.* Metabolism, 1990. **39**(9): p. 55-60.

218. Hamamoto, Y., et al., *Beneficial effect of pretreatment of islets with fibronectin on glucose tolerance after islet transplantation.* Hormone and metabolic research, 2003. **35**(08): p. 460-465.

219. Jiang, F.-X., G. Naselli, and L.C. Harrison, *Distinct distribution of laminin and its integrin receptors in the pancreas.* Journal of Histochemistry & Cytochemistry, 2002. **50**(12): p. 1625-1632.

220. Davis, N.E., et al., *Enhanced function of pancreatic islets co-encapsulated with ECM proteins and mesenchymal stromal cells in a silk hydrogel.* Biomaterials, 2012. **33**(28): p. 6691-7.

221. Lucas-Clerc, C., et al., *Long-term culture of human pancreatic islets in an extracellular matrix: morphological and metabolic effects.* Mol Cell Endocrinol, 1993. **94**(1): p. 9-20.

222. London, N., S. Swift, and H. Clayton, *Isolation, culture and functional evaluation of islets of Langerhans.* 2008.

223. Stendahl, J.C., et al., *Growth factor delivery from self-assembling nanofibers to facilitate islet transplantation.* Transplantation, 2008. **86**(3): p. 478.

224. Su, J., et al., *Anti-inflammatory peptide-functionalized hydrogels for insulin-secreting cell encapsulation.* Biomaterials, 2010. **31**(2): p. 308-314.

225. Montesano, R., et al., *Collagen matrix promotes reorganization of pancreatic endocrine cell monolayers into islet-like organoids.* J Cell Biol, 1983. **97**(3): p. 935-9.

226. Orci, L., *Macro-and micro-domains in the endocrine pancreas.* Diabetes, 1982. **31**(6): p. 538-565.

227. Zhang, Y., et al., *Three-dimensional scaffolds reduce islet amyloid formation and enhance survival and function of cultured human islets.* Am J Pathol, 2012. **181**(4): p. 1296-305.

228. Mason, M.N., C.A. Arnold, and M.J. Mahoney, *Entrapped collagen type 1 promotes differentiation of embryonic pancreatic precursor cells into glucose-responsive beta-cells when cultured in three-dimensional PEG hydrogels.* Tissue Eng Part A, 2009. **15**(12): p. 3799-808.

229. Charrier, A. and D.R. Brigstock, *Regulation of pancreatic function by connective tissue growth factor (CTGF, CCN2).* Cytokine & Growth Factor Reviews, (0).

230. Olsson, R. and P.O. Carlsson, *The pancreatic islet endothelial cell: emerging roles in islet function and disease.* Int J Biochem Cell Biol, 2006. **38**(5-6): p. 710-4.

231. Guney, M.A., et al., *Connective tissue growth factor acts within both endothelial cells and beta cells to promote proliferation of developing beta cells.* Proc Natl Acad Sci U S A, 2011. **108**(37): p. 15242-7.

232. Jansson, L., *Microsphere distribution in the pancreas of anesthetized rats. Alloxan stimulates the blood flow to all islets whereas glucose only affects the blood perfusion of a subgroup of islets.* Int J Pancreatol, 1996. **20**(1): p. 69-74.

233. Carlsson, P.O., et al., *Multiple injections of coloured microspheres for islet blood flow measurements in anaesthetised rats: influence of microsphere size.* Ups J Med Sci, 2002. **107**(2): p. 111-20.

234. *Unified nomenclature for Eph family receptors and their ligands, the ephrins. Eph Nomenclature Committee.* Cell, 1997. **90**(3): p. 403-4.

235. Klein, R., *Eph/ephrin signalling during development.* Development, 2012. **139**(22): p. 4105-9.

236. Himanen, J.P., et al., *Repelling class discrimination: ephrin-A5 binds to and activates EphB2 receptor signaling.* Nat Neurosci, 2004. **7**(5): p. 501-9.

237. Salvucci, O., et al., *EphB2 and EphB4 receptors forward signaling promotes SDF-1-induced endothelial cell chemotaxis and branching remodeling.* Blood, 2006. **108**(9): p. 2914-22.

238. Lee, E.J. and L.E. Niklason, *A novel flow bioreactor for in vitro microvascularization.* Tissue Eng Part C Methods, 2010. **16**(5): p. 1191-200.

239. *Real time PCR Ct values*. Available from: http://www.wvdl.wisc.edu/wp-content/uploads/2013/01/WVDL.Info_.PCR_Ct_Values1.pdf. Accessed: Sep 2014

240. Griffith, C.K., et al., *Diffusion limits of an in vitro thick prevascularized tissue.* Tissue Eng, 2005. **11**(1-2): p. 257-66.

241. Lang, N.R., et al., *Estimating the 3D pore size distribution of biopolymer networks from directionally biased data.* Biophys J, 2013. **105**(9): p. 1967-75.

242. Bentsi-Barnes, K., et al., *Detailed protocol for evaluation of dynamic perifusion of human islets to assess beta-cell function.* Islets, 2011. **3**(5): p. 284-90.

243. Jansson, L. and C. Hellerström, *Stimulation by glucose of the blood flow to the pancreatic islets of the rat.* Diabetologia, 1983. **25**(1): p. 45-50.

244. Purrello, F., et al., *Effects of high glucose on insulin secretion by isolated rat islets and purified beta-cells and possible role of glycosylation.* Diabetes, 1989. **38**(11): p. 1417-22.

245. Davalli, A.M., et al., *Abnormal sensitivity to glucose of human islets cultured in a high glucose medium: partial reversibility after an additional culture in a normal glucose medium.* J Clin Endocrinol Metab, 1991. **72**(1): p. 202-8.

246. Weber, L.M., K.N. Hayda, and K.S. Anseth, *Cell-matrix interactions improve beta-cell survival and insulin secretion in three-dimensional culture.* Tissue Eng Part A, 2008. **14**(12): p. 1959-68.

247. Jopling, C., S. Boue, and J.C.I. Belmonte, *Dedifferentiation, transdifferentiation and reprogramming: three routes to regeneration.* Nature reviews Molecular cell biology, 2011. **12**(2): p. 79-89.

248. Lu, J., et al., *Adult islets cultured in collagen gel transdifferentiate into duct-like cells.* World Journal Of Gastroenterology, 2005. **11**(22): p. 3426.

249. Li, J., et al., *Islet neogenesis-associated protein-related pentadecapeptide enhances the differentiation of islet-like clusters from human pancreatic duct cells.* Peptides, 2009. **30**(12): p. 2242-2249.

250. Bouwens, L., F. Braet, and H. Heimberg, *Identification of rat pancreatic duct cells by their expression of cytokeratins 7, 19, and 20 in vivo and after isolation and culture.* Journal of Histochemistry & Cytochemistry, 1995. **43**(3): p. 245-253.

251. Konstantinova, I. and E. Lammert, *Microvascular development: learning from pancreatic islets.* Bioessays, 2004. **26**(10): p. 1069-75.

252. Lammert, E., O. Cleaver, and D. Melton, *Role of endothelial cells in early pancreas and liver development.* Mech Dev, 2003. **120**(1): p. 59-64.

253. Song, H.J., et al., *Improved Islet Survival and Funtion With Rat Endothelial Cells In Vitro Co-Culture.* Transplantation Proceedings, 2009. **41**(10): p. 4302-4306.

254. Jaramillo, M. and I. Banerjee, *Endothelial cell co-culture mediates maturation of human embryonic stem cell to pancreatic insulin producing cells in a directed differentiation approach.* J Vis Exp, 2012(61).

255. Welsh, N., D.L. Eizirik, and S. Sandler, *Nitric oxide and pancreatic beta-cell destruction in insulin dependent diabetes mellitus: don't take NO for an answer.* Autoimmunity, 1994. **18**(4): p. 285-90.

256. Steiner, L., et al., *Endothelial cells as cytotoxic effector cells: cytokine-activated rat islet endothelial cells lyse syngeneic islet cells via nitric oxide.* Diabetologia, 1997. **40**(2): p. 150-155.

257. Fehsel, K., et al., *Islet cell DNA is a target of inflammatory attack by nitric oxide.* Diabetes, 1993. **42**(3): p. 496-500.

258. Kröncke, K.-D., et al., *Pancreatic islet cells are highly susceptible towards the cytotoxic effects of chemically generated nitric oxide.* Biochimica et Biophysica Acta (BBA)-Molecular Basis of Disease, 1993. **1182**(2): p. 221-229.

259. Montesano, R., L. Orci, and P. Vassalli, *In vitro rapid organization of endothelial cells into capillary-like networks is promoted by collagen matrices.* J Cell Biol, 1983. **97**(5 Pt 1): p. 1648-52.

260. Komorowski, J., et al., *Effect of thalidomide affecting VEGF secretion, cell migration, adhesion and capillary tube formation of human endothelial EA.hy 926 cells.* Life Sciences, 2006. **78**(22): p. 2558-2563.

261. Li, Z., et al., *Differentiation, Survival, and Function of Embryonic Stem Cell–Derived Endothelial Cells for Ischemic Heart Disease.* Circulation, 2007. **116**(11 suppl): p. I-46-I-54.

262. Aird, W.C., *Phenotypic heterogeneity of the endothelium: II. Representative vascular beds.* Circulation Research, 2007. **100**(2): p. 174-90.

263. Wang, H.U., Z.F. Chen, and D.J. Anderson, *Molecular distinction and angiogenic interaction between embryonic arteries and veins revealed by ephrin-B2 and its receptor Eph-B4.* Cell, 1998. **93**(5): p. 741-53.

264. Adams, R.H., et al., *Roles of ephrinB ligands and EphB receptors in cardiovascular development: demarcation of arterial/venous domains, vascular morphogenesis, and sprouting angiogenesis.* Genes Dev, 1999. **13**(3): p. 295-306.

265. Zanone, M.M., et al., *Expression of nephrin by human pancreatic islet endothelial cells.* Diabetologia, 2005. **48**(9): p. 1789-97.

266. Kaido, T., et al., *Impact of defined matrix interactions on insulin production by cultured human beta-cells: effect on insulin content, secretion, and gene transcription.* Diabetes, 2006. **55**(10): p. 2723-9.

267. Virtanen, I., et al., *Blood vessels of human islets of Langerhans are surrounded by a double basement membrane.* Diabetologia, 2008. **51**(7): p. 1181-91.

268. Iwashita, N., et al., *Impaired insulin secretion in vivo but enhanced insulin secretion from isolated islets in pancreatic beta cell-specific vascular endothelial growth factor-A knock-out mice.* Diabetologia, 2007. **50**(2): p. 380-9.

269. Lammert, E., et al., *Role of VEGF-A in vascularization of pancreatic islets.* Curr Biol, 2003. **13**(12): p. 1070-4.

270. Jabs, N., et al., *Reduced insulin secretion and content in VEGF-a deficient mouse pancreatic islets.* Exp Clin Endocrinol Diabetes, 2008. **116 Suppl 1**: p. S46-9.

271. Vasir, B., et al., *Hypoxia induces vascular endothelial growth factor gene and protein expression in cultured rat islet cells.* Diabetes, 1998. **47**(12): p. 1894-903.

272. Gorden, D.L., et al., *Vascular endothelial growth factor is increased in devascularized rat islets of Langerhans in vitro.* Transplantation, 1997. **63**(3): p. 436-43.

273. Christofori, G., P. Naik, and D. Hanahan, *Vascular endothelial growth factor and its receptors, flt-1 and flk-1, are expressed in normal pancreatic islets and throughout islet cell tumorigenesis.* Mol Endocrinol, 1995. **9**(12): p. 1760-70.

274. Tryggvason, K. and J. Wartiovaara, *Molecular basis of glomerular permselectivity.* Curr Opin Nephrol Hypertens, 2001. **10**(4): p. 543-9.

275. Beltcheva, O., et al., *Alternatively used promoters and distinct elements direct tissue-specific expression of nephrin.* J Am Soc Nephrol, 2003. **14**(2): p. 352-8.

276. Putaala, H., et al., *The murine nephrin gene is specifically expressed in kidney, brain and pancreas: inactivation of the gene leads to massive proteinuria and neonatal death.* Hum Mol Genet, 2001. **10**(1): p. 1-8.

277. Liu, L., et al., *Nephrin is an important component of the barrier system in the testis.* Acta Med Okayama, 2001. **55**(3): p. 161-5.

278. Lou, J., et al., *Expression of alpha-1 proteinase inhibitor in human islet microvascular endothelial cells.* Diabetes, 1999. **48**(9): p. 1773-8.

279. Zhang, B., et al., *α1-Antitrypsin protects β-cells from apoptosis.* Diabetes, 2007. **56**(5): p. 1316-1323.

280. Strom, T.B., *Saving islets from allograft rejection.* Proceedings of the National Academy of Sciences of the United States of America, 2005. **102**(36): p. 12651-12652.

281. Lewis, E.C., et al., *α1-Antitrypsin monotherapy induces immune tolerance during islet allograft transplantation in mice.* Proceedings of the National Academy of Sciences, 2008. **105**(42): p. 16236-16241.

282. Suschek, C., et al., *Primary cultures of rat islet capillary endothelial cells. Constitutive and cytokine-inducible macrophagelike nitric oxide synthases are expressed and activities regulated by glucose concentration.* Am J Pathol, 1994. **145**(3): p. 685-95.

283. Ding, Y. and R.S. Rana, *Nitric oxide does not initiate but potentiates glucose-induced insulin secretion in pancreatic beta-cells.* Biochem Biophys Res Commun, 1998. **251**(3): p. 699-703.

284. Laychock, S.G., M.E. Modica, and C.T. Cavanaugh, *L-arginine stimulates cyclic guanosine 3',5'-monophosphate formation in rat islets of Langerhans and RINm5F insulinoma cells: evidence for L-arginine:nitric oxide synthase.* Endocrinology, 1991. **129**(6): p. 3043-52.

285. Schmidt, H.H., et al., *Insulin secretion from pancreatic B cells caused by L-arginine-derived nitrogen oxides.* Science, 1992. **255**(5045): p. 721-3.

286. Spinas, G.A., *The dual role of nitric oxide in islet β-cells.* Physiology, 1999. **14**(2): p. 49-54.

287. Spinas, G., et al., *The early phase of glucose-stimulated insulin secretion requires nitric oxide.* Diabetologia, 1998. **41**(3): p. 292-299.

288. Willmott, N.J., A. Galione, and P.A. Smith, *Nitric oxide induces intracellular Ca< sup> 2+</sup> mobilization and increases secretion of incorporated 5-hydroxytryptamine in rat pancreatic β-cells.* FEBS letters, 1995. **371**(2): p. 99-104.

289. Åkesson, B. and I. Lundquist, *Influence of nitric oxide modulators on cholinergically stimulated hormone release from mouse islets.* J Physiol, 1999. **515**(2): p. 463-473.

290. Akesson, B., et al., *Islet constitutive nitric oxide synthase and glucose regulation of insulin release in mice.* Journal of endocrinology, 1999. **163**(1): p. 39-48.

291. Antoine, M.-H., et al., *Hydroxylamine, a nitric oxide donor, inhibits insulin release and activates K< sup>+</sup>< sub> ATP</sub> channels.* European journal of pharmacology, 1996. **313**(3): p. 229-235.

292. Gross, R., et al., *Alterations of insulin response to different beta cell secretagogues and pancreatic vascular resistance induced by N omega-nitro-L-arginine methyl ester.* Br J Pharmacol, 1995. **116**(3): p. 1965-72.

293. Henningsson, R., et al., *Chronic blockade of NO synthase paradoxically increases islet NO production and modulates islet hormone release.* Am J Physiol Endocrinol Metab, 2000. **279**(1): p. E95-E107.

294. Henningsson, R., et al., *Heme oxygenase and carbon monoxide: regulatory roles in islet hormone release: a biochemical, immunohistochemical, and confocal microscopic study.* Diabetes, 1999. **48**(1): p. 66-76.

295. Salehi, A., F. Parandeh, and I. Lundquist, *Signal transduction in islet hormone release: interaction of nitric oxide with basal and nutrient-induced hormone responses.* Cell Signal, 1998. **10**(9): p. 645-51.

296. Kim, J.A., et al., *Evidence that glucose increases monocyte binding to human aortic endothelial cells.* Diabetes, 1994. **43**(9): p. 1103-7.

297. Wang, X.L., et al., *Proteomic Analysis of Vascular Endothelial Cells-Effects of Laminar Shear Stress and High Glucose.* J. Proteomics Bioinform., 2009. **2**: p. 445.

298. Landsman, L., et al., *Pancreatic mesenchyme regulates epithelial organogenesis throughout development.* PLoS Biol, 2011. **9**(9): p. e1001143.

299. Golosow, N. and C. Grobstein, *Epitheliomesenchymal interaction in pancreatic morphogenesis.* Dev Biol, 1962. **4**: p. 242-55.

300. Nekrep, N., et al., *Signals from the neural crest regulate beta-cell mass in the pancreas.* Development, 2008. **135**(12): p. 2151-60.

301. Russ, H.A., et al., *In vitro proliferation of cells derived from adult human beta-cells revealed by cell-lineage tracing.* Diabetes, 2008. **57**(6): p. 1575-83.

302. Weinberg, N., et al., *Lineage tracing evidence for in vitro dedifferentiation but rare proliferation of mouse pancreatic beta-cells.* Diabetes, 2007. **56**(5): p. 1299-304.

303. Duan, Y., et al., *Shear-induced reorganization of renal proximal tubule cell actin cytoskeleton and apical junctional complexes.* Proceedings of the National Academy of Sciences, 2008. **105**(32): p. 11418-11423.

304. Song, C., et al., *Experimental study of rat beta islet cells cultured under simulated microgravity conditions.* Acta Biochim Biophys Sin (Shanghai), 2004. **36**(1): p. 47-50.